

Topics:
Dynamic load
Piping systems
Supports
Data bases
Failure
Testing

Dynamic Response of Pressurized Z-Bend Piping Systems Tested Beyond Elastic Limits and With Support Failures

— NOTICE —

THE ATTACHED FILES ARE OFFICIAL RECORDS OF THE DIVISION OF DOCUMENT CONTROL. THEY HAVE BEEN CHARGED TO YOU FOR A LIMITED TIME PERIOD AND MUST BE RETURNED TO THE RECORDS FACILITY BRANCH 016. PLEASE DO NOT SEND DOCUMENTS CHARGED OUT THROUGH THE MAIL. REMOVAL OF ANY PAGE(S) FROM DOCUMENT FOR REPRODUCTION MUST BE REFERRED TO FILE PERSONNEL. *50-206*

DEADLINE RETURN DATE *7/24/85*
8507260264

RECORDS FACILITY BRANCH

8507260271 850724
PDR ADCK 05000206
P PDR

R E P O R T S U M M A R Y

SUBJECTS	Risk assessment / Safety analysis	
TOPICS	Dynamic load Piping systems Supports	Data bases Failure Testing
AUDIENCE	Piping design and R&D engineers	

Dynamic Response of Pressurized Z-Bend Piping Systems Tested Beyond Elastic Limits and With Support Failures

A set of high-amplitude excitation tests demonstrated the wide safety margins allowed for dynamic loading in nuclear power plant piping specifications. This set of laboratory tests—the first of three sets—supports the argument that earthquake-resistance criteria for such piping systems are too conservative.

BACKGROUND	The ASME Boiler and Pressure Vessel Code bases its stress limits on data for ductile failure under statically applied loads. The piping system design standards for nuclear power plants, extrapolated from the static load data, are thought to be extremely conservative. An experimental data base is needed to address that conservatism.
OBJECTIVE	To establish an experimental data base for assessing the dynamic margin and failure capacities of piping and support systems in nuclear power plants.
APPROACH	Investigators set up two identical piping systems for laboratory testing. Each Z-shaped system of 4-in.-inside-diameter schedule 40 piping was 22 feet long. Three supports held each system in the vertical plane. Support hardware—frame, struts, mechanical snubbers, and hydraulic snubbers—was installed at the midpoint support. During testing, the hydraulic actuators sent a variety of input motions representing step forcing, sine dwell, random signals, and earthquakes through the support sleds to excite the system beyond the design-specified limits. Accelerometers, strain gages, displacement transducers, and load cells recorded piping and support responses.
RESULTS	The simple piping system successfully withstood repeated earthquakelike loadings that were three to five times those specified in the ASME Class 2 stress limit for service level D (the safe shutdown earthquake condition). Even in tests with a failed midpoint support, there was no leakage or plastic collapse. Snubber hardware did not fail until loads reached two to four times the manufacturer's specified load limits. (In one case, a mechanical snubber having a specified load maximum of 500 lb did not fail until the load was

1900 lb.) Pipe damping appeared at 2-4% of critical—higher than the 1-2% specified by NRC. Damping generally increased slightly with response amplitude.

EPRI PERSPECTIVE

This initial set of laboratory-based high-magnitude dynamic piping tests demonstrated that it is not easy to induce leakage or plastic collapse in high-pressure piping systems by applying earthquakelike dynamic loads. It also produced important reference data to use in validating both linear and nonlinear calculational procedures. A second set of tests is to be performed on more complex three-dimensional prototypical piping systems in EPRI project RP964-9, cosponsored by NRC. And in project RP1543, experiments are planned in which the dynamic loads increase until the test piping fails. Data from the three sets of pipe tests should provide solid evidence of the excessive conservatism in nuclear piping design code requirements. Such EPRI-sponsored research supports the activities of the Pressure Vessel Research Committee of the Welding Research Council in aiming for more realistic and efficient piping design rules. The damping data generated in this study can be used for further damping assessment and analytic method benchmarking. Brookhaven National Laboratory has already used them to perform a successful code benchmarking study for NRC.

PROJECT

RP964-3

EPRI Project Manager: Y. K. Tang

Nuclear Power Division

Contractor: ANCO Engineers, Inc.

For further information on EPRI research programs, call
EPRI Technical Information Specialists (415) 855-2411.

ORDERING INFORMATION EPRI NP-3746, Final Report, December 1984, 128 pages.

EPRI Members If this report is not available from your company libraries or your Technical Information Coordinator, you can order it from

Research Reports Center
P.O. Box 50490
Palo Alto, CA 94303
(415) 965-4081

Nonmembers You can order this report in print or microfiche from Research Reports Center.

Price: \$14.50 Overseas price: \$29.00
(California residents add sales tax.)
Payment must accompany order.

Dynamic Response of Pressurized Z-Bend
Piping Systems Tested Beyond Elastic Limits
and With Support Failures

NP-3746
Research Project 964-3

Final Report, December 1984

Prepared by

ANCO ENGINEERS, INC.
9937 Jefferson Boulevard
Culver City, California 90232-3591

Principal Investigators

G. E. Howard
W. B. Walton
B. A. Johnson

Prepared for

Electric Power Research Institute
3412 Hillview Avenue
Palo Alto, California 94304

EPRI Project Manager
Y. K. Tang

Risk Assessment Program
Nuclear Power Division

ORDERING INFORMATION

Requests for copies of this report should be directed to Research Reports Center (RRC), Box 50490, Palo Alto, CA 94303, (415) 965-4081. There is no charge for reports requested by EPRI member utilities and affiliates, U.S. utility associations, U.S. government agencies (federal, state, and local), media, and foreign organizations with which EPRI has an information exchange agreement. On request, RRC will send a catalog of EPRI reports.

Research Categories: Risk assessment
Safety analysis

Copyright © 1984 Electric Power Research Institute, Inc. All rights reserved.

NOTICE

This report was prepared by the organization(s) named below as an account of work sponsored by the Electric Power Research Institute, Inc. (EPRI). Neither EPRI, members of EPRI, the organization(s) named below, nor any person acting on behalf of any of them: (a) makes any warranty, express or implied, with respect to the use of any information, apparatus, method, or process disclosed in this report or that such use may not infringe privately owned rights; or (b) assumes any liabilities with respect to the use of, or for damages resulting from the use of, any information, apparatus, method, or process disclosed in this report.

Prepared by
ANCO Engineers, Inc.
Culver City, California

ABSTRACT

Results are presented for a series of high-amplitude dynamic tests of a simple pressurized piping system oriented in a vertical plane excited through various multiple piping supports. The four-inch diameter piping achieved response levels above yield when subjected to earthquake-like time history inputs and withstood--without leakage or gross distortion--dynamic inputs that were factors of three to five times greater than those inputs required to just achieve the ASME Class 2 stress limit for Service Level D, the Safe Shutdown Earthquake condition. Despite intentionally induced support failures in several tests, piping pressure integrity was maintained, and no plastic collapse occurred. Selected snubber hardware likewise exhibited large safety margins under transient loads. Calculated damping values were two to three times the values currently approved for use in seismic design.

CONTENTS

<u>Section</u>		<u>Page</u>
1	INTRODUCTION	1-1
2	PIPING SYSTEMS AND TESTING METHODS	2-1
	2.1 Piping Layout/Properties and Pipe End Boundary Conditions	2-1
	2.2 Piping Midpoint Support	2-8
	2.3 Bases Used for Base Motion	2-15
	2.4 Hydraulic Actuator System for Driving the Bases	2-15
	2.5 Instrumentation	2-18
	2.6 Data Acquisition and Analysis	2-18
	2.7 Tests Performed and Sample of Input Base Motions Used	2-26
3	PRESENTATION AND INTERPRETATION OF TEST RESULTS	3-1
	3.1 Response Levels Achieved During Testing	3-1
	3.1.1 Peak Base Motion and Pipe Response	3-1
	3.1.2 Achieved Base Motion Input Beyond That for Level D	3-8
	3.2 Support Influence on Piping Characteristics	3-22
	3.2.1 Support Influence With No Support Failures	3-22
	3.2.2 Support Influence With Support Failure	3-36
4	FINDINGS	4-1
5	REFERENCES	5-1
APPENDIX A	ULTRASONIC THICKNESS MEASUREMENTS OF PIPING RUNS	A-1
APPENDIX B	INSTRUMENTATION LAYOUTS	B-1
APPENDIX C	PHOTOGRAPHS OF PIPING SETUP	C-1

ILLUSTRATIONS

<u>Figure</u>	<u>Page</u>
2-1 Schematic Drawing of Bases and Pipeline	2-2
2-2 As-Built Pipe Dimensions--Phase I Tests	2-4
2-3 As-Built Pipe Dimensions--Phase II Tests	2-5
2-4 Thick Walled Tube at Ends of Test Pipeline	2-6
2-5 Box Frame Midpoint Support for Phase I Testing	2-10
2-6 Dimensions and Properties of Links Used in Phase II Testing	2-11
2-7 Midpoint Support Installed--Phase II Testing	2-13
2-8 Midpoint Support Installed--Phase III Testing	2-14
2-9 Basic Structure of Bases That is Generally Common to All Bases	2-16
2-10 Base Excitation System Flow Chart	2-17
2-11 Data Acquisition/Instrumentation Flowchart	2-20
2-12 Typical Arrangement of Strain Gages	2-22
2-13 Low-Level Base Input--Phase I Earthquake	2-35
2-14 Low-Level Base Input--Phase II Earthquake	2-37
2-15 Low-Level Base Input--Phase III Earthquake	2-39
3-1 Stress Ratio (Elbow at Point 3.0) for Just Below Level D Test--Grinnell Snubber	3-14
3-2 Stress Ratio (Elbow at Point 3.0) for Highest Level Test--Grinnell Snubber	3-15
3-3 Stress Ratio (Elbow at Point 3.0) for Level D Test--Bergen-Paterson Snubber	3-16
3-4 Stress Ratio (Elbow at Point 3.0) for Highest Level Test--Bergen-Paterson Snubber	3-17
3-5 Level D (for Elbow at Point 3.0) Base Motion Spectrum Compared to Highest Level Test With ITT Grinnell Snubber	3-19

<u>Figure</u>	<u>Page</u>
3-6 Level D (for Elbow at Point 3.0) Base Motion Spectrum Compared to Highest Level Test With Bergen-Paterson Snubber	3-20
3-7 Comparison of Actual and Scaled Relative Displacement for Point 3.0Z	3-27
3-8 Comparison of Actual and Scaled Relative Displacement for Point 3.0Z	3-29
3-9 Schematic Representation of Displacement Time Histories for Step-Loading Tests	3-32
3-10 Example of Change in Peak Response Due to Complete Break of Midpoint Support	3-38
3-11 Snubber Failure Test With PSA-1/4 Snubber	3-41
3-12 Snubber Failure Test With Weak Strut 2	3-42
3-13 Snubber Failure Test With A/D-40 Snubber	3-44
3-14 Attempted Snubber Failure Test With ITT Grinnell Snubber	3-45
3-15 Attempted Snubber Failure Test With Bergen-Paterson Snubber	3-46
3-16 Final Position and Shape of Pipeline After High-Level Earthquake Test (T1R7B)--Bergen-Paterson Snubber Used	3-48
A-1 Locations for Pipe Wall Thickness Measurements--Phase I Pipeline	A-4
A-2 Locations for Pipe Wall Thickness Measurements--Phase II Pipeline	A-5
B-1 Accelerometer, Displacement, and Pressure Transducer Locations--Phase I Tests	B-2
B-2 Strain Gage Locations--Phase I Tests	B-3
B-3 Accelerometer, Displacement, Force, and Pressure Transducer Locations--Phase II Tests	B-4
B-4 Strain Gage Locations--Phase II Tests	B-5
B-5 Accelerometer, Displacement, Force, and Pressure Transducer Locations--Phase III Tests	B-6
B-6 Strain Gage Locations--Phase III Tests	B-7

<u>Figure</u>	<u>Page</u>
C-1 End View of Z-Bend Piping System (as seen from Point 1.0)	C-2
C-2 Overall View of Z-Bend Piping System	C-3
C-3 Z-Bend Boundary Conditions	C-4
C-4 Midpoint Support	C-5

TABLES

<u>Table</u>	<u>Page</u>
2-1 Material Properties for Pipeline	2-7
2-2 Pipe Supports Used During Pipe Test Program	2-9
2-3 Description of Snubbers Used in Testing	2-12
2-4 Typical Postprocessing of Data	2-21
2-5 Comparison of Maximum Stress Ratios by Code Edition for 4-Inch Schedule 40 Piping, TLR6C Results	2-25
2-6 Phase I Tests Conducted	2-27
2-7 Phase II Tests Conducted	2-28
2-8 Phase III Tests Conducted	2-31
3-1 Peak Base Motion and Peak Pipe Response for Tests Without Planned Support Failure (earthquake base motion only)	3-2
3-2 Peak Base Motion and Peak Pipe Response for Tests With Planned Support Failure (earthquake base motion only)	3-5
3-3 Amplification Factor--Phase I Earthquake	3-9
3-4 Amplification Factor--Phase II Earthquake	3-10
3-5 Amplification Factor--Phase III Earthquake	3-11
3-6 Tests for Which Comparisons Were Made Between Level D Input and Highest Level Input	3-18
3-7 Comparison of Level D Base Input Spectral Amplitude With That for the Highest Level Test	3-21
3-8 Natural Frequencies for Support Configurations	3-24
3-9 Average Log Decrement Damping (First Mode) as a Function of Excitation Level and Free Vibration Cycle Number	3-33
3-10 Log Decrement Damping (First Mode) Obtained for Point 3.0Z Displacement Channel	3-35
3-11 Earthquake Tests Inducing Pipe Support Failure	3-39

Table

Page

A-1	Pipe Wall Thickness Measurements--Phase I Pipeline
A-2	Pipe Wall Thickness Measurements--Phase II Pipeline

A-2
A-3

SUMMARY

This report presents the methodology used and the results thereof of a laboratory research program investigating the dynamic response of pressurized piping and response levels up to and above-pipeline yield. The four-inch Schedule 40 piping system studied was mounted on three moving supports simulating seismic inputs to the piping system. The middle pipe support was varied to include typical pipe restraint hardware in the test program.

The limited testing conducted demonstrated the feasibility of executing, in a laboratory environment, multiple support excitation experiments inducing severe piping dynamic response. In addition, test data were generated for a relatively simple piping system for benchmarking both linear and nonlinear calculational tools. The data include the case of intentionally induced support failure in the course of dynamic loading.

The tested piping systems successfully withstood repeated earthquake-like loading at input levels three to five times those necessary to just exceed the ASME Class 2 Level D stress limit for primary loads. Even with mid-point support failure, piping pressure integrity was maintained. The tests demonstrated the difficulty of inducing pressurized piping failure (leakage or plastic collapse) with dynamic loads and provided limited evidence of the large safety margins that are believed to exist for nuclear power plant piping subjected to seismic loads.

In addition, the seismic testing of the piping indicated that the snubber hardware used had apparent failure loads that were two to four times the manufacturer's specified allowable load. Piping system damping was observed to range from about two percent to four percent of critical, generally increasing somewhat with response amplitude and varying with support type. The observed damping was at least twice the one percent used in U.S. design

practice for the Operating Basis Earthquake for four-inch piping, and up to twice the damping currently used for the Safe Shutdown Earthquake condition.

Subsequent extension of the work has included a large increase in dynamic capacity of the hydraulic drive system and erection and testing of a four- and five-support, fully three-dimensional layout of a six-inch and/or eight-inch Schedule 40 piping system with and without branch lines.* Included in the planned testing have been investigations of damping as a function of support design at response levels at and above the Operating Basis Earthquake and Safe Shutdown Earthquake stress limits.

* A joint EPRI/NRC research program

Section 1

INTRODUCTION

This report summarizes the results of multiple support excitation tests of a four inch Schedule 40 piping system excited to response levels up to and exceeding that required to achieve permanent deformation in the piping material.

Experimental objectives included:

- demonstrating the feasibility of executing high-amplitude, multiple-support excitation studies of a piping system of moderate size,
- obtaining elastic response benchmark data for a pressurized piping system with various piping support conditions,
- obtaining nonlinear response benchmark data for pressurized piping driven well above piping elastic response limits, including the case of support failures and
- a limited demonstration of piping design margins for dynamic loads by exciting the piping system to response levels which were multiples of those accepted for ASME Code Class 2 design.*

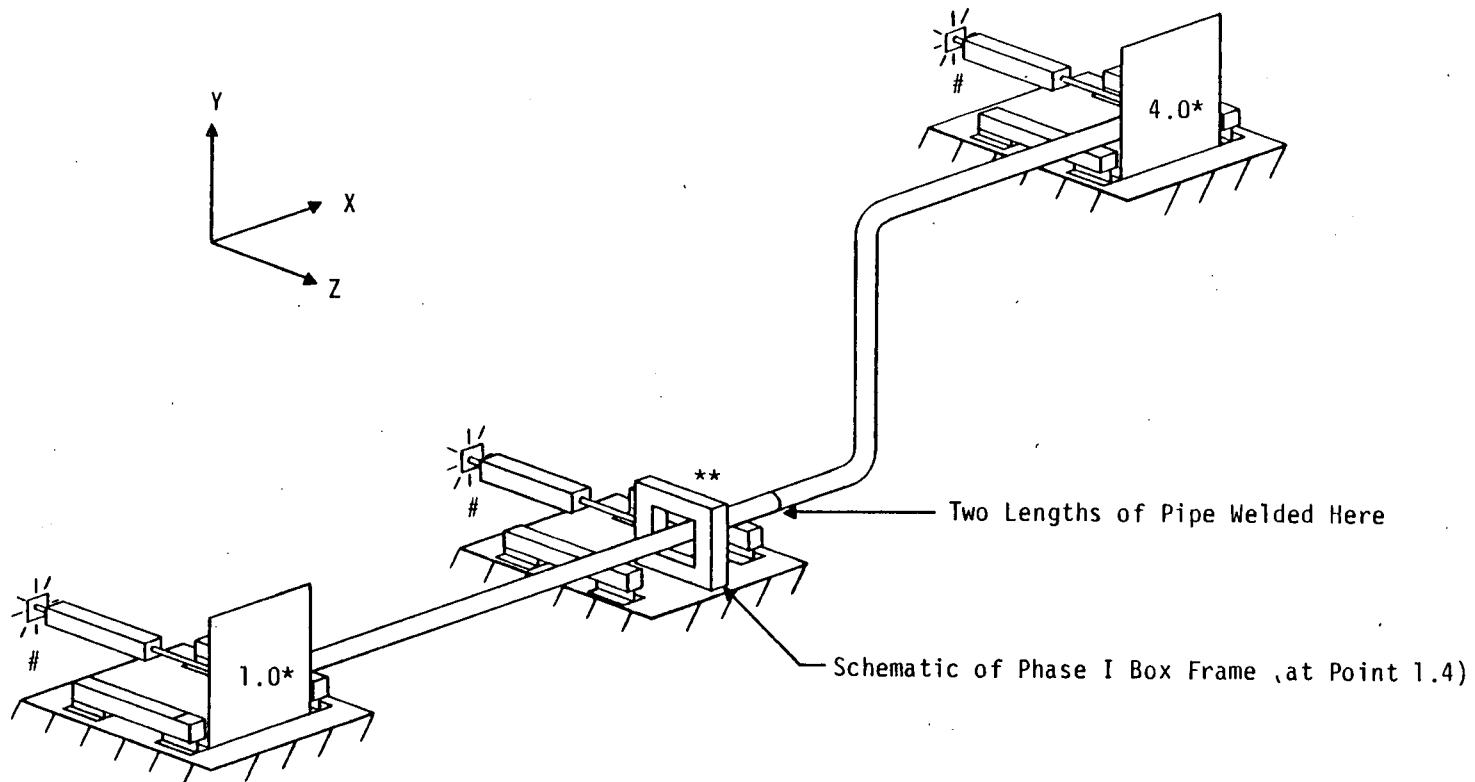
The work reported herein was motivated, in part, by the desire to examine the postulate that the dynamic design margins of nuclear power plant piping systems are very large. Very little data exist, however, regarding piping dynamic response characteristics and capacity for loading near and well above accepted design limits. Static test results appear to form the basis for current design criteria. The tests described herein provide some of the data necessary for a reassessment of piping design criteria for cyclic dynamic loads. In addition, apparent piping system damping values are reported herein as a function of support type and response amplitude.

*The term "Code" refers to Section III of the ASME Boiler and Pressure Vessel Code, Division 1.

The selected test specimens were two separate 20-ft (6-m) water-filled runs of ASTM A-106 Grade B carbon steel 4-in. Schedule 40 piping. The piping layout was a Z-shape in a vertical plane with two elbows and with two or three supports. Dynamic inputs were applied to the piping through the motion of the piping supports, which were in turn driven by hydraulic actuators providing earthquake-like excitation to the support hardware.

The piping runs were excited to various peak response levels while at the Code allowable working pressure (at room temperature) of 1,500 psig (10.3 MPa). The two identical piping runs were tested in several phases as the work scope was expanded to include testing of various supports. The first piping specimen was tested in Phase I and the second in Phases II and III. High-level dynamic loads above the elastic range of the piping material and above the ASME Class 2 Level D stress limit (i.e., the stress limit typically used for the Safe Shutdown Earthquake [SSE] design condition) were induced in the piping system.

The various piping systems, including the types and sizes of supports, that were tested are described in Section 2. Also discussed in that section are (1) the instrumentation used, (2) the method used to acquire test data, and (3) the possible types of data analysis that could be done. Section 3 presents a summary of the test results. The data analysis results are given. Such items as maximum response levels achieved, systems nonlinearities, support influence, and damping are discussed. Finally, Section 4 contains the conclusion.



- * Pinned Supports at Points 1.0 and 4.0
- ** Variable Support at Point 1.4
- # Actuators at Points 1.0, 1.4, and 4.0

Figure 2-1. Schematic Drawing of Bases and Pipeline

Section 2

PIPING SYSTEMS AND TESTING METHODS

One pipeline layout, including pipe end boundary conditions, was used for all the tests. The pipeline was replaced once during the testing. The pipe midpoint support was varied during the test program and included as hardware a box frame, a strut, a mechanical snubber, a hydraulic snubber, and the case of no support at all.

The method of exciting the pipe was identical in all testing. The pipe was driven by hydraulically moving the bases (sleds) to which the piping was attached--i.e., base motion was used. There were three bases which were used to support the piping system. These were each given approximately the same motion.* The moving bases translated on rails which in turn were anchored to a concrete foundation.

The pipeline/mid-support was instrumented with a variety of transducers; signals from them were digitized and stored (on a magnetic medium) using a computer-based data acquisition/analysis system. The data obtained during the testing were used to help guide the direction of the test program.

In the following subsections, the topics discussed above will be expanded upon, and some additional topics will be covered.

2.1 Piping Layout/Properties And Pipe End Boundary Conditions

The pipeline layout consisted of three straight lengths of pipe and two elbows (see Figure 2-1). The piping system was in a flat plane which was nearly vertical.** The pipeline was attached to the bases (one-dimensional

* Drive signals were identical, but the hydraulic drive system could not produce the commanded motion at each base with perfect fidelity.

** The plane normal of the piping system was rotated approximately five degrees above the +Z axis.

shake tables) at Points 1.0 and 4.0 using pin connections (to be discussed later). It was supported at Point 1.4 (called the pipe midpoint) using a one-dimensional support between the pipe and base. This support was in the Z (horizontal) direction. (This is discussed in Section 2.2.)

There were three phases of testing (Phases I through III). The pipeline for Phases I and II was virgin material, and the pipeline for Phase III was that used for Phase II. As-built drawings of the essentially identical pipelines are presented herein (see Figures 2-2 and 2-3) and include instrumentation locations. Both pipelines were about 21 ft (6.4 m) long and had 90-degree elbows each with a radius of curvature of 9 in. (22.9 cm). The pipelines were made out of two straight lengths of pipe. One length of pipe was bent in two places to form the two elbows. The bends were made in such a way that essentially no ovalization occurred.

The pipelines were constructed of 4-in. Schedule 40 pipe; the outside diameter and wall thickness* were nominally 4.50 in. and 0.237 in., respectively. For all tests the piping was filled with water at room temperature and 1500 psig pressure, producing a weight per unit length of pipe plus water of 16.3 lbm/ft (24.3 kg/m).

To ensure that the material at the pipeline ends remained elastic during testing, thus permitting loads extraction from strain gage measurements, additional pipe lengths were added at both ends in order to reinforce the test specimen (Figure 2-4).

The material used for both Phase I and II pipelines was ASTM A106 Grade B carbon steel; the material properties reported by the manufacturer are given in Table 2-1.

* Appendix A tabulates piping wall thickness measurements for both pipelines tested.

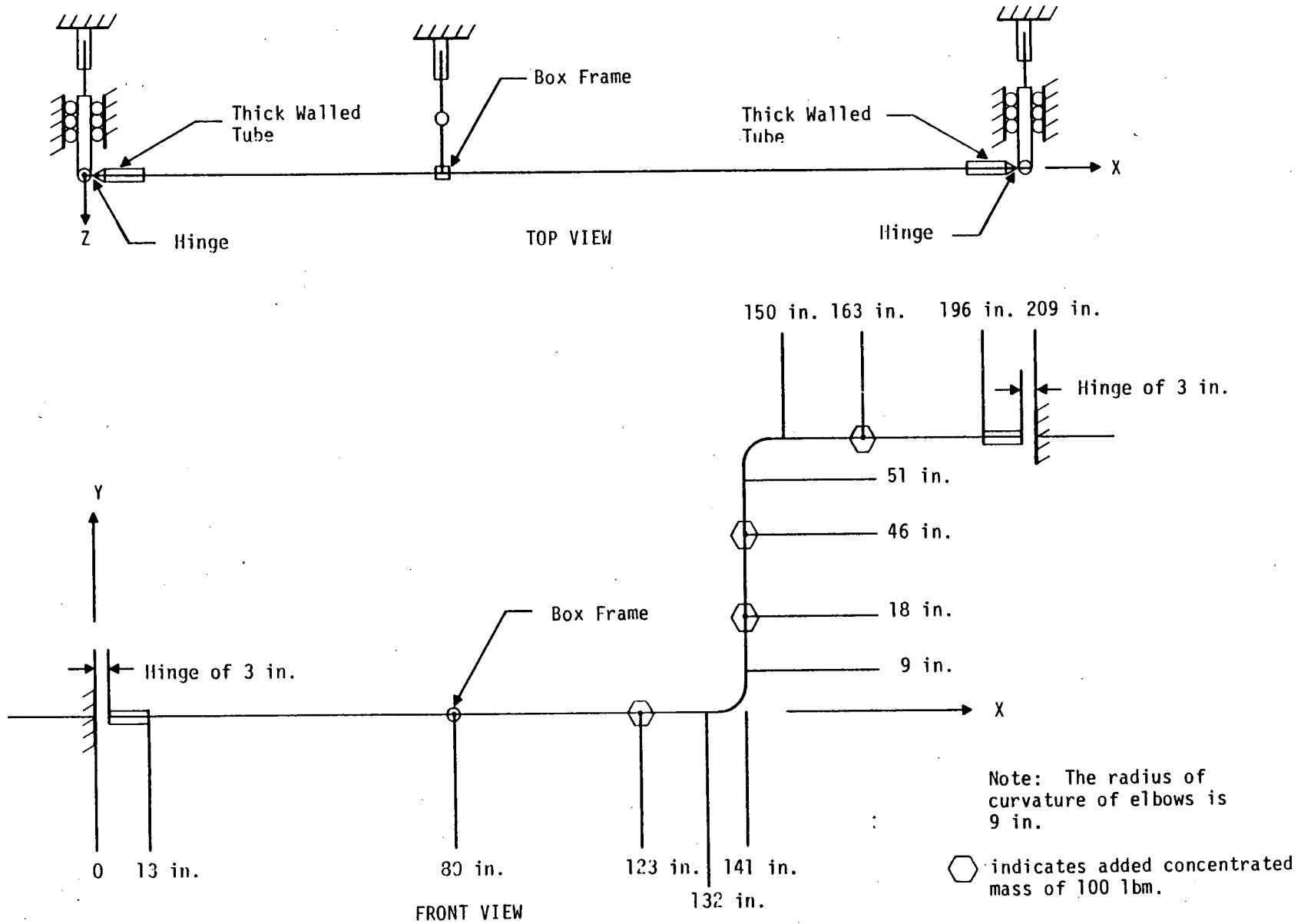
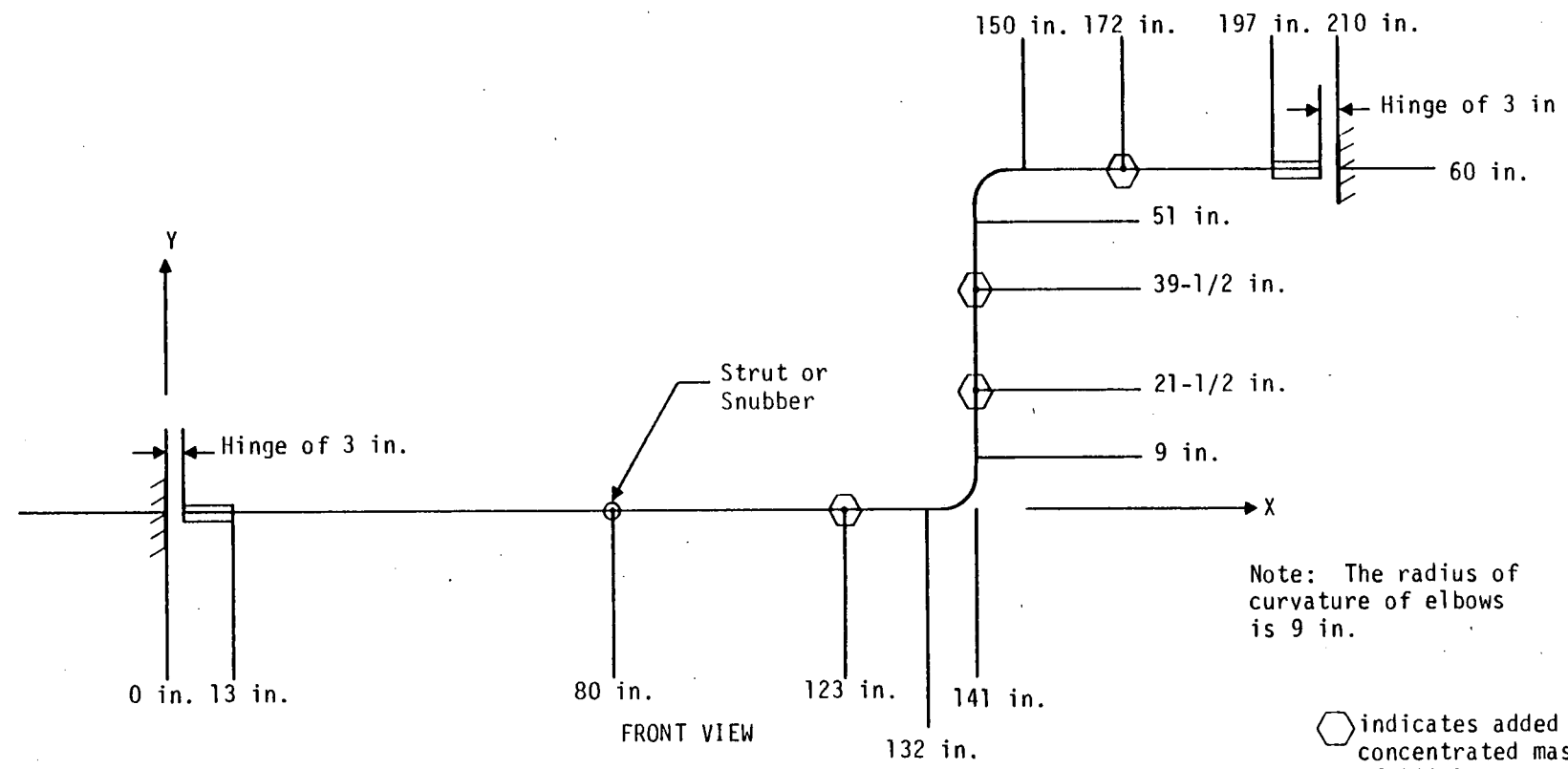
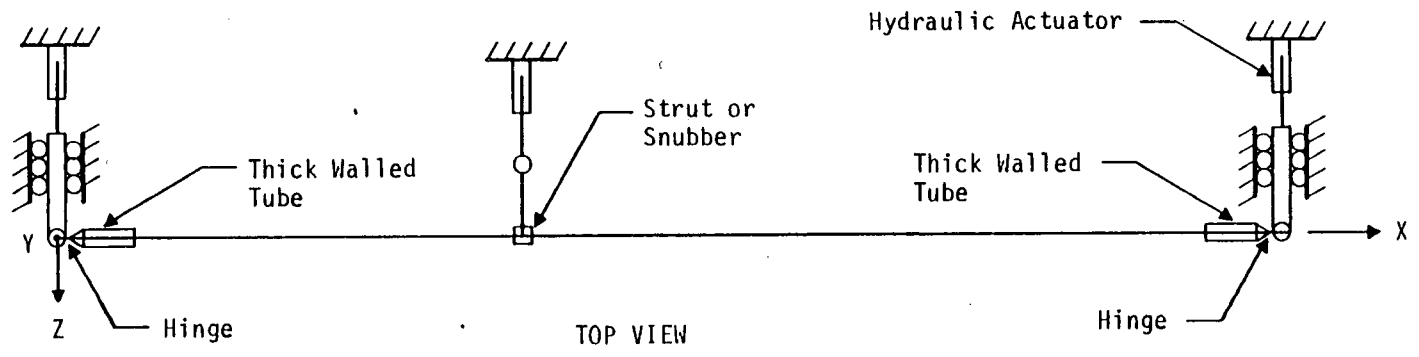


Figure 2-2. As-Built Pipe Dimensions--Phase I Tests



Note: The radius of curvature of elbows is 9 in.

⬡ indicates added concentrated mass of 100 lbm.

Figure 2-3. As-Built Pipe Dimensions--Phase II Tests

2-5

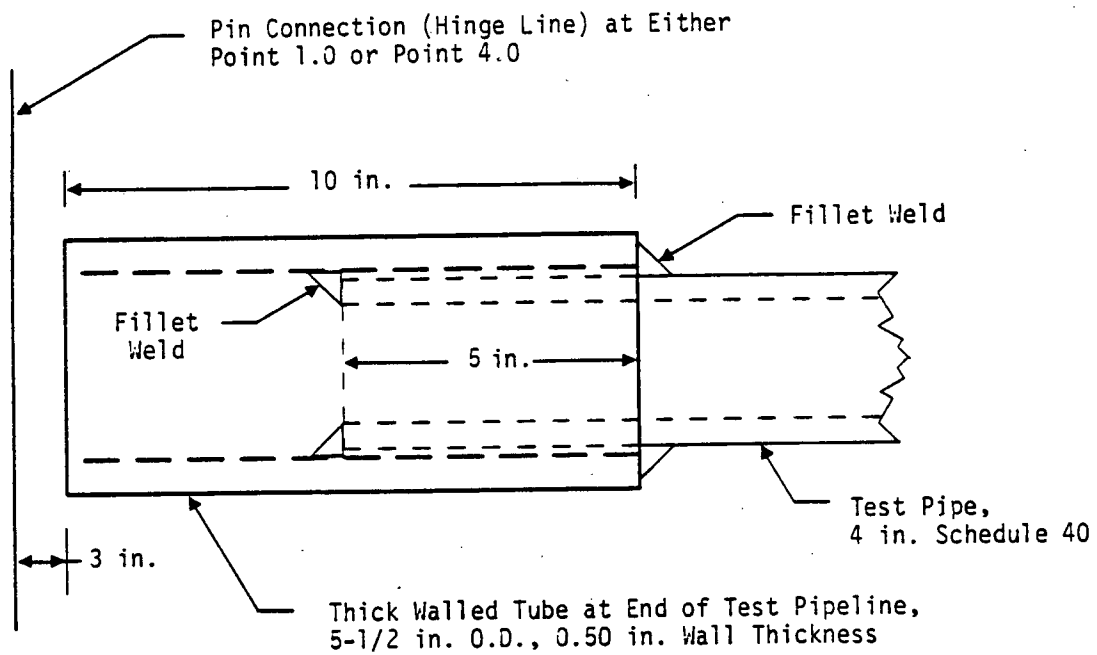


Figure 2-4. Thick Walled Tube at Ends of Test Pipeline

Table 2-1
MATERIAL PROPERTIES FOR PIPELINE

<u>Pipe Segment</u>	<u>Yield Point (psi)</u>	<u>Ultimate Strength (psi)</u>	<u>Percent Elongation</u>
Phase I Pipe			
1. Test pipe, Point 1.0 to weld	45,300	73,000	35.0
2. Test pipe, weld to Point 4.0	45,300	73,000	35.0
Phase II Pipe			
1. Test pipe, Point 1.0 to weld	49,800	75,100	38.0
2. Test pipe, weld to Point 4.0	45,300	73,000	35.0
<u>Tube at Pipe Ends</u>	<u>Brinell Number</u>	<u>Hardness</u>	
Phase I	**	**	
Phase II	207	J57-6 J55-8	

* These are the thick walled tubes at the ends of the test pipe (reference Figure 2-4). The yield point, ultimate strength, and percent elongation were not available for the thick walled tube.

** These values were not obtained; however, they are probably the same as those for Phase II.

As mentioned previously, the pipeline ends were attached to the bases (at Points 1.0 and 4.0) through pin connections, allowing rotation about only a vertical axis. The pipe ends were constrained, relative to the pipe end bases, for the remaining five degrees-of-freedom. That is, the end bases could transmit, to the pipe ends, a pipe axial load, two perpendicular shear forces, a moment about the Z axis, and a torsional moment about the X axis. The moment about the Y axis would be zero at both pipe ends.

2.2 Piping Midpoint Support

The midpoint support provided the interface between the pipe (at Point 1.4) and corresponding base. The sled provided the frame to which the support could be anchored at one end. The other end of the support was anchored to the pipe. (In the case of the Phase I tests, the support [box frame] was not attached to the pipe, but surrounded it.) When the midpoint base was driven (moved) by its hydraulic actuator, the base in turn drove one end of the midpoint support. The support then drove the pipe.

A variety of supports were used for the tests, as summarized in Table 2-2. The box frame, used for Phase I, is described by Figure 2-5. This type of support was selected because it is used, in some cases, for similarly sized piping. The struts used for the Phase II tests are described in Figure 2-6. The strut stiffnesses were chosen to vary from being much greater than prototypical values to somewhat less than prototypical values. Some of the properties of the snubbers (shock arrestors) used for Phase II and III testing are described in Table 2-3.

The method used to install the supports was different for each phase of testing. The box frame for Phase I was installed simply by welding its bottom surface to the midpoint sled. The midpoint supports for Phases II and III were installed as shown in Figures 2-7 and 2-8, respectively. The supports were held into place by pin connections at both of their ends. For the Phase II tests the pins used for the connections, were Strainert load cell clevis pins. Where necessary, the ends of the supports were modified so the load cells (1 in. in diameter) would fit through them. For the

Table 2-2

PIPE SUPPORTS USED DURING PIPE TEST PROGRAM

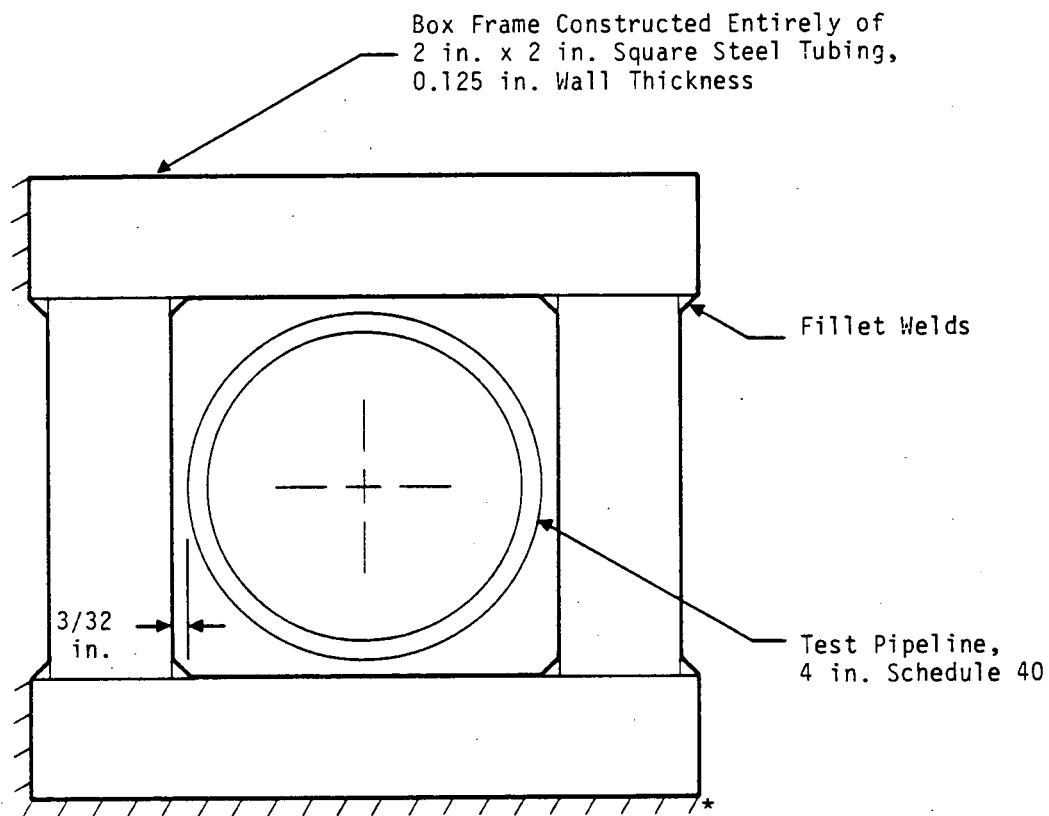
<u>Phase</u>	<u>Box Frame</u>	<u>Struts</u>	<u>PSA-1*</u>	<u>PSA-1/4*</u>	<u>AD-40**</u>	<u>ITT Fig. 200#</u>	<u>BP2525-3##</u>
I	x						
II		x	x	x			
III				x	x	x	x

* Pacific Scientific mechanical shock arrester

** Anchor/Darling mechanical shock arrester

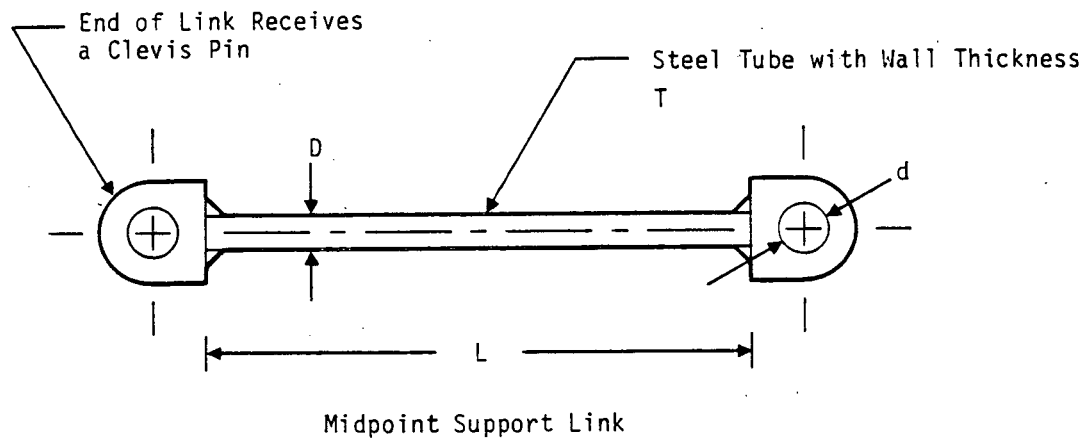
ITT Grinnell hydraulic shock arrester

Bergen-Paterson hydraulic shock arrester



* These surfaces welded to pipe midpoint base.

Figure 2-5. Box Frame Midpoint Support for Phase I Testing



Link-Type Support	L (in.)	D (in.)	T (in.)	d (in.)	P_u (lbf)*
Rigid	16	1.00	0.250	1.0	31,000
Weak Link 1	16	0.50	0.028	1.0	2,900
Weak Link 2	16	0.75	0.035	1.0	5,500

* Ultimate load for the support. It is based on an ultimate strength of 70,000 psi.

Figure 2-6. Dimensions and Properties of Links Used in Phase II Testing

Table 2-3

DESCRIPTION OF SNLBBERS USED IN TESTING

<u>Manufacturer Model</u>	<u>Type</u>	<u>Midspan Length (Pin-to-Pin) (in.)</u>	<u>A/B (Design(Load (lbf)</u>	<u>C/D Load (lbf)</u>
Pacific Scientific PSA-1	Mechanical	17.0	1,500	2,100
Pacific Scientific PSA-1/4	Mechanical	12.10	350	500
Anchor/Darling AD-40	Mechanical	10.50	400	530
Bergen-Paterson BP2525-3	Hydraulic	25.75	3,000	4,000
ITT Grinnell FIG 200	Hydraulic	17.3125	3,000	4,000

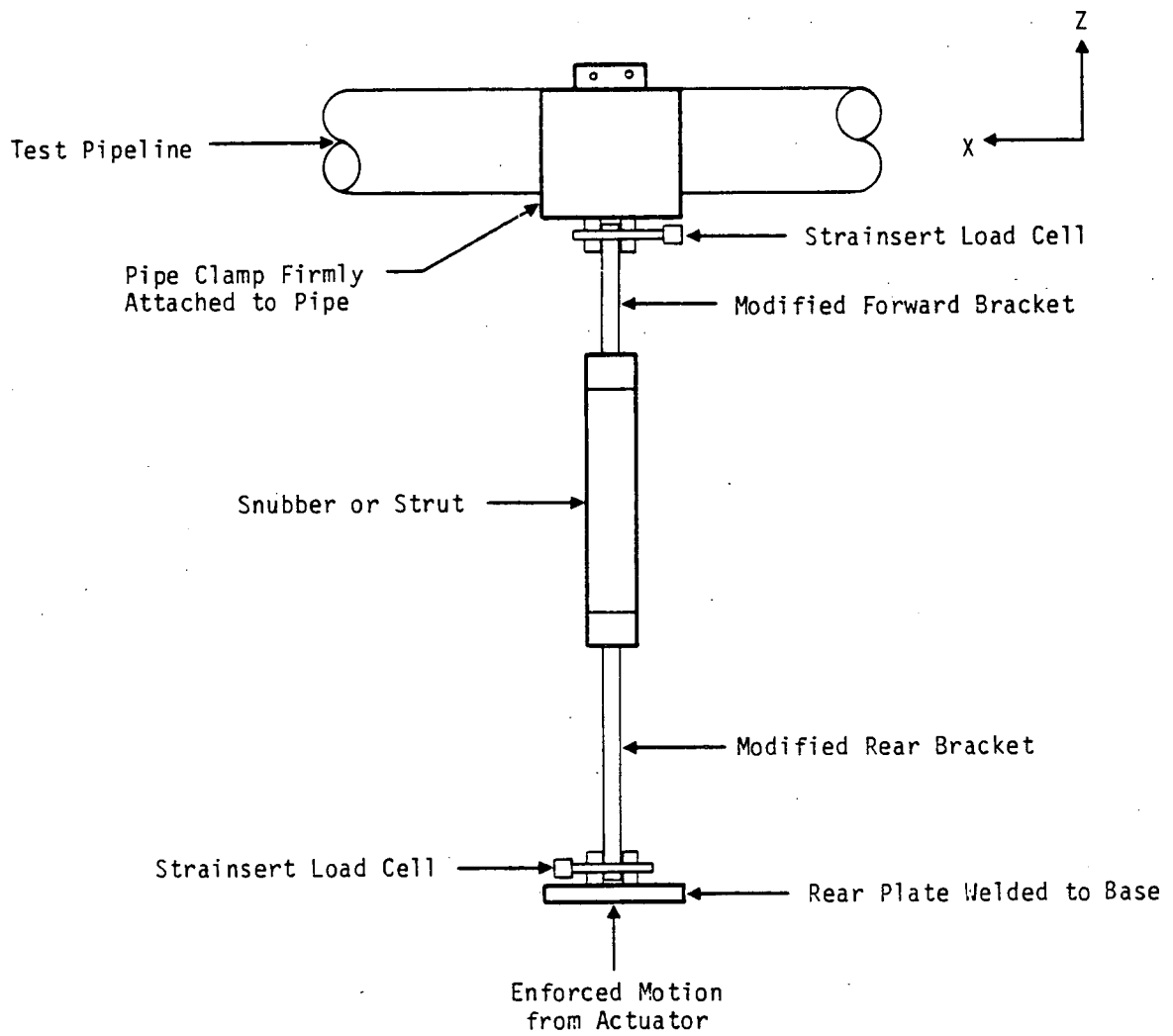


Figure 2-7. Midpoint Support Installed--Phase II Testing

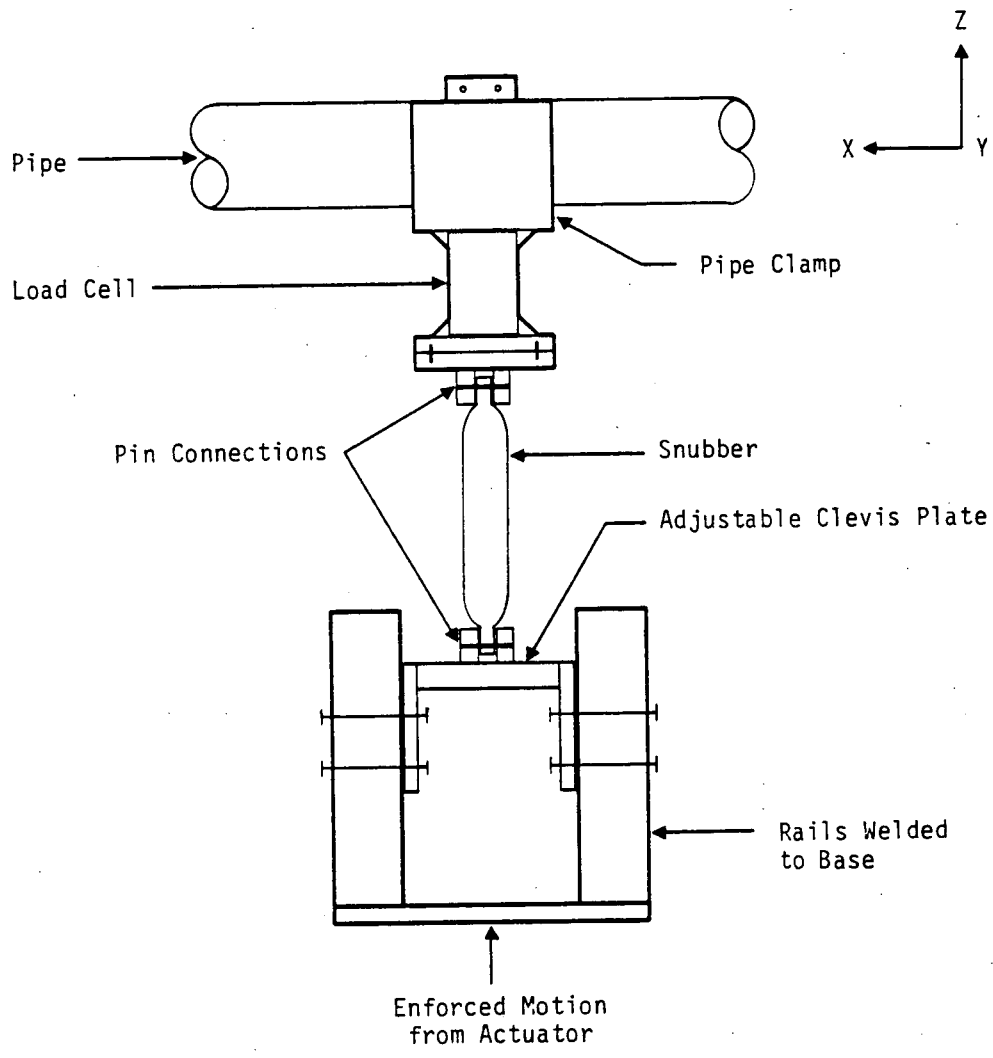


Figure 2-8. Midpoint Support Installed--Phase III Testing

Phase III tests, the connection pins used were steel rods (dowels); they were not load cells. This is because all of the snubber hardware would have required customization to accept the load cells, and this was undesirable. Instead, a load cell was fabricated from square steel tubing by instrumenting it with strain gauges so that the axial load in it could be determined.

2.3 Bases Used for Base Motion

A base consisted of a very stiff welded frame supported by four linear bearings (reference Figure 2-9). There was a bearing at each corner of the base. The bearings rode on two circular steel shafts, with the shafts supported by a common steel plate. The steel plate in turn was bolted to a reinforced concrete foundation. The pipe end bases each incorporated the pin connections for the pipe. The pipe midpoint base included the necessary mating piece for the midpoint support.

2.4 Hydraulic Actuator System For Driving The Bases

Each of the bases was driven by its own hydraulic actuator. The 11,000-lbf capacity actuators were servo-controlled extending or contracting in proportion to a supplied displacement signal and were driven by a 25-gpm, 3,000-psi hydraulic power supply. Four 10-gallon accumulators provided smooth rates of flow (of hydraulic fluid) and ensured adequate supply pressure during dynamic events. A flow chart of the sled excitation system is shown in Figure 2-10.

The base motion acceleration time histories are stored in digital format on a Data General NOVA3 minicomputer. The time history to be used for a test is transferred through a digital-to-analog (D/A) converter and stored on FM tape. During a test, the analog time history was reproduced by the FM recorder, and the signal was conditioned and filtered prior to its insertion into the actuator controllers. A strip chart recorder with built-in medium gain amplifiers was used for monitoring purposes.

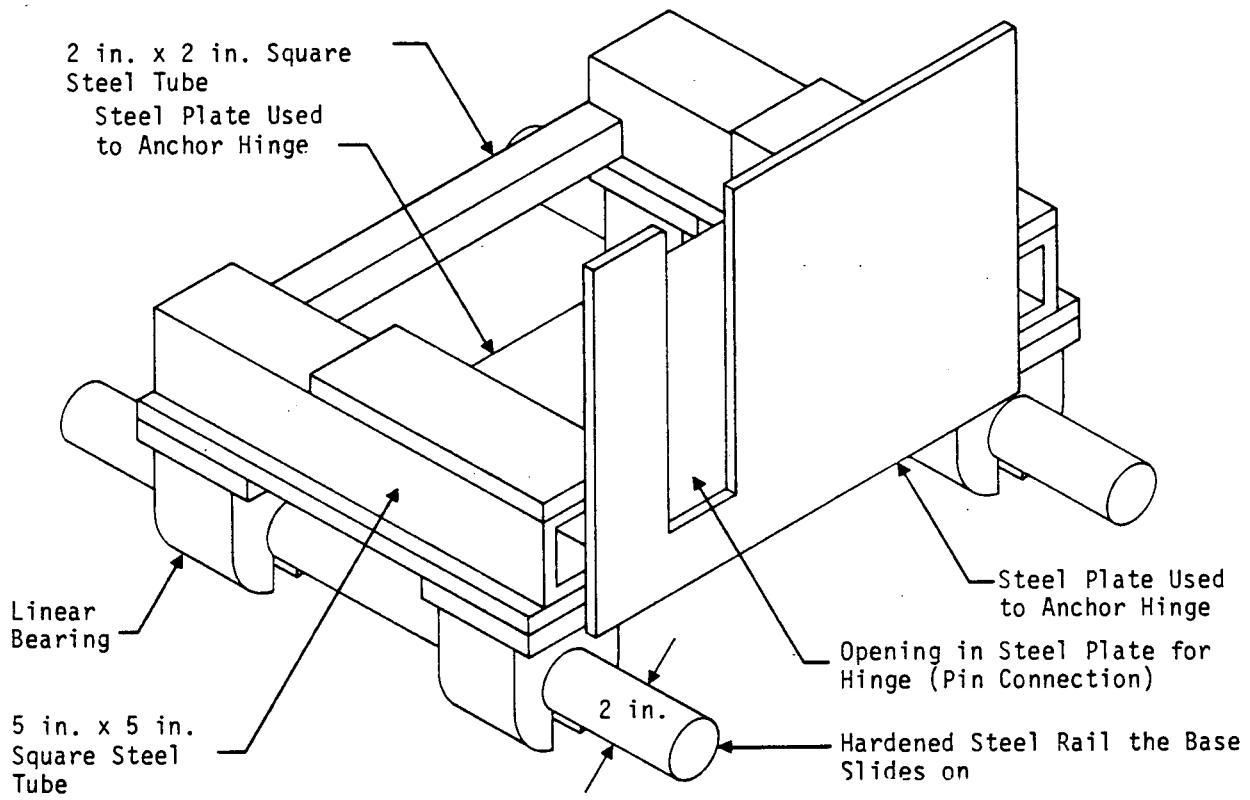


Figure 2-9. Basic Structure of Bases That is Generally Common to All Bases

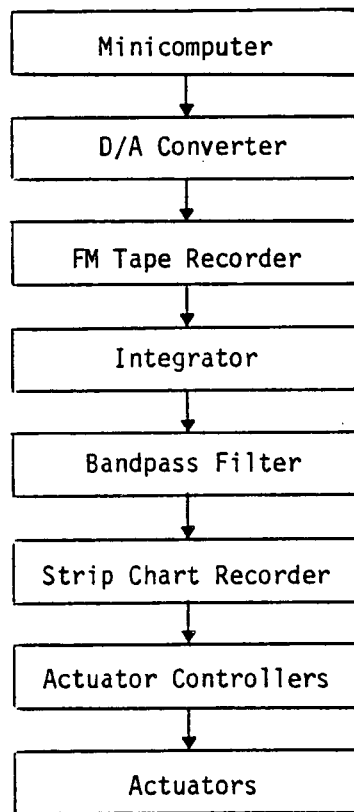


Figure 2-10. Base Excitation System Flow Chart

2.5 Instrumentation

For Phase I testing, forty-eight channels of data were obtained using piezoelectric accelerometers, bonded strain gauges, and displacement transducers. Phase II testing incorporated the use of fifty-two channels, with the inclusion of two load cells and one pressure transducer. (For some tests an additional accelerometer channel was added.) The instrumentation used for Phase III testing was similar to that for Phase II, with the exception that some of the strain gauges were oriented differently, and only one load cell (at Point 1.4) was used. All voltage, acceleration, force, and resistance instruments used during calibration had documentation which was traceable to the National Bureau of Standards. Appendix B describes in detail the instrumentation layouts used for the testing.

2.6 Data Acquisition And Analysis

Data acquisition was provided by ANCO's computerized vibration test and analysis system (CVTAS). The system, based on a Data General NOVA-3 mini-computer, consists of the following:

1. 12-slot NOVA-3/12 chassis
2. 256 k-byte memory and CPU
3. 10-Mbyte disk drive with adapter
4. 9-track digital tape system
5. CRT interactive terminal
6. DEC Writer II printing terminal
7. Houston Instruments DP-11 incremental plotter
8. Computer Products Real Time Peripheral (RTP) System with 64 channels of A/D converters and 4 channels of D/A converters
9. 64 channels of STI differential amplifier/anti-aliasing filters

A flow chart of the data acquisition instrumentation used is shown in Figure 2-11.

Analog output from the transducers is low pass filtered, using the STI amplifier-filter system and then is digitized, using the RTP system and the program XFAST. In addition to creating a file containing the digitized test data, XFAST sets up all title, test, and run information and the digitizing time step and time duration of data acquisition as a part of the data file. For Phase I and Phase III testing the following filter/digitizing parameters were used:

- low pass cutoff frequency = 42.6 Hz
- sample rate per channel = 100 data points/s
- duration of acquisition = 20.48 s

For Phase II testing the following parameters were used:

- low pass cutoff frequency = 42.6 Hz
- sample rate per channel = 125 data points/s
- duration of acquisition = 16.384 s

By sampling at 100 points/s or greater, a minimum resolution of 6-8 points per cycle could be obtained for data signals with a dominant (or total) frequency content corresponding to the first two system natural frequencies (7 Hz and 15 Hz). This allowed an accurate determination of the peak response, signal frequency, and log decrement damping. Following execution of a test, the data were corrected for time interval shifts and subsequently processed to generate the categories of information illustrated in Table 2-4.

A few comments need to be made about the calculation of the pipe cross-sectional loads and the ASME stress ratio. Various pipe cross sections were instrumented with strain gauges. An example of a typical arrangement of gauges is given in Figure 2-12. For the strain gauge arrangement in Figure 2-12, it is possible to determine all six

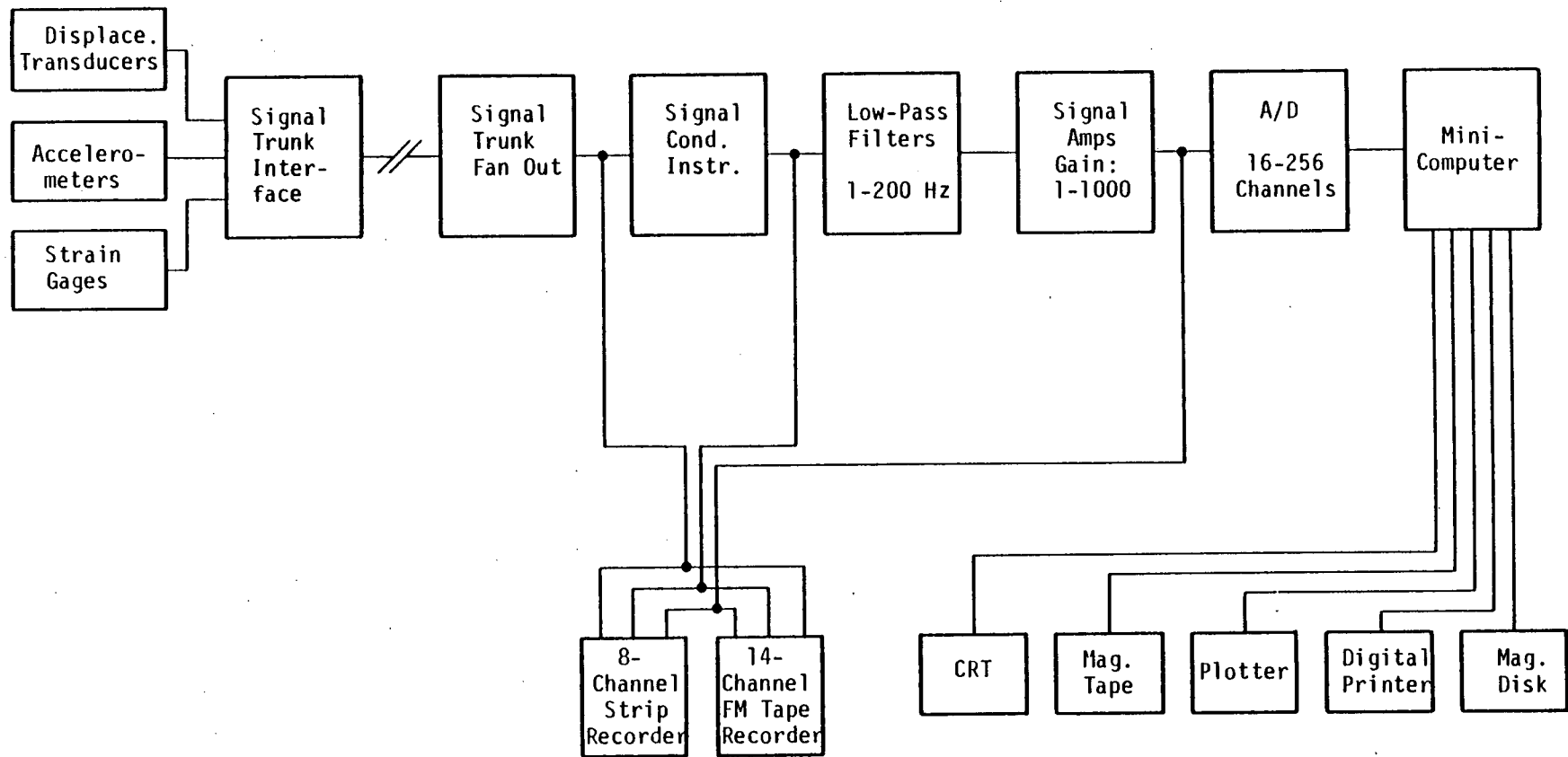


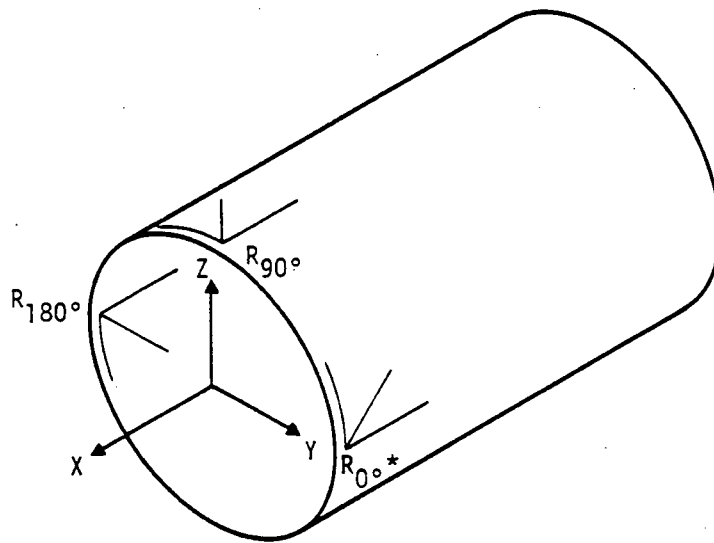
Figure 2-11. Data Acquisition/Instrumentation Flowchart

Table 2-4

TYPICAL POSTPROCESSING OF DATA

<u>Information That Can Be Obtained</u>	<u>Method Used</u>
1. Extreme values of response for each data channel.	Computer code TIMEPEAK* searches channel by channel for maximum and minimum.
2. Time history plots of data.	TIMEPLOT plots transducer amplitude as a function of time.
3. Pipe cross-sectional loads and ASME stress ratio as a function of time.	For pipe cross sections with appropriate strain gage instrumentation, LOADS is used.
4. Principal strains and von Mises ratios for locations on pipe outer surface.	For points on pipe surface with strain gage rosettes, STRESS is used.
5. Fourier transform of transient data.	XFILT is used to obtain transform, and also to filter data and obtain inverse transform.
6. Plot Fourier transform of data.	FOURPLOT plots real and imaginary components or modulus and phase.
7. Response spectrum.	XBETLS and XCETLDP calculates and plots response spectra for accelerometer channels of interest, respectively.
8. Determine time history which is a linear combination of various data time histories; this can be used to determine the relative motion (to the base motion) of the pipe.	LINCOM and TIMEDGEN calculates the new time history and adds header information to the new file, respectively.

* Words with all letters capitalized (e.g., LOADS) refer to computer codes.



* R_θ refers to a strain gage rosette configuration of gages located at θ degrees from the Y axis. The adjacent gages in a rosette are 45° from each other.

Figure 2-12. Typical Arrangement of Strain Gages

cross-sectional loads. For other arrangements, less than six loads can be calculated. (Of course, it is assumed that the pipe material is behaving linearly, so loads can be calculated from strains.) The computer code LOADS is used to calculate stresses from strains. The stresses are then used to calculate cross-sectional loads (e.g., bending moments, shear forces).

Of key importance is the calculation of the two bending moments, M_y and M_z , and the torsion, M_x , at a given pipe cross-section. LOADS does this (given the necessary strain gauges) for each time point of a transient event. It then calculates the resultant sectional moment, $M_1(t)$, from the following:

$$M_1(t) = (M_x^2(t) + M_y^2(t) + M_z^2(t))^{1/2} \quad (2-1)$$

The resultant moment calculated by Equation 2-1, includes the effects of the dynamic response (stresses due to occasional loads, e.g., earthquakes). If the strain gauge settings are not nulled (zeroed) out after pressurization of the pipe, the calculated resultant moment will also include the effect of the pipe internal pressure (a sustained load).

Once having calculated the resultant moment, LOADS then calculates the ASME Code stress ratio using the following equation:

$$SR(t) = S_{OL}(t)/CSL = (B_1(PD_o/2t) + B_2(M_1(t)/Z))/CSL \quad (2-2)$$

where $SR(t)$ = ASME stress ratio (t = time)

$S_{OL}(t)$ = stress due to occasional loads (i.e., earthquake), as calculated by the method described in the ASME Boiler and Pressure Vessel Code*; the stress is due to primary loads

CSL = ASME Code stress limit

$P(t)$ = pipe internal pressure

D_o = outside pipe diameter

t = pipe wall thickness

$M_1(t)$ = resultant cross-sectional moment

* The term ASME Code refers to the ASME Boiler and Pressure Vessel Code, Section III, Division 1.

- Z = section modulus
- B₁ = stress index for pipe pressure term
- B₂ = stress index for moment term

The Winter Addenda of the 1981 edition of the ASME Code for Class 2 piping was used in response evaluations. An important point should be made concerning the resultant moment for Class 2 piping. The computer code LOADS calculates the resultant moment due to any effects seen by the recorded strain data. Thus, if the strain gauge settings are not nulled out before a dynamic test (as was the case for these tests) the calculated resultant moment reflects both the pipe pressure and dynamic effects. However, the stress equation for primary loads for Class 2 piping has its moments in the form $M_A + M_B(t)$, where M_A and M_B are the resultant moments due to sustained and occasional loads, respectively. For the tests performed, the difference between the resultant moments calculated by both approaches was negligible, i.e., M_i was essentially equal to $M_A + M_B$. The values of the constant terms in Equation 2-2, used for calculating the stress ratio, are given as follows:

- D_o = 4.500 in.
- t = 0.237 in.
- Z = 3.220 in.³
- B₁ = 0.088
- B₂ = 2.160
- CSL = 3.0S_h = 45,000 psi (Level D stress limit)

Table 2-5 shows a comparison of stress ratio evaluations for one particular test using two different editions of the code. As may be seen, the Winter 1981 addenda is more restrictive for elbows in the 4-in. Schedule 40 system and less restrictive for straight pipes than was the earlier edition [1].

Table 2-5

COMPARISON OF MAXIMUM STRESS RATIOS BY CODE EDITION
FOR 4-INCH SCHEDULE 40 PIPING, TIR6C RESULTS

<u>Element</u>	<u>Winter 1981 Addenda</u>	<u>1977</u>
Elbow: 4-in. Sch. 40, 9-in. radius of curvature	1.01	0.83
Straight: 4-in. Sch. 40, $D_o = 4.5$ in., $t = 0.237$ in.	0.61	0.76

2.7 Tests Performed and Sample of Input Base Motions Used

Four types of tests were performed for this test series; they were (1) earthquake, (2) base step (all bases were moved simultaneously from one position to another, and then held fixed), (3) sine dwell, and (4) random vibration. All tests were base motion tests. The tests conducted for the three testing phases are listed in Tables 2-6 through 2-8.

Fundamentally different earthquakes (different skyline shapes and frequency content) were used for each of the three phases of testing. For a given phase of testing, the approach used to generate earthquake motion with a desired peak response was to linearly scale up in amplitude a specified (basic) earthquake trace. A specified basic earthquake was used for all the tests for a given phase--the basic earthquake was not varied. One variation from this was for Phase I testing--see Table 2-6. The basic earthquakes used, for the three phases of testing, are given in Figures 2-13 through 2-15. The response spectra corresponding to the input earthquakes are also shown.

The spectra for Phase I and Phase II are somewhat similar in that they have about the same shape. Their shapes were selected so that the first mode would be excited much more than any other mode. The spectrum for Phase III is different from that of the other phases. It was selected to excite the second mode the most. This was done to provide data for support failure where the piping response was radically different than that of the Phase II tests. This gave support failure data for two fundamentally different base excitations.

Table 2-6

PHASE I TESTS CONDUCTED*

<u>Test/Run</u>	<u>Date</u>	<u>Comments</u>
Pressure Only**	9/22/81	No dynamic motion.
1/1	9/21/81	Scaled up basic input.#
1/2	9/22/81	Scaled up basic input.
1/3	9/22/81	Scaled up basic input.
1/4	9/22/81	Bandpass filtered (6 Hz to 8 Hz) basic input, then scaled up.
1/5	9/22/81	Bandpass filtered (6.5-Hz to 6.5+Hz) basic input, then scaled up.

* The midpoint support used for all of these tests was a box frame, which surrounded the pipe. All base motion input was earthquake excitation.

** The pipeline was pressurized to 1,500 psig for this test and all subsequent tests.

The "basic" input was a preselected earthquake trace which was stored on magnetic tape. When the earthquake signal was reproduced, it was amplified and then used in driving the hydraulic actuators.

Table 2-7
 PHASE II TESTS CONDUCTED

<u>Test/Run</u>	<u>Midpoint Support</u>	<u>Base Excitation</u>	<u>Date</u>	<u>Comments</u>
2/1	Rigid Link	Static Base Displacement	12/3/81	The three bases were given a static step displacement--check out of transducers.
2/2	Rigid Strut	Static Test	12/3/81	The load cells were checked out.
2/3	Rigid Strut	Earthquake	12/4/81	Low-level input--bases in phase.*
2/4	Rigid Strut	Earthquake	12/8/81	Low-level input--bases out of phase.**
2/5	Rigid Strut	Base Step	12/7/81	All actuators displaced - 2 in.
2/6	Rigid Strut	Random	12/8/81	Random base input.
2/7C	Rigid Strut	Sine Dwell	12/9/81	Transient data taken at first mode.
2/8	Rigid Strut	Earthquake	12/11/81	Moderate-level input--bases in phase.
2/9	Rigid Strut	Earthquake	12/11/81	Moderate-level input--bases out of phase.
2/10	Rigid Strut	Base Step	12/11/81	All actuators displaced - 1 in.
2/11	Rigid Strut	Random	12/14/81	Moderate-level input.
2/12C	Rigid Strut	Sine Dwell	12/14/81	Transient data taken at first mode.

Table 2-7 (Continued)

PHASE II TESTS CONDUCTED

<u>Test/Run</u>	<u>Midpoint Support</u>	<u>Base Excitation</u>	<u>Date</u>	<u>Comments</u>
3/1	PSA1	Static Pressure	12/17/81	No dynamic motion, internal pressure was 1,500 psig.
3/2	PSA1	Static Base Displacement	12/17/81	Base at Point 4.0 was displaced - 2 in., other bases were not moved.
3/3	PSA1	Base Step	12/17/81	All actuators displaced - 1 in.
3/4B	PSA1	Sine Dwell	12/17/81	Transient data taken at 7.6 Hz.
3/5B	PSA1	Sine Dwell	12/18/81	Transient data taken.
3/6	PSA1	Earthquake	12/21/81	Low-level input--bases in phase.
3/7B	PSA1	Sine Dwell	12/22/81	Transient data taken at 7.6 Hz.
3/8	PSA1	Random	12/24/81	Moderate-level input.
3/9B	PSA1	Sine Dwell	12/24/81	Transient data taken at 7.4 Hz.
3/10	PSA1	Earthquake	12/22/81	Moderate-level input--bases in phase.
3/11	PSA1	Earthquake	12/22/81	High-level input--bases in phase.
3/12	PSA1	Earthquake	12/22/81	Highest-level input--bases in phase.
3/13	PSA 1/4	Earthquake	12/22/81	High-level input--bases in phase.

Table 2-7 (Concluded)

PHASE II TESTS CONDUCTED

<u>Test/Run</u>	<u>Midpoint Support</u>	<u>Base Excitation</u>	<u>Date</u>	<u>Comments</u>
4/1	Weak Strut 1	Static Base Displacement	12/26/81	Base at Point 4.0 was displaced - 1 in., other bases were not moved.
4/2	Weak Strut 1	Base Step	12/26/81	All actuators displaced - 1 in.
4/3	Weak Strut 1	Earthquake	12/26/81	Low-level input--bases in phase.
4/4	Weak Strut 2	Earthquake	12/28/81	Low-level input--bases in phase.
4/5	Weak Strut 2	Earthquake	12/28/81	Moderate-level input--bases in phase.

* "Bases in phase" refers to all three bases moving in the same direction at each point in time.

** "Bases out of phase" refers to one base moving in the opposite direction from that of the other bases.

Table 2-8
PHASE III TESTS CONDUCTED

<u>Test/Run</u>	<u>Midpoint Support</u>	<u>Base Excitation</u>	<u>Date</u>	<u>Comments</u>
1/1	BP*	Base Step	5/1/82	All actuators displaced 0.15 in.
1/2	BP	Base Step	5/12/82	All actuators displaced 0.5 in.
1/3	BP	Base Step	5/12/82	All actuators displaced 1.5 in.
1/4	BP	Earthquake**	5/12/82	Input scaling test.
1/5	BP	Earthquake	5/12/82	Test to generate 50% of A/B load in support.
1/5C	BP	Earthquake	6/1/82	Repeat of Test 1, Run 5.
1/6	BP	Earthquake	5/12/82	Test to generate 100% of A/B load in support.
1/6B	BP	Earthquake	6/1/82	Repeat of Test 1, Run 6.
1/6C	BP	Earthquake	6/1/82	Repeat of Test 1, Run 6.
1/7	BP	Earthquake	5/17/82	Support failure test.
1/7B	BP	Earthquake	6/1/82	Repeat of Test 1, Run 7.
2/1	AD#	Base Step	5/14/82	All actuators displaced - 1 in.
2/2	AD	Base Step	5/14/82	All actuators displaced 0.1 in.
2/3	AD	Base Step	5/14/82	All actuators displaced 0.15 in.

Table 2-8 (Continued)
 PHASE III TESTS CONDUCTED

<u>Test/Run</u>	<u>Midpoint Support</u>	<u>Base Excitation</u>	<u>Date</u>	<u>Comments</u>
2/4	AD	Earthquake	5/14/82	Input scaling test.
2/5	AD	Earthquake	5/14/82	Test to generate 50% of A/B load in support.
2/6	AD	Earthquake	5/14/82	Test to generate 100% of A/B load in support.
2/7	AD	Earthquake	5/17/82	Support failure test.
3/1	ITT##	Base Step	5/13/82	All actuators displaced - 1 in.
3/2	ITT	Base Step	5/13/82	All actuators displaced - 1.25 in.
3/3	ITT	Base Step	5/13/82	All actuators displaced - 1.25 in.
3/4	ITT	Earthquake	5/13/82	Input scaling test.
3/5	ITT	Earthquake	5/13/82	Test to generate 50% of A/B load in support.
3/5B	ITT	Earthquake	5/28/82	Repeat of Test 3, Run 5.
3/5C	ITT	Earthquake	5/28/82	Repeat of Test 3, Run 5.
3/5D	ITT	Earthquake	6/1/82	Repeat of Test 3, Run 5.
3/6	ITT	Earthquake	5/13/82	Test to generate 100% of A/B load in support.

Table 2-8 (Continued)
 PHASE III TESTS CONDUCTED

<u>Test/Run</u>	<u>Midpoint Support</u>	<u>Base Excitation</u>	<u>Date</u>	<u>Comments</u>
3/6B	ITT	Earthquake	6/1/82	Repeat of Test 3, Run 6.
3/6C	ITT	Earthquake	6/1/82	Repeat of Test 3, Run 6.
3/7	ITT	Earthquake	5/17/82	Support failure test.
3/7B	ITT	Earthquake	6/1/82	Repeat of Test 3, Run 7.
4/1	PSA 1/4†	Base Step	5/15/82	All actuators displaced 0.1 in.
4/2	PSA 1/4	Base Step	5/15/82	All actuators displaced 0.13 in.
4/3	PSA 1/4	Base Step	5/15/82	All actuators displaced 0.175 in.
4/4	PSA 1/4	Earthquake	5/15/82	Input scaling test.
4/5	PSA 1/4	Earthquake	5/15/82	Test to generate 50% of A/B load in support.
4/6	PSA 1/4	Earthquake	5/15/82	Test to generate 50% of A/B load in support.
4/7	PSA 1/4	Earthquake	5/17/82	Support failure test.
4/7B	PSA 1/4	Earthquake	6/1/82	Repeat of Test 4, Run 7.
4/8	Rigid Strut	Earthquake	5/17/82	Support failure test.
4/8B	Rigid Strut	Earthquake	6/1/82	Repeat of Test 4, Run 8.

Table 2-8 (Concluded)
 PHASE III TESTS CONDUCTED

<u>Test/Run</u>	<u>Midpoint Support</u>	<u>Base Excitation</u>	<u>Date</u>	<u>Comments</u>
4/9	No Support	Earthquake	5/17/82	Maximum input test.

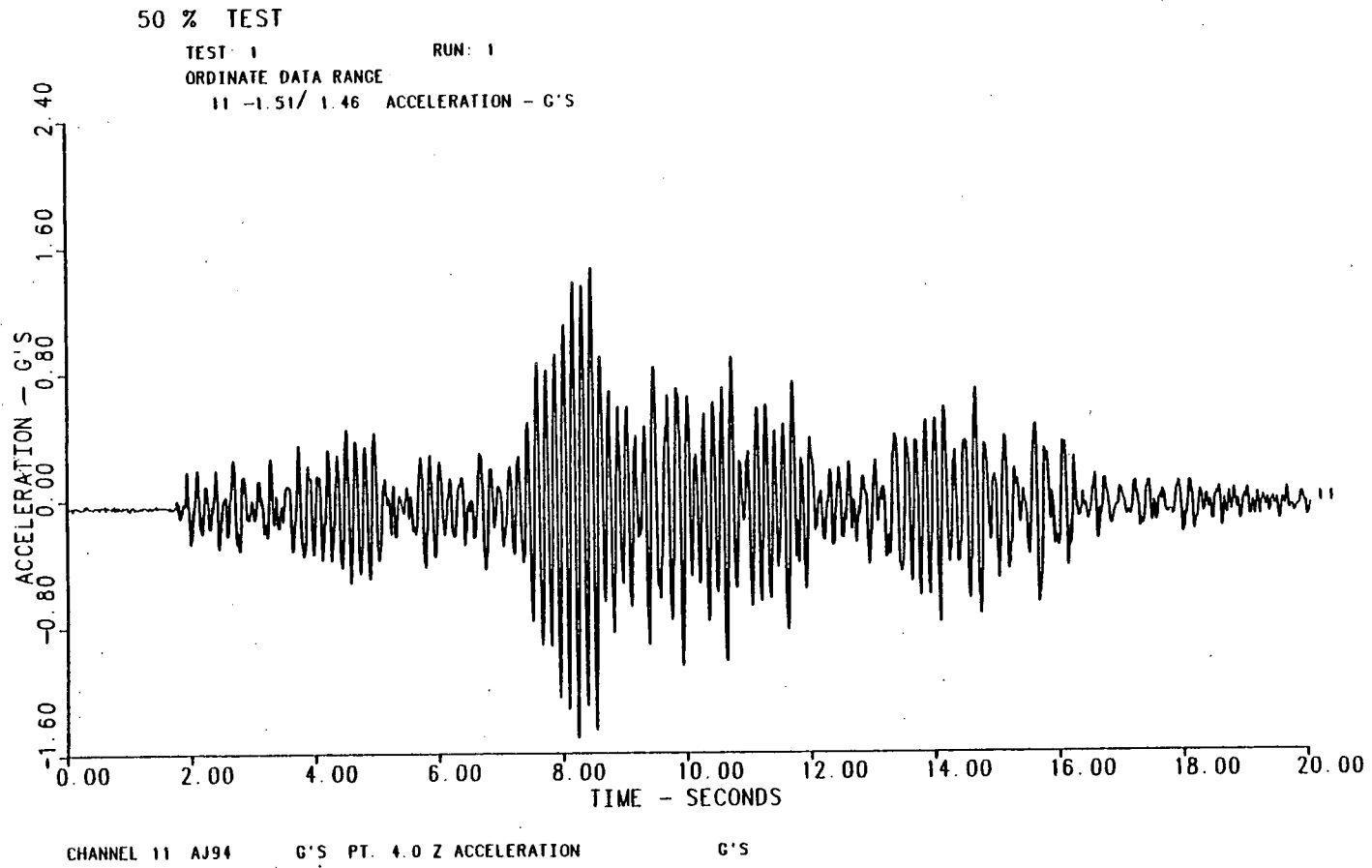
* Bergen-Paterson 2525-3 hydraulic shock arrester.

** All earthquake tests were with in-phase motion of the bases.

Anchor/Darling-40 mechanical shock arrester.

ITT Grinnell Figure 200 hydraulic shock arrester.

† Pacific Scientific 1/4 mechanical shock arrester.



(a) Time History

Figure 2-13. Low-Level Base Input--Phase I Earthquake

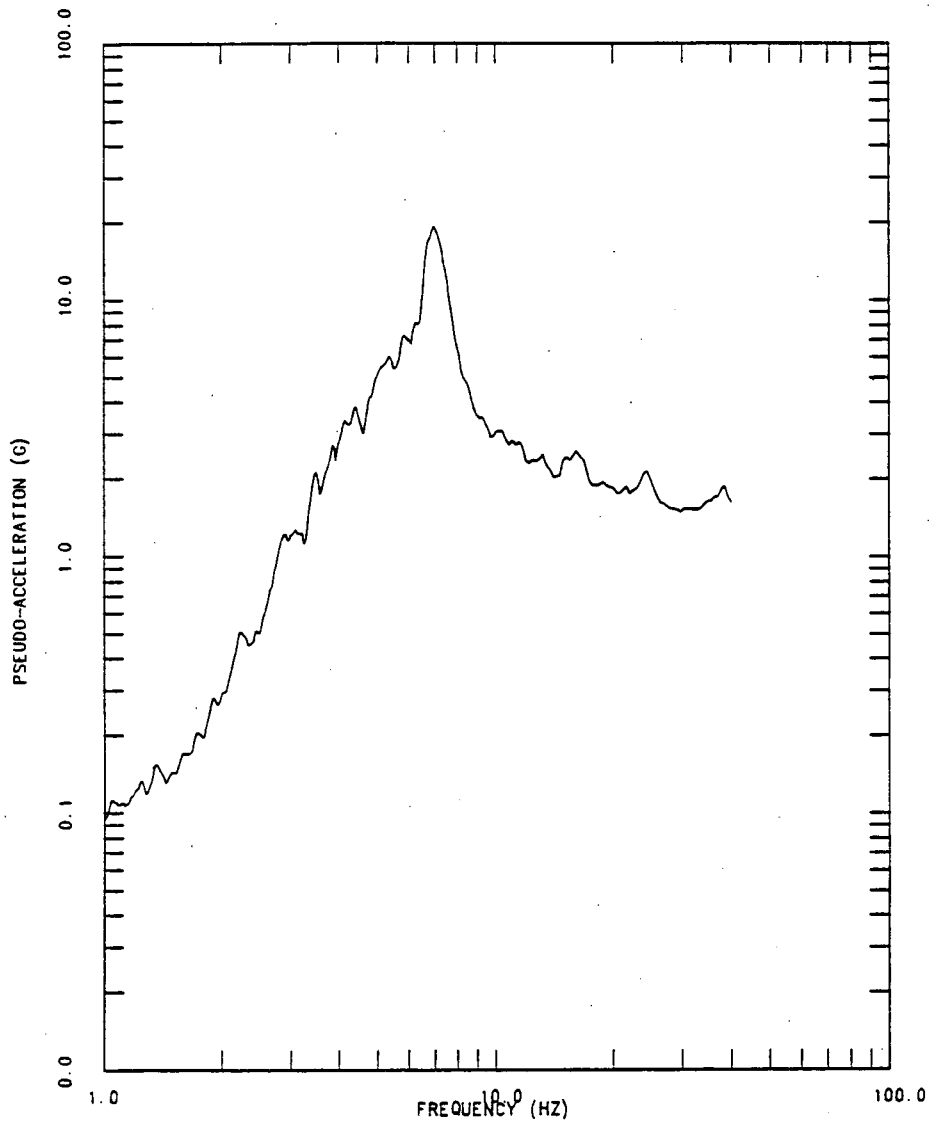
50 % TEST

AJ94 G'S PT. 4.0 Z ACCELERATION

G'S

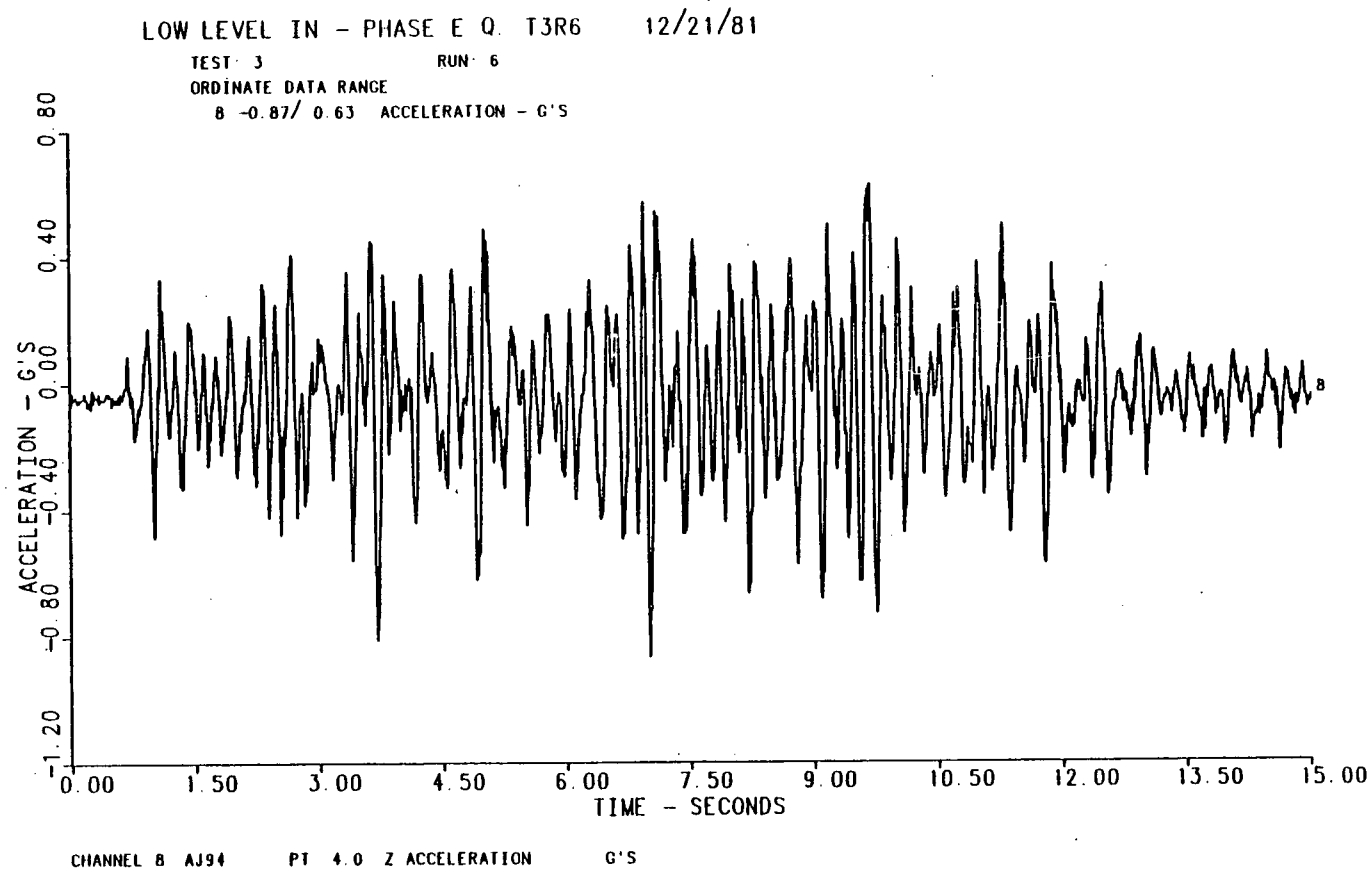
CHANNEL 11

DAMPING = 0.020



(b) Base Spectrum (Point 4.0Z)--2% Damping

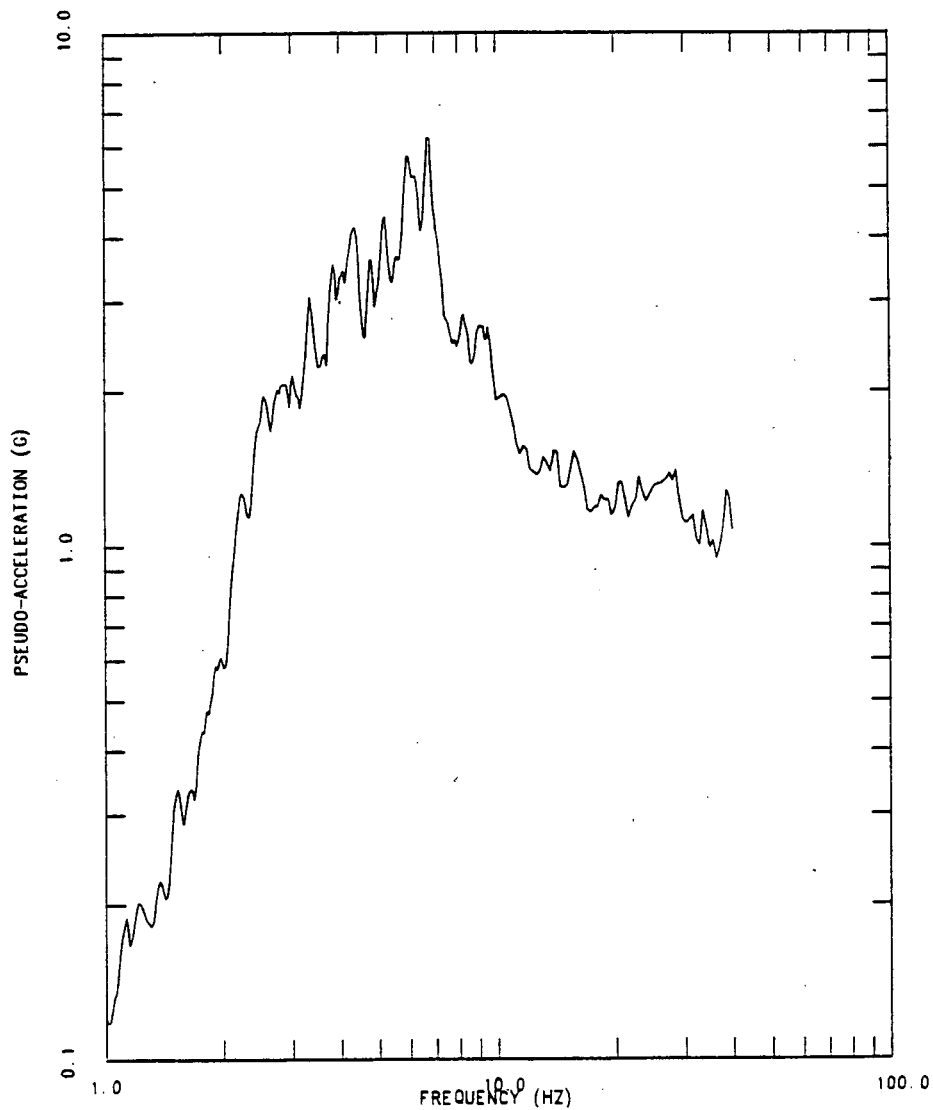
Figure 2-13. (Concluded)



(a) Time History

Figure 2-14. Low-Level Base Input--Phase II Earthquake

LOW LEVEL IN - PHASE E. O. T3R6 12/21/81
AJ94 PT. 4.0 Z ACCELERATION G'S
CHANNEL B DAMPING = 0.020

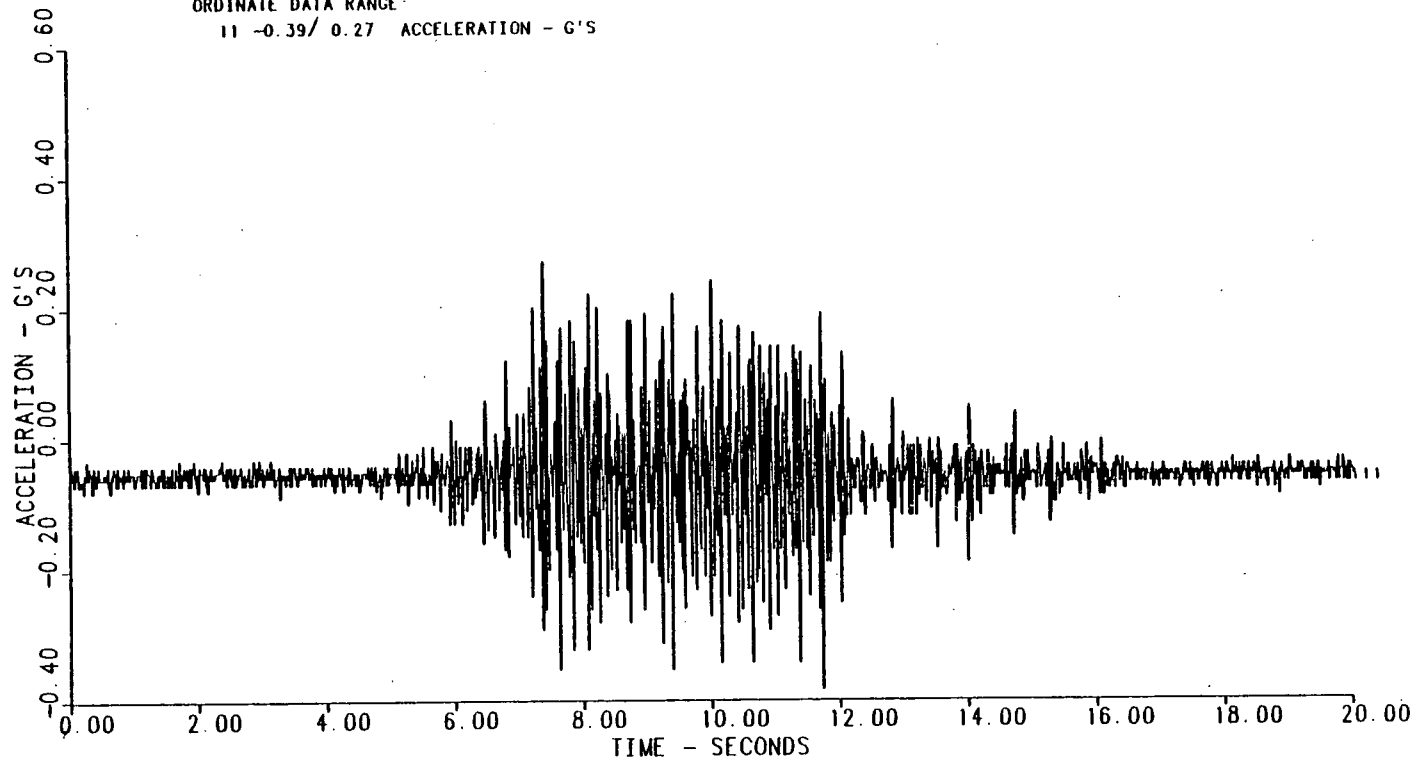


(b) Base Spectrum (Point 4.0Z)--2% Damping

Figure 2-14. (Concluded)

E. Q. INPUT SCALING TEST PSA 1/4 SNUBBER

TEST: 4 RUN: 4
ORDINATE DATA RANGE
11 -0.39/ 0.27 ACCELERATION - G'S

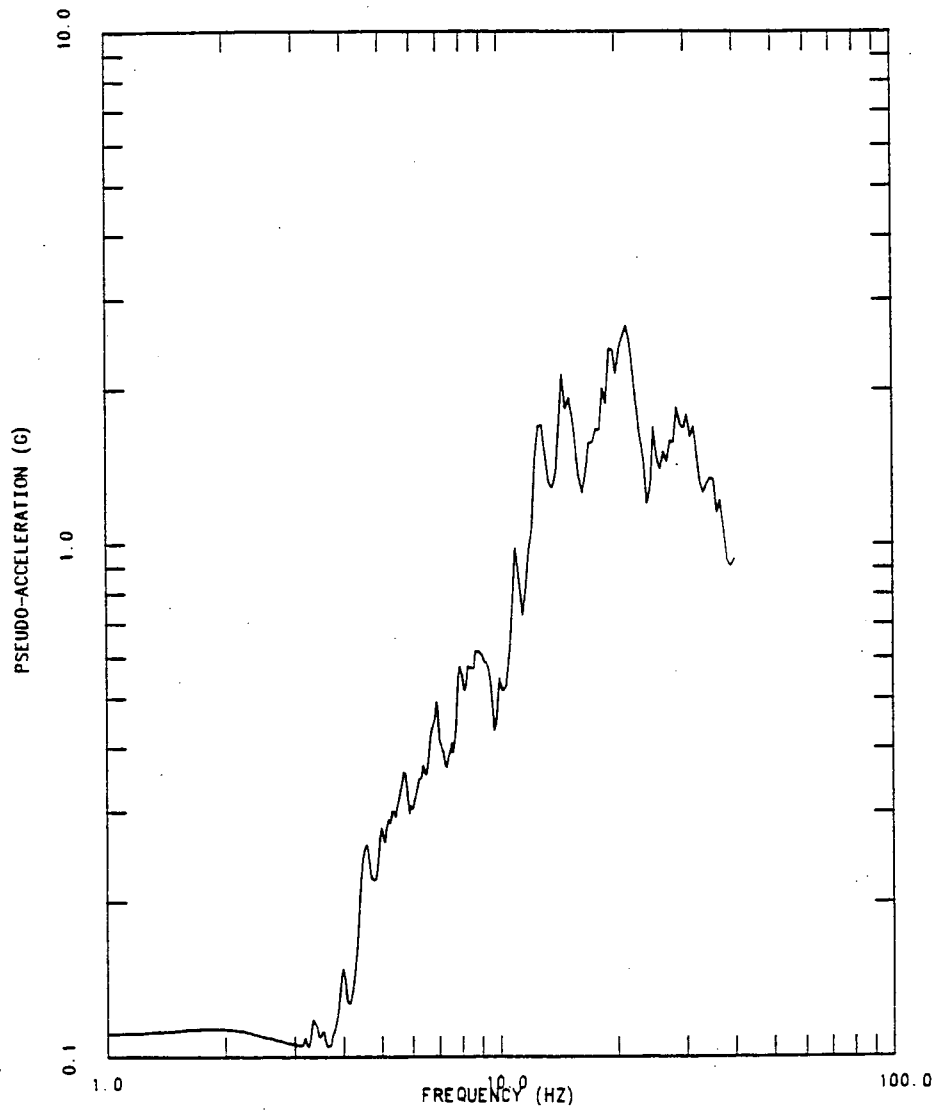


CHANNEL 11 AL88 PT 4.0 Z ACCELERATION G'S

(a) Time History

Figure 2-15. Low-Level Base Input--Phase III Earthquake

E. Q. INPUT SCALING TEST PSA 1/4 SNUBBER
AL88 PT 4.0 Z ACCELERATION G'S
CHANNEL 11 DAMPING = 0.020



(b) Base Spectrum (Point 4.0Z)--2% Damping

Figure 2-15. (Concluded)

Section 3

PRESENTATION AND INTERPRETATION OF TEST RESULTS

From all the testing performed (Phases I through III), there are two major topic areas that should be discussed: (1) the response levels achieved; and (2) the influence of the different types of supports on the pipe system characteristics (i.e., nonlinear behavior and damping). These two topics encompass some of the important items that can be investigated in analyzing the test data. The concept of the testing phases (I through III) is not focused on this section; instead, some of the important research topics are. The topics discussed will utilize the test data from all three phases of testing.

3.1 Response Levels Achieved During Testing

Basically two topics (items) will be discussed which describe something about the input motion to the piping system and the resulting response. These are: (1) a presentation and discussion of the peak base motion (input motion to the piping system) and corresponding peak pipe response, together with the corresponding amplifications; and (2) a comparison of the base motion spectra necessary to achieve a Level D condition, with the maximum base motion spectra achieved for some of the support configurations.

3.1.1 Peak Base Motion And Pipe Response

Two tables of peak piping base motion and response are given. The first (Table 3-1) gives the results for the tests that did not produce any support failure. The second (Table 3-2) gives the results for the tests for which there were planned support failures. The base motion quantities

Table 3-1

PEAK BASE MOTION AND PEAK PIPE RESPONSE FOR TESTS WITHOUT PLANNED SUPPORT FAILURE
(earthquake base motion only)

Midpoint Support	Test	Measured Base Motion		Measured Pipe Response			Support Condition	
		Displacement (in.)	Acceleration (g)	Absolute Displacement (in.)	Acceleration (g)	ASME Stress Ratio ^{††}	Pipe Support Load (lbf)	Percent of A/B Level
Bergen-Paterson	T1R5C	0.22	4.6	0.89 (3.0)#	14.2 (1.2)	0.68	1,920	64
Bergen-Paterson	T1R6C	0.34	6.7	1.35 (3.0)	16.4 (1.2)	1.01	3,000	100
ITT Grinnell	T3R5D	0.24	4.4	0.87 (3.0)	9.9 (1.2)	0.63	1,860	62
ITT Grinnell	T3R6C	0.39	6.8	1.30 (3.0)	19.7 (1.2)	0.95	2,710	90
Anchor/Darling	T2R5	0.06	0.6	0.09 (3.0)	1.5 (1.2)	0.11	160	40
Anchor/Darling	T2R6	0.12	2.3	0.24 (3.0)	5.2 (1.2)	0.25	635	159
Pacific Scientific-1/4	T4R6	0.05	0.6	0.10 (3.0)	1.2 (1.2)	0.09	180	51
Pacific Scientific-1/4	T4R5	0.07	1.1	0.21 (3.0)	2.8 (1.2)	0.19	410	117
Pacific Scientific-1	T3R6	0.52	0.9	0.95 (3.0)	4.4 (3.0)	0.57	1,340	89

Table 3-1 (Continued)

PEAK BASE MOTION AND PEAK PIPE RESPONSE FOR TESTS WITHOUT PLANNED SUPPORT FAILURE
(earthquake base motion only)

Midpoint Support	Test	Measured Base Motion		Measured Pipe Response			Support Condition	
		Dis- placement (in.)	Accel- eration (g)	Absolute Displacement (in.)	Acceleration (g)	ASME Stress Ratio ††	Pipe Support Load(lbf)	Percent of A/B Level
Pacific Scientific-1	T3R10	0.51	0.8	0.94 (3.0)	4.2 (3.0)	0.56	1,470	98
Pacific Scientific-1	T3R11	2.04	5.0	3.32 (3.0)	14.3* (3.0)	1.54	5,940	396
Weak Strut 2	T4R4	0.60	1.0	1.22 (3.0)	6.0 (3.0)	0.88	2,080	38**
Rigid Strut	T2R3	0.48	0.2	0.49 (3.0)	0.3 (3.0)	0.15	150	0.5**
Rigid Strut	T2R8	1.31	0.9	1.84 (3.0)	4.9 (3.0)	0.65	1,880	6**
Box Frame	T1R1	0.38	1.5	1.61 (3.0)	8.1 (3.0)	1.14	†	-
Box Frame	T1R2	0.84	3.3	3.46 (3.0)	16.6*(3.0)	2.39	†	-
Box Frame	T1R3	1.62	6.8	4.67 (3.0)	##	3.05	†	-
Box Frame	T1R4	2.33	12.0	5.42 (3.0)	22.3(3.0)	3.35	†	-

Table 3-1 (Concluded)

PEAK BASE MOTION AND PEAK PIPE RESPONSE FOR TESTS WITHOUT PLANNED SUPPORT FAILURE
(earthquake base motion only)

Midpoint Support	Test	Measured Base Motion		Measured Pipe Response			Support Condition	
		Dis- placement (in.)	Accel- eration (g)	Absolute Displacement (in.)	Acceleration (g)	ASME Stress Ratio ††	Pipe Support Load(lbf)	Percent of A/B Level
Box Frame	TIR5	2.50	10.9	5.41 (3.0)	21.2*(3.0)	3.39	†	-

* The transducer excitation amplitude exceeded the linear range (≤ 14.1 g) of the internal amplifier and signal distortion is likely. This problem occurred with the ENDEVCO 5241A accelerometers. For other tests, a different type of transducer was used.

** There is not a specified A/B load for the ANCO designed struts; this is the percent of the ultimate load for the strut.

The numbers in parentheses, (), are the locations of the corresponding pipe response. The given responses are in the Z direction.

Transducer failure.

† The box frame was not instrumented, so the loads into it could not be determined.

†† The ASME stress ratio is based on the Level D stress limit; it is for the elbow at Point 3.0. Ratios greater than unity are difficult to interpret because of section yielding.

Table 3-2

PEAK BASE MOTION AND PEAK PIPE RESPONSE FOR TESTS WITH PLANNED SUPPORT FAILURE
(earthquake base motion only)

Midpoint Support	Test	Measured Base Motion		Measured Pipe Response			Support Condition		
		Displacement (in.)	Acceleration (g)	Absolute Displacement (in.)	Acceleration (g)	ASME Stress Ratio ##	Pipe Support Load(lbf)	Percent of C/D Level	Support Failed
Bergen-Paterson	T1R7B	1.41	15.1	37.8 (2.1)#	37.5 (1.2)	2.51	6,150	154	No
ITT Grinnell	T3R7B	1.47	15.1	3.86 (2.1)	42.6 (1.2)	2.79	5,440	136	No
Anchor/Darling	T2R7	0.59	8.6	1.31 (2.0)	18.6*(1.2)	0.86	1,120	210	Yes
Pacific Scientific-1/4	T4R7B	1.00	15.8	2.58 (2.1)	40.4 (1.2)	1.24	1,900	380	Yes
Pacific Scientific-1/4	T3R13	3.29	12.9	9.55 (1.6)	17.7*(1.6)	3.25	1,900	380	Yes
Pacific Scientific-1	T3R12	3.21	14.9*	6.28 (1.4)	18.2*(3.0)	2.04	6,900	329	No

Table 3-2 (Concluded)

PEAK BASE MOTION AND PEAK PIPE RESPONSE FOR TESTS WITH PLANNED SUPPORT FAILURE
(earthquake base motion only)

Midpoint Support	Test	Measured Base Motion		Measured Pipe Response			Support Condition		
		Dis- placement (in.)	Accel- eration (g)	Absolute Displacement (in.)	Acceleration (g)	ASME Stress Ratio ##	Pipe Support Load(lbf)	Percent of C/D Level	Support Failed
Weak Strut 1	T4R3	0.81	1.1	2.56 (1.6)	16.0*(1.6)	1.05	1,670	106**	Yes
Weak Strut 2	T4R5	2.92	9.03	10.6 (1.6)	18.4 (3.0)	2.73	4,700	157**	Yes

* The transducer excitation amplitude exceeded the linear range (≤ 14.1 g) of the internal amplifier and signal distortion is likely. This problem occurred with the Endevco 5241A accelerometers. For other tests, a different type of transducer was used.

** There is not a specified C/D load for the ANCO designed struts; this is the percent of the minimum yield load for the strut.

The numbers in parentheses, (), are the locations of the corresponding pipe response. The given responses are in the Z direction.

The ASME stress ratio is based on the Level D stress limit; it is for the elbow at Point 3.0.

listed are the displacement (absolute--relative to the fixed foundation) and the acceleration (absolute). The pipe response quantities are the absolute displacement, acceleration (absolute), ASME stress ratio for specified elbow (based on the 1981 edition, Winter addenda, of the code), and midpoint support load.

The extreme values of base motion, for all the tests reported in Table 3-1, are 0.05 in. to 2.5 in. displacement and 0.2 g to 12.0 g acceleration. The extreme values of pipe response for Table 3-1 are 0.09 in. to 5.42 in. displacement, 0.3 g to 19.7 g acceleration, and 0.09 to 3.39 Level D ASME stress ratio. These values are not the most extreme values for the testing, because Table 3-1 is for the tests without planned midpoint support failure. For the tests with planned support failure (Table 3-2), the extreme response values are, in general, much greater. The extreme values of base motion, for Table 3.2, are 0.81 in. to 3.29 in. displacement and 1.1 g to 15.8 g acceleration. The extreme values of pipe response, for Table 3-2, are 1.31 in. to 10.60 in. displacement, 16.0 g to 42.6 g acceleration, and 0.86 to 3.25 Level D ASME stress ratio. A comment must be made about the values reported for the Level D ASME stress ratio. Values greater than one do not have any meaning because these values indicate that the pipe material yielded. Thus, stresses and moments calculated from strain data, using linear relationships, would be meaningless. Therefore, the stress ratios greater than one would be meaningless. The values are given only as a rough qualitative measure of how much the material strained plastically.

A topic worth briefly looking at is the amount of amplification the pipeline experienced above that of its base. The quantity to be looked at, as a function of peak base displacement, is the ratio of the peak pipe absolute displacement to the base displacement. It is given by the following equation:

$$\text{amplification } (i,j) = z_{pi}^a / z_{bj} \quad (3-1)$$

Where z_{pi}^a is the peak absolute z-direction displacement of the pipe at the i th node point, and z_{bj} is the peak base motion (z-direction) displace-

ment of the j th base (sled). For Equation 3-1 to be correct, the peak values would have to occur at the same time. However, in general, they will occur at different times. For some of the tests performed, they were at the same time. For other tests, they were at different times (from 0.5-s to 2.0-s difference). Therefore, Equation 3-1 will be used only as a rough measure of the amplification.

The tests listed in Tables 3-1 and 3-2 which had common base motion spectra (the same spectra linearly scaled up or down) were compared. The amplification (Equation 3-1) was determined for three sets of data (each set had a different common base spectra). The results are given in Tables 3-3 through 3-5. For a linear system, the amplification factor is constant for the base motion, at one level, linearly scaled to another level. It is apparent that the amplification factor is not constant for all levels of excitation for the three phases of testing. In some cases, the amplification remained fairly constant. This was generally the case, although not always, at the lower response levels. There are a number of reasons for the variation of the amplification; they are (1) piping system nonlinearities, and (2) limitations in the hydraulic actuator system. The piping system nonlinearities could be due to (1) midpoint support nonlinear action--opening and closing of gaps or locking and unlocking of the snubber, and (2) plastic deformation of the pipeline. The limitations of the hydraulic actuator system result in the system being able to drive all three bases with the same desired motion, provided that the desired motion is not too great. Once the prescribed base motion exceeds certain limits, the hydraulic actuator system is unable to deliver exactly what is desired. The generated base motion has different amplitude and frequency characteristics than the desired motion. The peak pipe response location would then probably change. This is seen in the data presented in Tables 3-4 and 3-5.

3.1.2 Achieved Base Motion Input Beyond That For Level D

A significant question to be addressed is: given a particular midpoint support configuration (i.e., Bergen-Paterson snubber at point 1.4), how large was the input for the highest level earthquake test compared to the input for a test that resulted in just achieving a Level D stress limit? The approach used to address this question is described below. The general

Table 3-3

AMPLIFICATION FACTOR--PHASE I EARTHQUAKE

<u>Midpoint Support</u>	<u>Base Motion-- Displacement (in.)</u>	<u>Amplification*</u>
Box Frame	0.38	4.24 (3.0)
	0.84	4.12 (3.0)
	1.62	2.88 (3.0)
	2.33**	2.33 (3.0)
	2.50**	2.16 (3.0)

* The amplification factor is defined by Equation 3-1. The location of the maximum pipe response used in calculating the amplification is given in parentheses, (). The base motion used is that of the base at Point 4.0.

** The base motion time histories for these two tests were different from the other three tests, and they were slightly different from each other. The last two base motion time histories were developed by bandpass filtering the same time history that was used for the other tests.

Table 3-4
AMPLIFICATION FACTOR--PHASE II* EARTHQUAKE

<u>Midpoint Support</u>	<u>Base Motion-- Displacement (in.)</u>	<u>Amplification**</u>
Pacific Scientific-1	0.52	1.83 (3.0)
	0.51	1.84 (3.0)
	2.04	1.63 (3.0)
	3.21	1.96 (1.4) 1.34 [3.0]
Pacific Scientific-1/4	3.29	2.90 (1.6)
Rigid Strut	0.48	1.02 (3.0)
	1.31	1.40 (3.0)
Weak Strut 1	0.81	3.16 (1.6)
Weak Strut 2	0.60	2.03 (3.0)
	2.92	3.63 (1.6) 1.86 [3.0]

* The same basic (unscaled) earthquake signal was used in operating the hydraulic actuator system for all Phase II tests. The basic earthquake was linearly scaled up for the tests.

** The amplification factor is defined by Equation 3-1. The location of the maximum pipe response, used in calculating the amplification, is given in parentheses, (). Other pipe response locations are given in brackets, []. The base motion used is that of the base at Point 4.0.

Table 3-5
AMPLIFICATION FACTOR--PHASE III* EARTHQUAKE

<u>Midpoint Support</u>	<u>Base Motion-- Displacement (in.)</u>	<u>Amplification**</u>
Bergen- Paterson	0.22	4.05 (3.0)
	0.34	3.97 (3.0)
	1.41	2.74 (2.1) 2.41 [3.0]
ITT Grinnell	0.24	3.63 (3.0)
	0.39	3.33 (3.0)
	1.47	2.63 (2.1) 2.54 [3.0]
Anchor/ Darling-40	0.06	1.50 (3.0)
	0.12	2.00 (3.0)
	0.59	2.22 (2.0) 1.61 [3.0]
Pacific Scientific-1/4	0.05	2.00 (3.0)
	0.07	3.00 (3.0)
	1.00	2.58 (2.1) 1.59 [3.0]

The same basic (unscaled) earthquake signal was used in operating the hydraulic actuator system for all Phase III tests. The basic earthquake was nearly scaled up for the tests.

*
h
11

**
max
pare
The

The amplification factor is defined by Equation 3-1. The location of the minimum pipe response, used in calculating the amplification, is given in parenthesis, (). Other pipe response locations are given in brackets, []. The base motion used is that of the base at Point 4.0.

approach used was to select a test which resulted in an ASME stress condition at or below, but as close as possible to Level D. Then, it was determined how much the dynamic input for this test must be linearly scaled up in order to achieve a Level D condition. The scaled up input spectra (Level D spectra) was compared with the largest input spectra achieved. The comparison should be done at the pipe system natural frequencies.

The steps followed in making the comparisons between the Level D spectra and largest input spectra are described as follows:

1. Select a midpoint support configuration
2. From the available strain data, calculate the maximum ASME stress ratio* achieved for each test
3. Select the test ("Reference Test") whose maximum stress ratio is as close to one as possible, but not greater than one. This stress ratio is SR_b^m , and its corresponding resultant dynamic moment is M_{Bb}^m
4. Calculate the value of the dynamic moment, corresponding to the pipe location of the maximum stress ratio, necessary to achieve a Level D condition; this is done by solving the following equation** for the dynamic limit moment, M_B^L :

$$B_1(P_{\max} D_o / 2t) + B_2(M_A + M_B^L) / Z = 3.0S_h$$

the expression for the dynamic limit moment is given by.

$$M_B^L = (Z/B_2)(3.0S_h - B_1[P_{\max} D_o / 2t]) - M_A$$

* The stress ratio is calculated using the Level D stress limit.

** This equation is the primary loads ASME stress equation evaluated at the Level D stress limit condition; the stress equals $3.0S_h$. Some of the terms in the equation are defined for Equation 2-2.

5. Calculate the scale factor, k , necessary to scale up Reference Test (test in 3 above) base input by, so the scaled base input would result in a Level D condition (maximum stress in system is $3.0S_H$)

$$k = M_B^L / M_{Bb}^m$$

6. Multiply the base input for the below Level D test (test in 3 above) by the factor k , and compare it with the base input for the highest level test:

$$s_D^I(f) = k s_b^I(f) \text{ compared to } s_H^I(f) ,$$

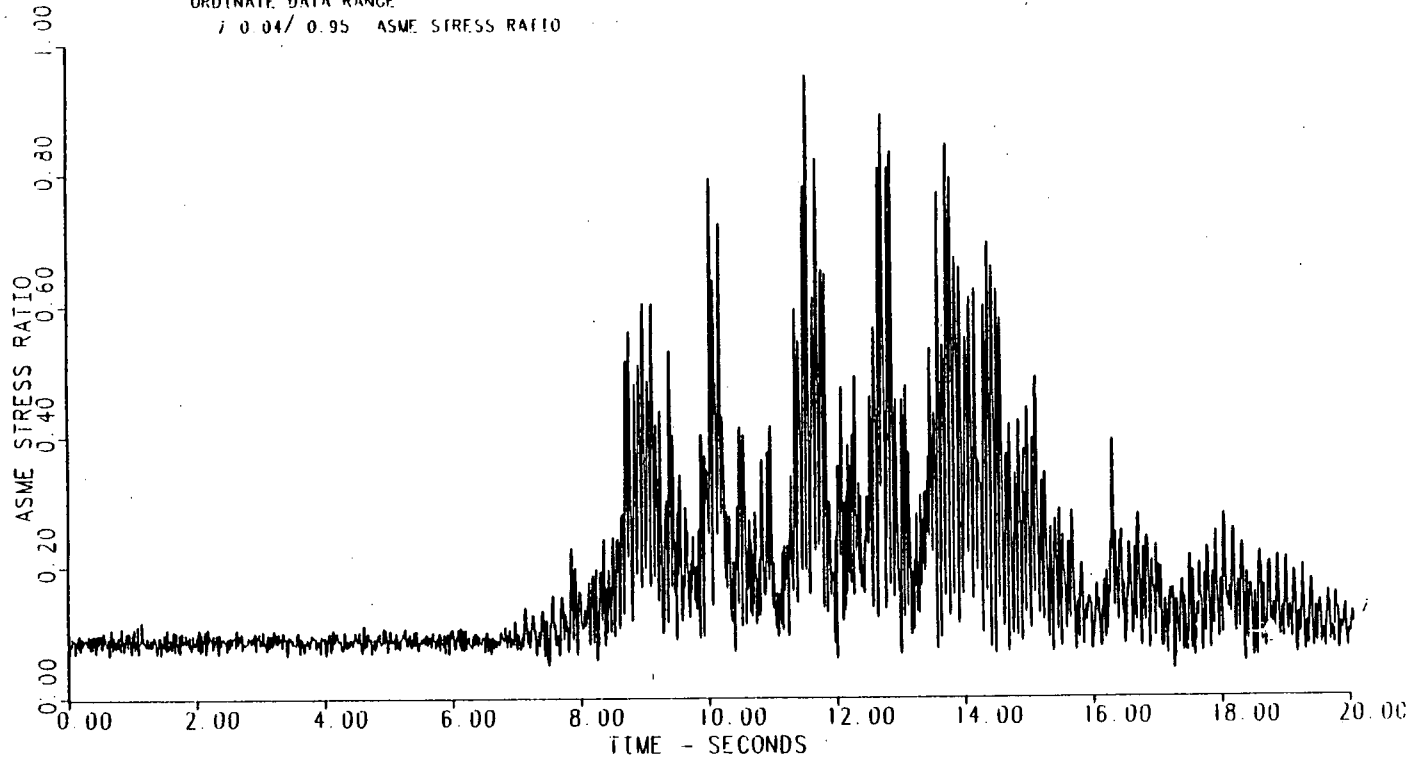
where $s^I(f)$ is an input (base) spectra, f is frequency, and D , b , and H refer to Level D stress condition, below Level D, and highest stress level condition, respectively. The comparison is made at the most important system natural frequencies.

This method of scaling up the below Level D input to Level D, and then comparing it with the highest level input is approximate. However, it does provide a first order estimate of how large a base input, relative to the Level D input, was achieved.

The above described method of comparing inputs was applied to two support configurations (see Table 3-6). These support configurations were chosen because the supports used had adequate load carrying capability, so they were not undersized or oversized for the subject pipe line and the input earthquake levels used. Figures 3-1 through 3-4 give transient data plots of the ASME stress ratio for the elbow at Point 3.0 for the tests listed in Table 3-6. The dynamic base input for the below Level D tests were scaled up by the factor k , and plotted together with the highest level base inputs achieved. The results are given in Figures 3-5 and 3-6. A tabular comparison at selected frequencies between the two curves (Level D and highest), for a given support is given in Table 3-7. The data in this table indicate that at the first two natural frequencies of the systems, the

100% A/B LOAD REPEAT TEST 2. EARTHQUAKE INPUT. GRINNELL SNUBBER

TEST 3 RUN 6C
ORDINATE DATA RANGE
7 0 04/ 0.95 ASME STRESS RATIO

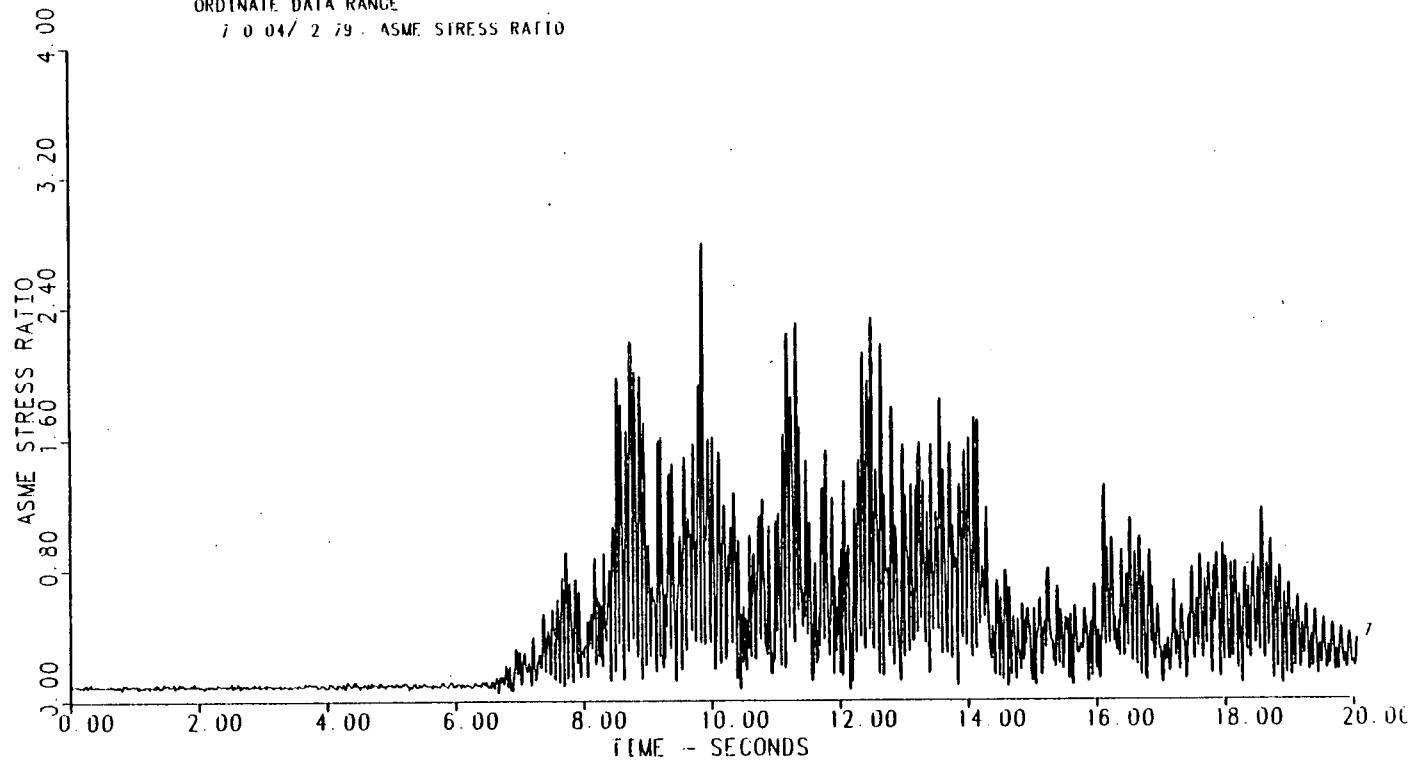


CHANNEL 7 1981 ASME LEVEL D STRESS RATIO

Figure 3-1. Stress Ratio (Elbow at Point 3.0) For Just Below Level D Test--Grinnell Snubber

FAILURE TEST REPEAT, EARTHQUAKE INPUT, GRINNELL SNUBBER

TEST: J RUN: 7B
ORDINATE DATA RANGE
7 0 04/ 2 79 ASME STRESS RATIO

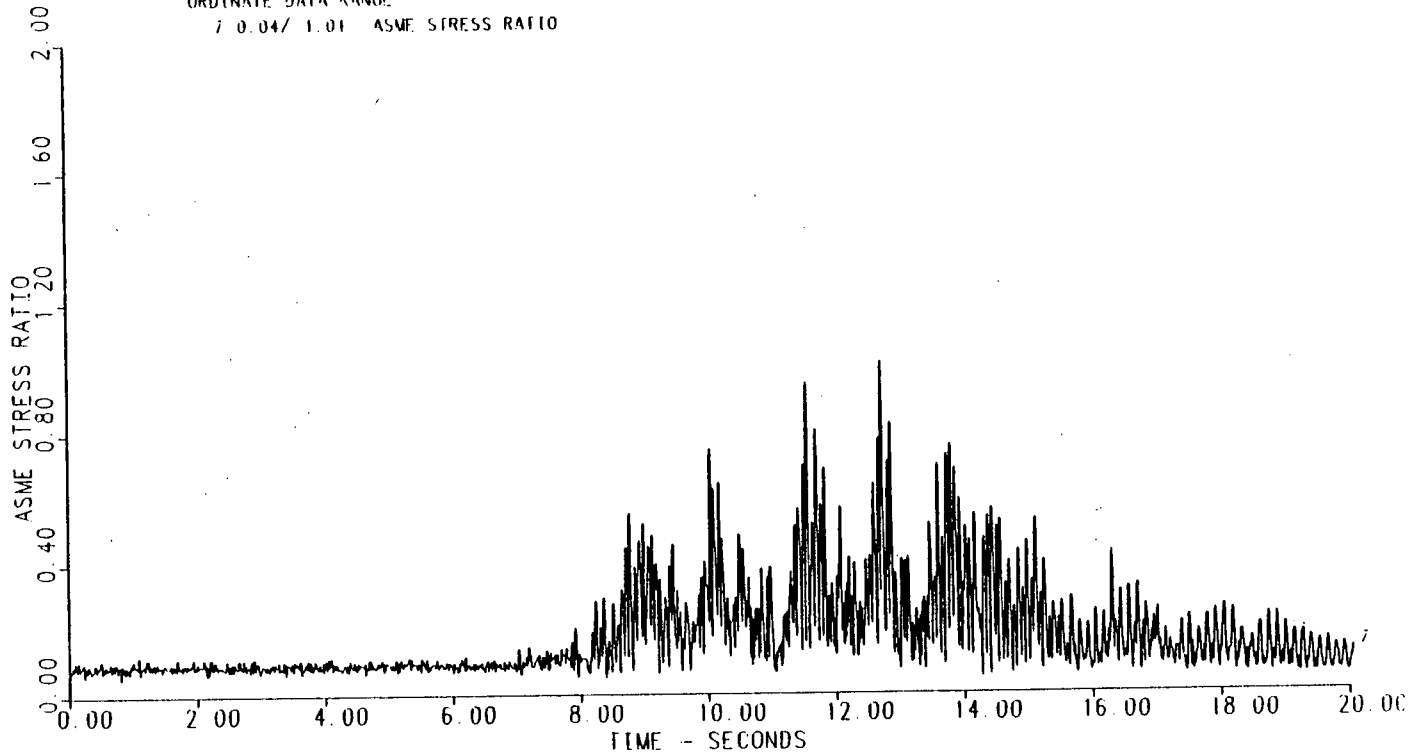


CHANNEL 7 1981 ASME LEVEL D STRESS RATIO

Figure 3-2. Stress Ratio (Elbow at Point 3.0) For Highest Level Test--Grinnell Snubber

100% A/B LOAD REPEAT TEST 2, EARTHQUAKE INPUT, BP-2525-3 SNUBBER

TEST 1 RUN: 60
ORDINATE DATA RANGE
7 0.04/ 1.01 ASME STRESS RATIO

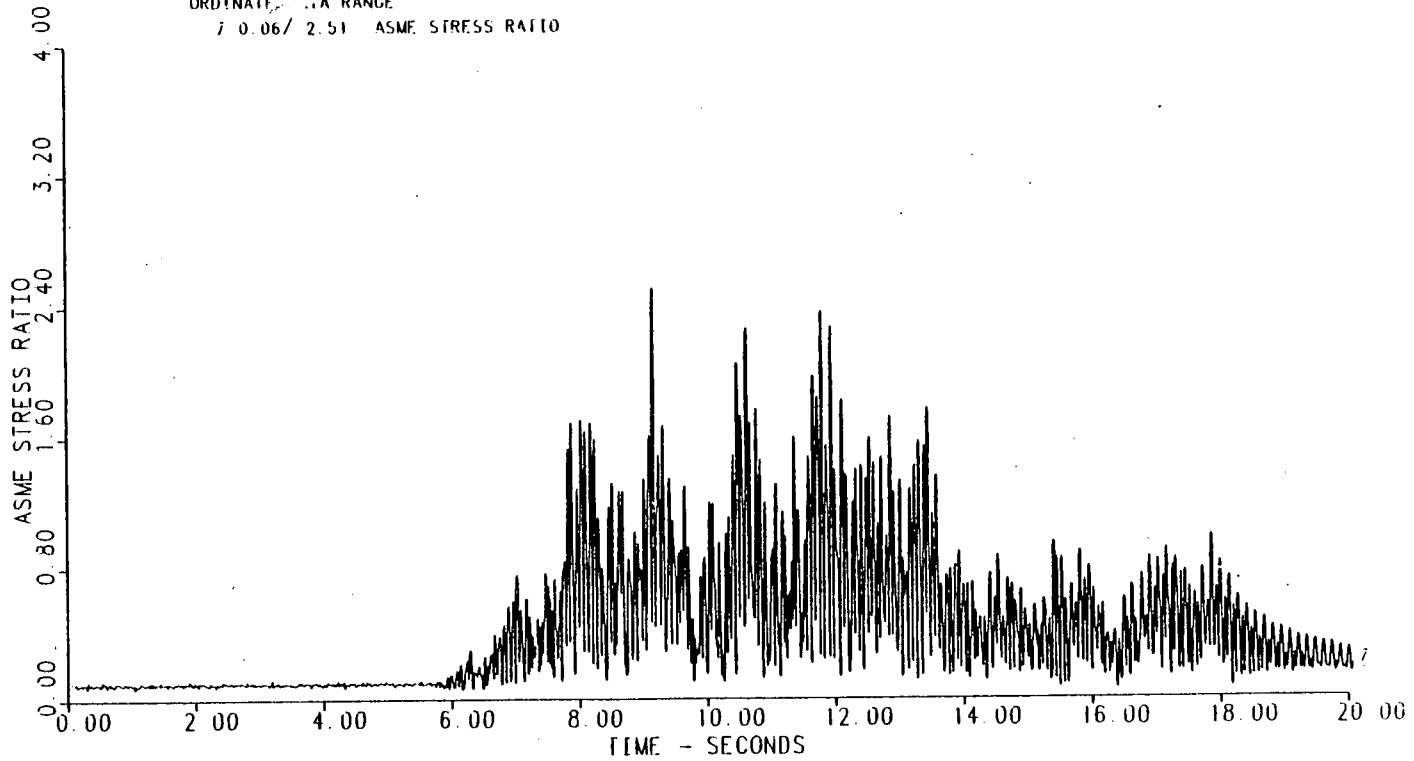


CHANNEL 7 1981 ASME LEVEL D STRESS RATIO

Figure 3-3. Stress Ratio (Elbow at Point 3.0) For Level D Test--Bergen-Paterson Snubber

FAILURE TEST REPEAT EARTHQUAKE INPUT, BP-2525-3 SNUBBER

TEST 1 RUN 7B
ORDINATE RANGE
1 0.06/ 2.51 ASME STRESS RATIO



CHANNEL 7 1981 ASME LEVEL D STRESS RATIO

Figure 3-4. Stress Ratio (Elbow at Point 3.0) For Highest Level Test--Bergen-Paterson Snubber

Table 3-6

TESTS FOR WHICH COMPARISONS WERE MADE BETWEEN
LEVEL D INPUT AND HIGHEST LEVEL INPUT

Midpoint Support Type	Below Level D Test	Maximum Stress Ratio, SR_b^m	Maximum Dynamic Moment, M_{Bb}^m (lbf-in.)	Scale Factor, k**	Highest Level Test
ITT Grinnell	T3R6C	0.95	57,894	1.06	T3R7B
Bergen- Paterson	T1R6C	1.00	61,533	1.00	T1R7B

* The entries in this table are for the pipe elbow at Point 3.0.

** The dynamic limit moment for the elbow at Point 3.0 is 61,248 lbf-in.
(6,923 Nm).

Higher Spectra: T3R7B
Lower Spectra: T3R6C Scaled to Level D
Damping: 2%

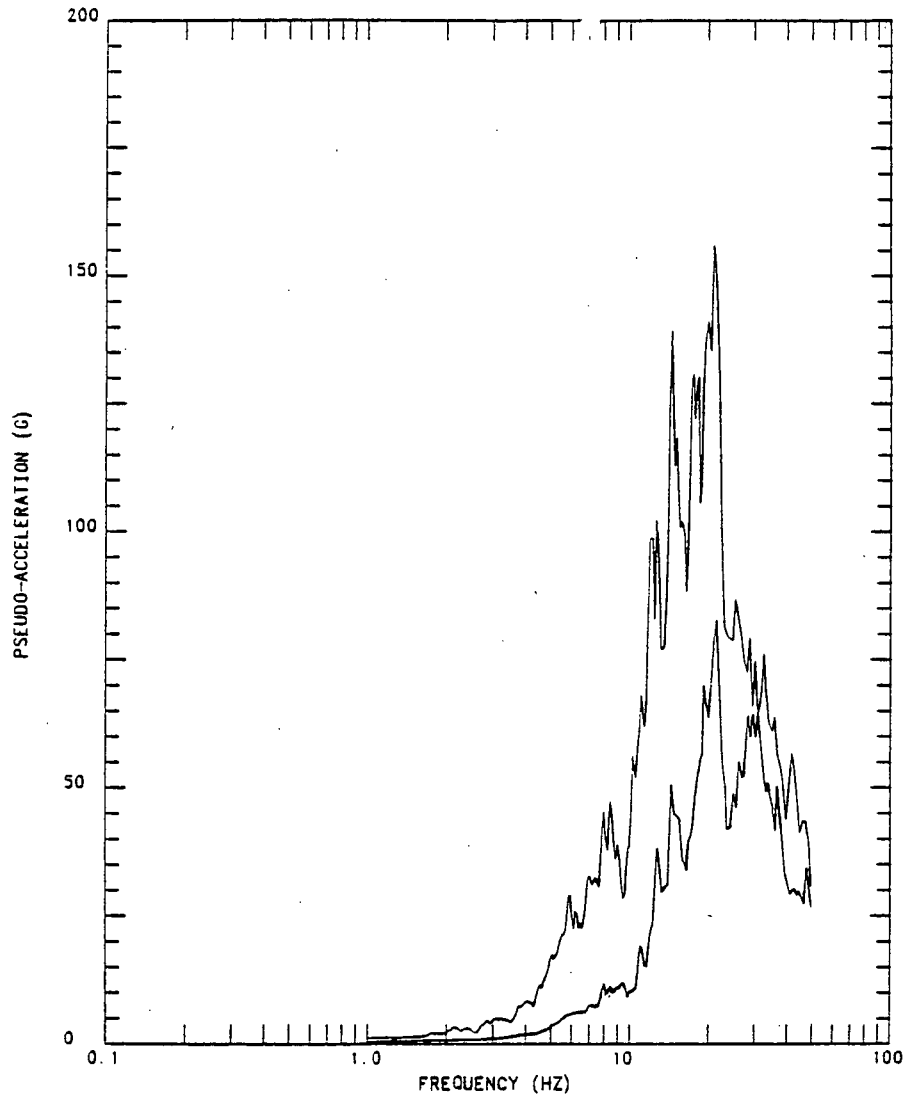


Figure 3-5. Level D (For Elbow at Point 3.0) Base Motion Spectrum Compared to Highest Level Test with ITT Grinnell Snubber

Higher Spectra: T1R7B
Lower Spectra: T1R6C Scaled to Level D
Damping: 2%

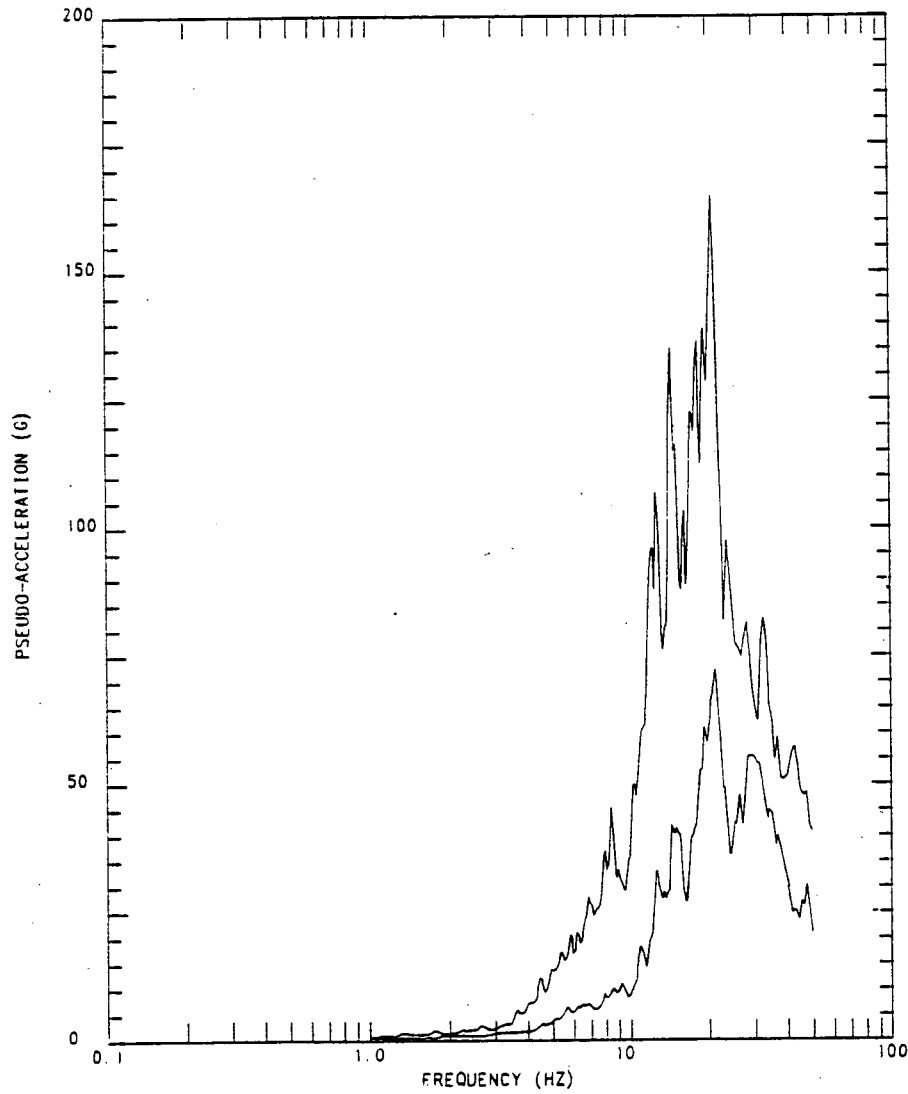


Figure 3-6. Level D (For Elbow at Point 3.0) Base Motion Spectrum Compared to Highest Level Test with Bergen-Paterson Snubber

Table 3-7

COMPARISON OF LEVEL D BASE INPUT SPECTRAL AMPLITUDE
WITH THAT FOR THE HIGHEST LEVEL TEST*

Spectral Frequency (Hz)	<u>Multiples of Level D Base Input**</u>	
	<u>ITT Grinnell</u>	<u>Bergen-Paterson</u>
5.0	4.75	3.10
7.3#	4.35	4.45
10.0	3.85	3.90
14.6#	2.75	3.20
20.0	2.20	2.20
25.0	1.60	1.95
30.0	1.25	1.20
40.0	1.30	1.70
50.0	1.15	2.00

* The values given in this table were obtained from the data presented in Figures 3-5 and 3-6.

** The entries are the number of times the highest level base input is of the Level D base input, as a function of spectral frequency.

These are the first two natural frequencies for the two test systems.

highest level base input was from 4.5 to 3.0 times the Level D input (for the given snubbers). (The first mode was excited considerably more than the other modes.) While base motion input spectral comparison is not a precise method of comparing the achieved loading to the Code limit conditions, the approach herein is useful for evaluation purposes. What Table 3-7 may suggest to the designer is that the tested piping successfully withstood earthquake inputs which were about four and one half times the maximum inputs acceptable by current Code rules.

3.2 Support Influence on Piping Characteristics

Pipe supports (i.e., struts, snubbers) and their corresponding anchor/connection mechanisms (i.e., clevis pin through holes) affect a piping system in numerous ways. They are the source of some types of system nonlinearities. This includes such things as (1) hardening or softening effects that result in a change in the system natural frequencies as the response level changes [2]; (2) changes in actual damping with changes in response level; and (3) because of the changing natural frequencies and damping, nonlinearities of varying degrees are introduced into the transient and frequency response.

Another effect of supports on piping is that of increased damping. Depending on the piping system and types of supports, different support introduce different amounts of damping into the piping system. A strut type of support contributes less damping than a snubber support. A strut support (less its clevis pin connections) undergoing elastic deformation has only structural damping. This damping is small compared to the portion of snubber damping due to the action of the snubber internals, including lockup of the snubber. For some models, mechanical snubbers contribute more damping than hydraulic snubbers. Support influence on piping will be discussed below for two cases: (1) no support failure; and (2) support failure.

3.2.1 Support Influence With No Support Failure

The topic areas discussed below are (1) natural frequencies, (2) response nonlinearities, and (3) piping system damping.

3.2.1.1 Natural Frequencies

The natural frequencies of a piping system are affected by the stiffness properties of its support system (supports plus attachment devices). These stiffness properties can be linear or nonlinear. Possible nonlinear properties could be due to gaps at various places in the piping system. The gaps could be due to a loose fit around clevis pins for the strut ends; in this case they might be small (i.e., 0.002 in.). The gaps could be due to clearance between the pipe and a surrounding restraint frame; in this case the gaps might be large (i.e., 0.1 in. to 1 in.).

Another source of nonlinear behavior could be due to the locking and unlocking of snubbers. As this takes place the stiffness of the system changes. Piping systems with snubbers tend to be hardening systems. Also, the internal snubber mechanisms can introduce nonlinearities into a system.

All the above described sources of nonlinear behavior, and others not described, will cause a piping system's instantaneous natural frequencies* to change over time. When a transient test is performed, from which natural frequencies can be determined, there is only one resonant peak (Fourier transform modulus peak) per mode. There is not a separate peak for some of the instantaneous values of a particular natural frequency. Instead, the peak for the particular frequency (mode) is broadened to the degree that the frequency changes over time.

Two types of transient tests were performed on the subject piping system to determine its natural frequencies. They were (1) base step and (2) white noise base motion. The first two frequencies were determined for many of the support configurations and are given in Table 3-8. Even though there is no evidence, from presently analyzed data, to indicate it, it is suspected

* Instantaneous natural frequencies are the natural frequencies corresponding to the system stiffness at a particular point in time, t . They are determined from the following: $[[k(t)] - \omega^2(t)[m]] = 0$, where $[k(t)]$ is the tangent stiffness matrix at time t , $\omega(t)$ is the natural frequency, and $[m]$ is the mass matrix.

Table 3-8

NATURAL FREQUENCIES FOR SUPPORT CONFIGURATIONS

<u>Midpoint Support</u>	<u>Test</u>	<u>Test Type*</u>	<u>Natural Frequency (Hz)</u>		<u>Peak Input Acceleration (g)</u>
			<u>First</u>	<u>Second</u>	
No Support	NRC#	Sine	3.5	12.2	0.2, 0.7#
Rigid Strut	T2R5	Step	7.0	**	5.0
	T2R6	Noise	7.4	16.2	0.7
	T2R11	Noise	7.4	15.8	5.0
Weak Strut 1	T4R2	Step	7.4	16.0	4.7
Pacific Scientific-1	T3R3	Step	7.4	16.2	5.2
	T3R8	Noise	7.4	15.4	5.8
ITT Grinnell	T3R2	Step	7.2	14.6	5.4
	T3R3	Step	7.3	14.6	7.2
Bergen-Patterson	T1R2	Step	7.3	15.0	5.2
	T1R3	Step	7.3	14.6	7.0

* Sine, step, and noise refer to sine dwell base motion, base step, and white noise, respectively.

** The Fourier transforms of the data did not show a distinct sharp spike for the second mode; the peak was flat and broad.

This test was done as part of a U.S. Nuclear Regulatory Commission research program. The peak input accelerations 0.2 g and 0.7 g are for forcing at the first and second natural frequencies, respectively.

that the piping configurations are hardening systems [2]. It may be that hardening effects are small for the range of input motions used in these tests.

3.2.1.2 System Nonlinearities

There are several sources of nonlinear behavior for the Z-Bend piping system. These include gap closure, coulomb damping, snubber lockup, midpoint support failure, and plastic deformation of the pipe. For this discussion, midpoint support failure is not considered. The object of this investigation is to gain some insight as to how nonlinearly the pipe systems behaved during earthquake testing. It is desired to focus on tests which generated stress levels between the Level B and Level D ASME Code stress limits.

In comparing the Z-Bend pipeline with strut-type supports installed with the pipeline with snubber supports installed, the piping system with snubber supports would, in general, behave the most nonlinearly of the two. (This assumes the gaps in the system are the same.) For this reason, this discussion will focus on midpoint snubber supports. Another type of midpoint support used--a box frame for Phase I testing. This type of support is definitely nonlinear. When the pipe response levels are great enough to close some of the gaps, the system stiffness changes. This type of support is less common than the strut/snubber type of support. It is used for pipe whip control. From past experience [3], it is seen that piping systems, with this type of support (box frame), cannot be modeled with a great degree of accuracy using linear methods.

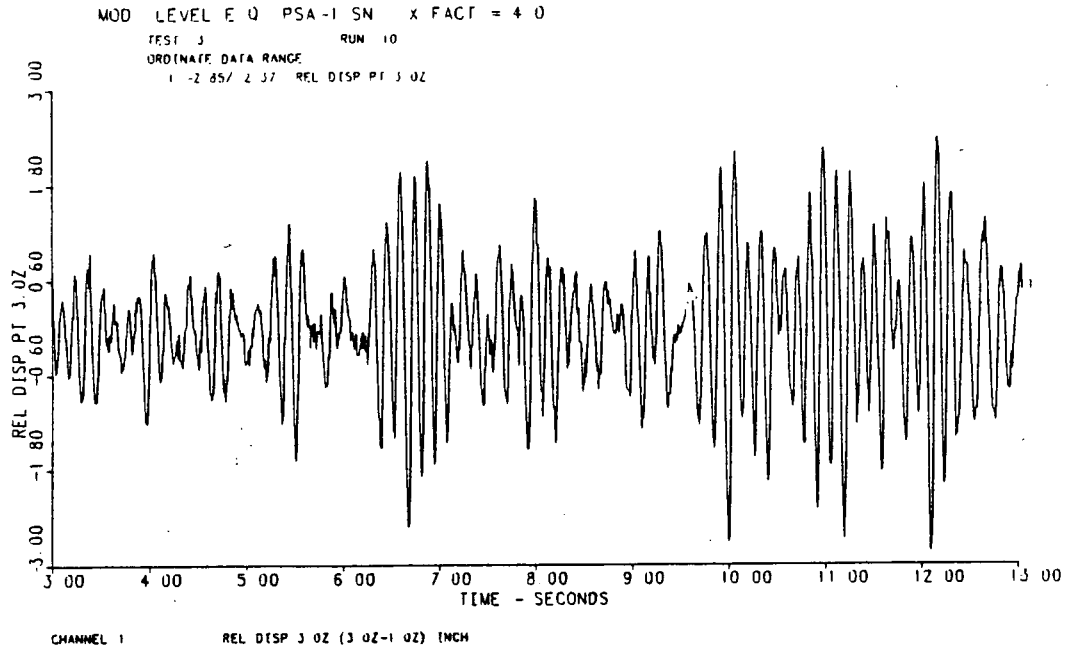
Two snubbers are locked at. They are (1) PSA-1 mechanical snubber and (2) ITT Grinnell hydraulic snubber. They were selected because they were fairly close to being the proper size for the earthquake levels used for testing. The method used to establish the degree of nonlinearity achieved during testing is qualitative. A point on the pipeline which experienced the greatest displacement was selected for study. This always turned out to be Point 3.0, with the displacement in the Z direction. The relative

displacement of this point was calculated. (The relative displacement is the difference between the absolute motion of Point 3.0 and the base motion.) This was done for two different levels of earthquakes. The relative displacement for the lower level earthquake was linearly scaled to the level of the highest level earthquake. The actual and scaled relative displacements, corresponding to the highest level earthquake, were then compared. This was done for each of the two snubbers. The results are presented in Figures 3-7 and 3-8. As can be seen, the comparisons indicate a substantial degree of linearity. Both the frequency content and amplitudes compare very well. This is especially meaningful considering the response levels achieved (see the figures).

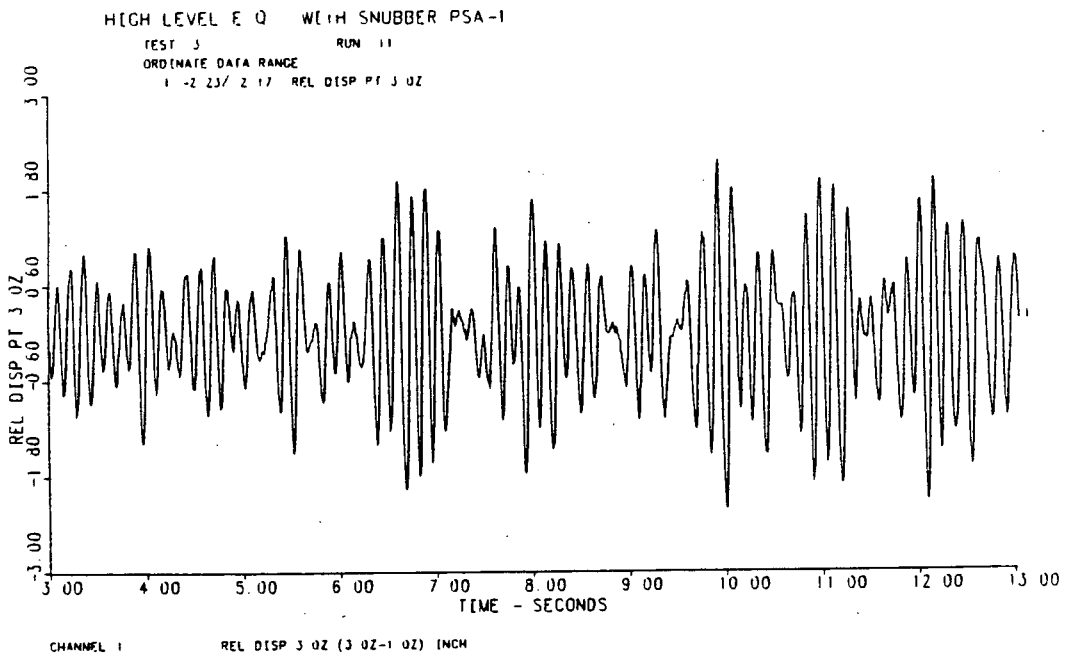
The point whose relative displacement was studied (Point 3.0) was about midway between the snubber and the base at Point 4.0. Its displacement was much greater than that of the pipe at the snubber attachment point (Point 1.4). The displacement of Point 1.4 was relatively small because of the locking action of the snubber. Thus, even though the snubber displacement would indicate substantial nonlinear behavior (with respect to the pipe displacement at Point 1.4), it is not surprising that the Point 3.0 displacement showed largely linear behavior--the Point 3.0 displacement was not made to be nonlinear by the much smaller nonlinear displacement motion at Point 1.4. This result is similar to some of the results of an earlier pipe testing/analysis project [2,4]. A general conclusion is that for piping systems with snubbers that are undergoing earthquake excitation, the nonlinear response (action) of the snubbers can be neglected. (This assumes that the level of the response is great enough to cause substantial locking of the snubbers.) The overall pipeline can then be treated as a linear system. (This latter comment assumes that the response levels are low enough to prevent plastic deformation of the pipe and support material.)

3.2.1.3 Damping Characteristics

The damping values presented herein are for four different types of midpoint (Point 1.4 in Figure 2-1) supports for the test pipeline. The supports were either of the strut or snubber type. The damping was calculated using test data from base step tests in which the three pipe

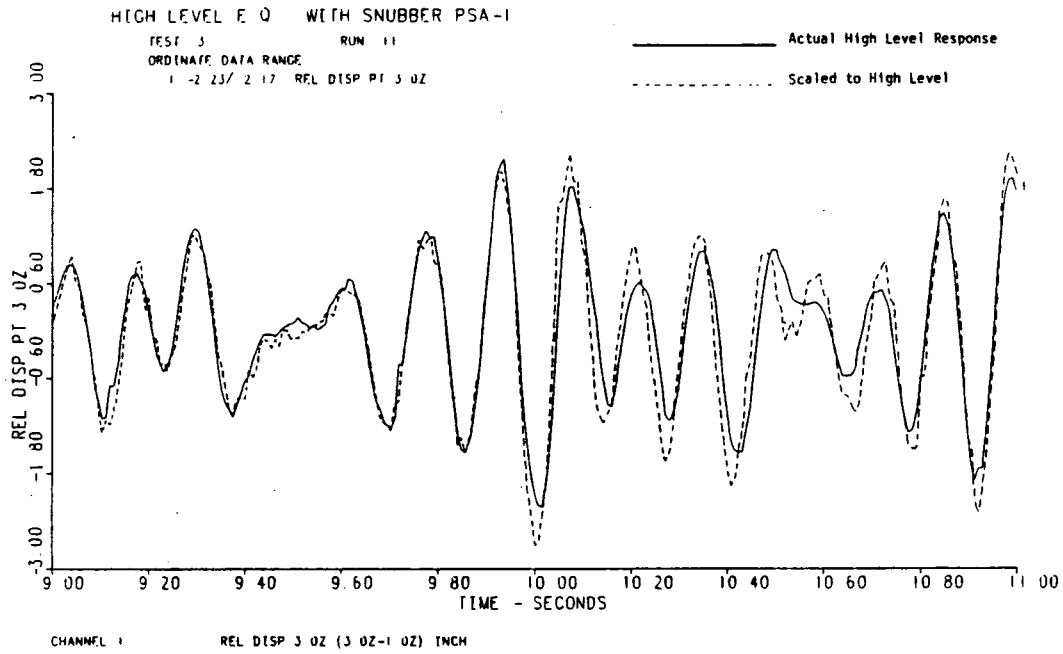


(a) Response Scaled to Level of Higher Level Earthquake [Earthquake for Figure 3-7(b)]



(b) Actual Response for Higher Level Earthquake

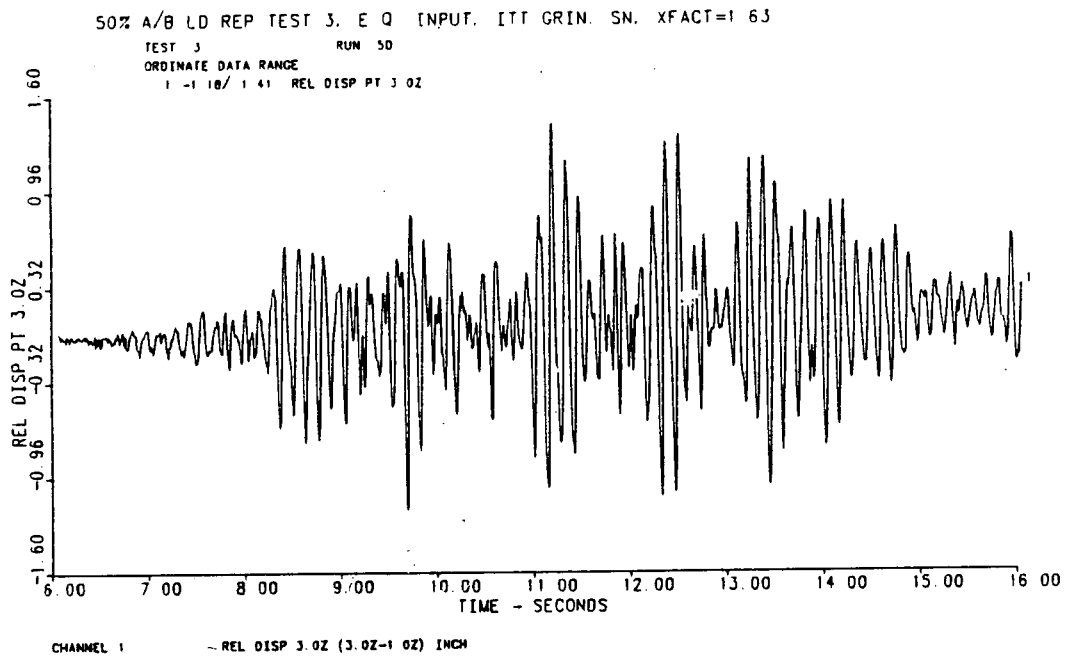
Figure 3-7. Comparison of Actual and Scaled Relative Displacement for Point 3.0Z



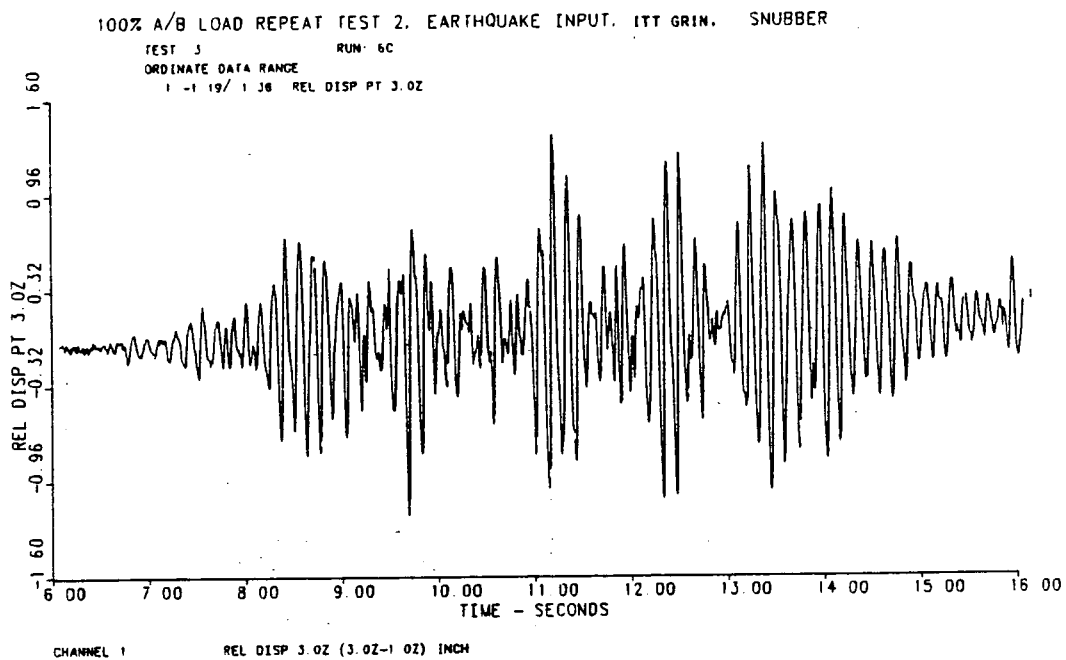
(c) Overlay of Actual and Scaled Relative Displacement for Portion of Event Where Responses were Greatest

Note:	<u>Test</u>	<u>Peak ASME Stress Ratio</u>	<u>Percent of A/B Load</u>
	Lower Level (T3R10)	0.56	93
	Higher Level (T3R11)	1.54	396

Figure 3-7. (Concluded)

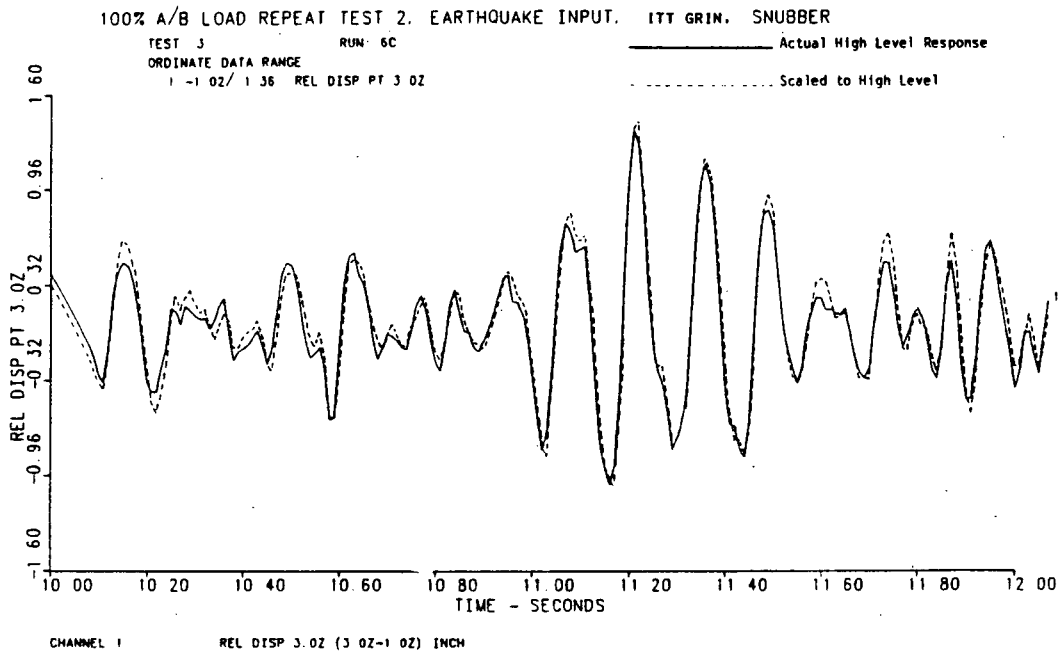


(a) Response Scaled to Level of Higher Level Earthquake [Earthquake for Figure 3-8(b)]



(b) Actual Response for Higher Level Earthquake

Figure 3-8. Comparison of Actual and Scaled Relative Displacement for Point 3.0Z



(c) Overlay of Actual and Scaled Relative Displacement for Portion of Event Where Responses were Greatest

Note:	Test	Peak ASME Stress Ratio	Percent of A/B Load
	Lower Level (T3R5D)	0.63	62
	Higher Level (T3R6C)	0.95	90

Figure 3-8. (Concluded)

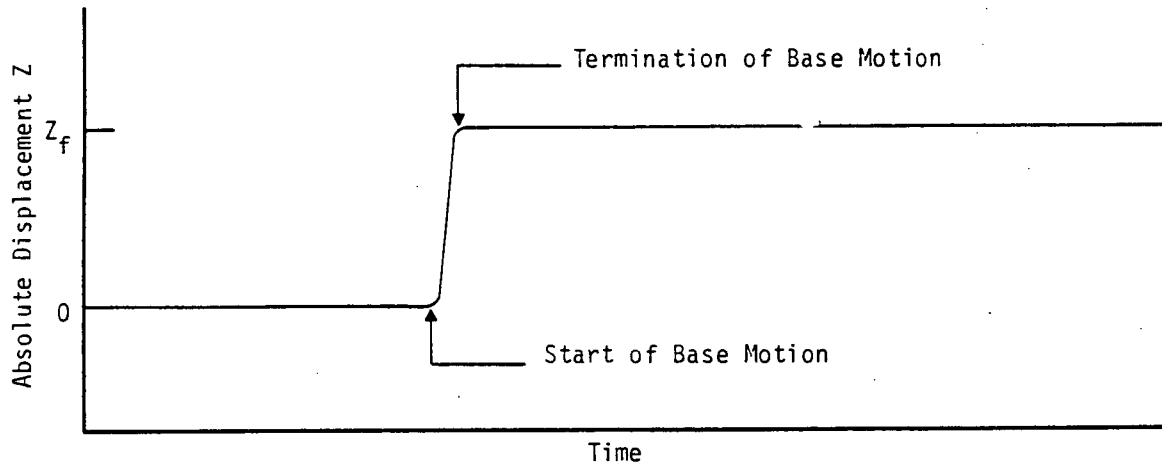
support bases were given a sudden simultaneous equal displacement from one value to another (see Figure 3-9[a]). Once the bases had stopped moving, the pipeline continued to undergo decaying free vibration motion (see Figure 3-9[b]). After the transient motion of the pipe had decayed to zero, the final displacement of the pipe was equal to that of the bases. The displacement motion of the pipe in the Z direction was almost entirely dominated by the first mode (natural frequency of about 7.3 Hz) for all the support configurations. Thus, it was easy to use the log decrement method for obtaining estimates of damping for each configuration. The log decrement damping formula is:

$$\beta^{(1)} = \ln(z_0/z_1)/2\pi f$$

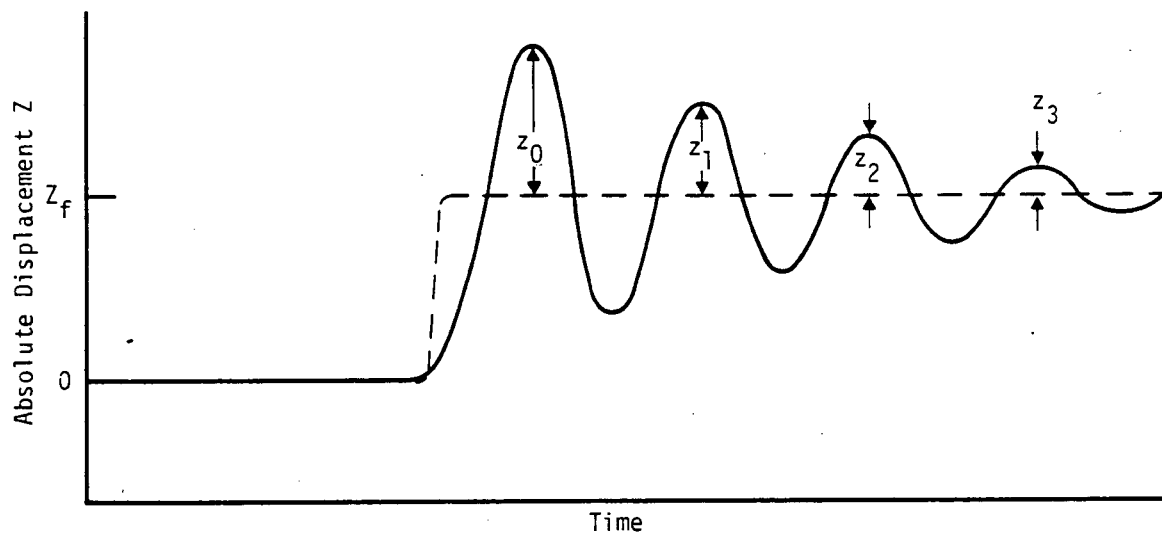
where z_0 and z_1 are the relative amplitudes of the peaks of the o th and i th cycles, respectively. In making the damping calculations, the o th cycle was taken at the first peak in the displacement time trace. All the calculations for a given time trace were based on this o th cycle. Calculations were done for the first three cycles of oscillation. For each set of test results that were analyzed, the three largest response channels (always displacement channels) were used for damping calculations; they corresponded to three of the following four locations/directions: Points 2.0Z, 2.1Z, 3.0Z, and 3.1Z. For a given cycle of oscillation, the average value of damping was determined from the three channels. The extreme deviation from the average value was also determined. Table 3-9 presents the results of all the damping calculations that were performed for the various support configurations.*

Several observations may be made regarding the averaged damping results. First, for the first cycle of motion, the apparent damping increased with response level; for the second cycle, the damping increased or remained constant. Second, for a given midpoint support type and excitation level,

* Only the first-mode damping was calculated. This is because only the log decrement method was used for damping estimation, and the transient response data, to which this method was applied, was dominated essentially by only the first mode.



(a) Motion of All Bases (Base Input)



(b) Motion of a Point on the Pipeline (Not at a Base)

Figure 3-9. Schematic Representation of Displacement Time Histories for Step-Loading Tests

Table 3-9

AVERAGE LOG DECREMENT DAMPING (FIRST MODE) AS A FUNCTION
OF EXCITATION LEVEL AND FREE VIBRATION CYCLE NUMBER

Support Type	<u>Lower Level Response Damping (%)*</u>			<u>Higher Level Response Damping (%)*</u>		
	<u>Cycle 1</u>	<u>Cycle 2</u>	<u>Cycle 3</u>	<u>Cycle 1</u>	<u>Cycle 2</u>	<u>Cycle 3</u>
Weak Strut 1	**			1.9 ± 0.3 (2,300 lbf, 1.15 in., 9.3 g, 605 µε)	1.8 ± 0.1	1.7 ± 0.2
PSA-1 Snubber	1.6 ± 0.1 (1,250 lbf, 0.53 in., 4.6 g, 395 µε)	2.2 ± 0.1	2.3 ± 0.1	2.4 ± 0.3 (2,200 lbf, 1.07 in., 9.3 g, 590 µε, 0.87)	2.2 ± 0.2	1.8 ± 0.1
Grinnell Snubber	2.7 ± 0.1 (1,600 lbf, 0.72 in., 4.3 g, 470 µε)	3.1 ± 0.1	2.9 ± 0.1	3.0 ± 0.2 (3,300 lbf, 2.01 in., 10.9 g, 1,040 µε, 0.79)	3.1 ± 0.2	3.1 ± 0.1
Bergen-Paterson Snubber	2.3 ± 0.2 (1,300 lbf, 0.51 in., 3.2 g, 350 µε)	2.8 ± 0.2	2.7 ± 0.0	4.0 ± 0.3 (2,700 lbf, 1.53 in., 8.7 g, 773 µε, 1.05)	3.8 ± 0.1	3.5 ± 0.1

* The damping values presented in this table are average values and the corresponding extreme variations from average. The data used to calculate the average damping were taken from displacement channels corresponding to locations Point 2.0Z, Point 2.1Z, Point 3.0Z, and Point 3.1Z.

** Tests of the breakable strut were not performed at a lower level of excitation.

NOTE: The quantities in parentheses, (), are the peak (maximum) support load (at Point 1.4), peak relative displacement (Point 3.0Z), peak absolute acceleration (Point 3.0Z), peak strain (Point 3.0/+Z face of pipe/axial gage), and peak ASME stress ratio (curved pipe at Point 2.0 or 3.0). The ASME stress ratio was calculated using the 1981 edition, Winter addenda, of the code; it was calculated for only some of the higher level tests.

as the cycle number increased (the response decreased) the damping could either increase or decrease, depending on the excitation level. The question might be raised as to why the damping increased with increasing response in some cases and increased with decreasing response for other cases. A possible answer to this question, for the case of the snubbers, could consist of the following: (1) as the response level of the pipe at its midpoint (Point 1.4) continued to increase beyond a threshold value, the snubber locked up more and more, thus dissipating more and more energy (the snubber lockups would tend to act somewhat like impacts--an energy dissipation mechanism); (2) as the response level at the snubber continued to decrease towards and below the threshold value, the energy loss because of snubber lockup decreased (below the response threshold, the snubber never locked up); (3) at high levels of response, the energy loss (because of Coulomb and other frictional effects) was probably negligible compared to the loss due to snubber lockup; and (4) at low response levels, the Coulomb and other frictional effects were much more important than snubber lockup. It may be postulated that at high response levels, damping was influenced greatly by snubber lockup, with the damping increasing as the response level increased. At low response levels, the damping was due largely to the energy loss from Coulomb and other frictional effects, with the damping increasing as the response level decreased.*

The above discussion is based on the average damping data presented in Table 3-9. In addition to these data, the damping corresponding to a particular data channel (Point 3.0Z displacement) was investigated to see if the same trends were apparent for both average and channel damping (see Table 3-10). This data channel (Point. 3.0Z) generally had the largest response. As can be seen, both the average and channel damping show generally the same trends; hence, the tentative conclusion given above (concerning the variation of damping with response) appears to be reasonable.

Base step tests (producing free vibrations) were not executed for the Phase I tests (box frame support). Thus, damping estimates, for Phase I, must be extracted by using earthquake simulation damping which produces a best fit between predicted and experimental piping response.

Table 3-10

LOG DECREMENT DAMPING (FIRST MODE) OBTAINED
FOR POINT 3.0Z DISPLACEMENT CHANNEL

<u>Support Type</u>	<u>Lower Level Response Damping (%)*</u>			<u>Higher Level Response Damping (%)*</u>		
	<u>Cycle 1</u>	<u>Cycle 2</u>	<u>Cycle 3</u>	<u>Cycle 1</u>	<u>Cycle 2</u>	<u>Cycle 3</u>
Weak Strut 1	*			2.2 (2,300 lbf; 1.15 in.; 9.3 g; 605 $\mu\epsilon$)	2.0 (2,300 lbf; 1.15 in.; 9.3 g; 605 $\mu\epsilon$)	1.8 (2,300 lbf; 1.15 in.; 9.3 g; 605 $\mu\epsilon$)
PSA-1 Snubber	1.7 (1,250 lbf; 0.53 in.; 4.6 g; 395 $\mu\epsilon$)	2.3 (1,250 lbf; 0.53 in.; 4.6 g; 395 $\mu\epsilon$)	2.2 (1,250 lbf; 0.53 in.; 4.6 g; 395 $\mu\epsilon$)	2.0 (2,200 lbf; 1.07 in.; 9.3 g; 590 $\mu\epsilon$; 0.87)	2.0 (2,200 lbf; 1.07 in.; 9.3 g; 590 $\mu\epsilon$; 0.87)	2.0 (2,200 lbf; 1.07 in.; 9.3 g; 590 $\mu\epsilon$; 0.87)
Grinnell Snubber	2.8 (1,600 lbf; 0.72 in.; 4.3 g; 470 $\mu\epsilon$)	3.0 (1,600 lbf; 0.72 in.; 4.3 g; 470 $\mu\epsilon$)	3.0 (1,600 lbf; 0.72 in.; 4.3 g; 470 $\mu\epsilon$)	3.0 (3,300 lbf; 2.01 in.; 10.9 g; 1,040 $\mu\epsilon$; 0.79)	3.3 (3,300 lbf; 2.01 in.; 10.9 g; 1,040 $\mu\epsilon$; 0.79)	3.1 (3,300 lbf; 2.01 in.; 10.9 g; 1,040 $\mu\epsilon$; 0.79)
Bergen-Paterson Snubber	2.4 (1,300 lbf; 0.51 in.; 3.2 g; 350 $\mu\epsilon$)	2.9 (1,300 lbf; 0.51 in.; 3.2 g; 350 $\mu\epsilon$)	2.7 (1,300 lbf; 0.51 in.; 3.2 g; 350 $\mu\epsilon$)	3.9 (2,700 lbf; 1.53 in.; 8.7 g; 773 $\mu\epsilon$; 1.05)	3.7 (2,700 lbf; 1.53 in.; 8.7 g; 773 $\mu\epsilon$; 1.05)	3.4 (2,700 lbf; 1.53 in.; 8.7 g; 773 $\mu\epsilon$; 1.05)

* Tests of the struts were not performed at the lower level.

NOTE: The quantities in parentheses, (), are the peak (maximum) support load (at Point 1.4), peak relative displacement (Point 3.0Z), peak absolute acceleration (Point 3.0Z), peak strain (Point 3.0/+Z face of pipe/axial gage), and peak ASME stress ratio (curved pipe at Point 2.0 or 3.0).

The log decrement method of calculating the damping from experimental response data was chosen because it appears to be the most reliable method at present for damping estimation. There are numerous methods currently available for calculating damping (e.g., half-power, least squares). All of them are based on the definition of a linear theoretical model. When the physical system, for which damping is to be calculated, is even slightly nonlinear, the damping estimates obtained by frequency domain methods (e.g., half-power) can possess substantial error because of resonant peak broadening [2]. The log decrement damping is not influenced by a change in the period (for the mode in question)--for this reason, it appears to be a better measure of damping for certain types of nonlinear systems.

3.2.2 Support Influence With Support Failure

Some high-level earthquake tests were planned for which the midpoint support was to fail. The purpose of these tests was to obtain benchmark data for the failure of struts, mechanical snubbers, and hydraulic snubbers. These data could be used to study (1) damping changes, (2) higher or lower stress levels due to the pipe response transients associated with going from a system with one set of natural frequencies and modes to a different one, and (3) support capacity and failure mechanisms.

When a pipe support fails, it can do so in a variety of ways. For a strut type of support, the only failure mode is a complete, or essentially complete, break at some point in the support. For a snubber type of support, the possible failure modes include the following: (1) damage of snubber internals, or other parts, resulting in a complete separation of the snubber into two or more parts (support effectively removed from pipe system); (2) damage to snubber, resulting in permanent snubber lockup (for pipe response below the level necessary to achieve a complete break [disconnection]); and (3) damage resulting in malfunctioning of snubber mechanism (internals), but without a complete break or permanent lockup.

When there is a complete break in a pipe support some of the mode shapes change, together with a corresponding change in the natural frequencies. This can be seen for the subject piping system (see Table 3-8) Natural frequencies were determined for a variety of midpoint supports. The first two natural frequencies were essentially the same: 7.3 Hz, 0.13 Hz, and 15.4 Hz, 0.70 Hz for the average natural frequency and standard deviation

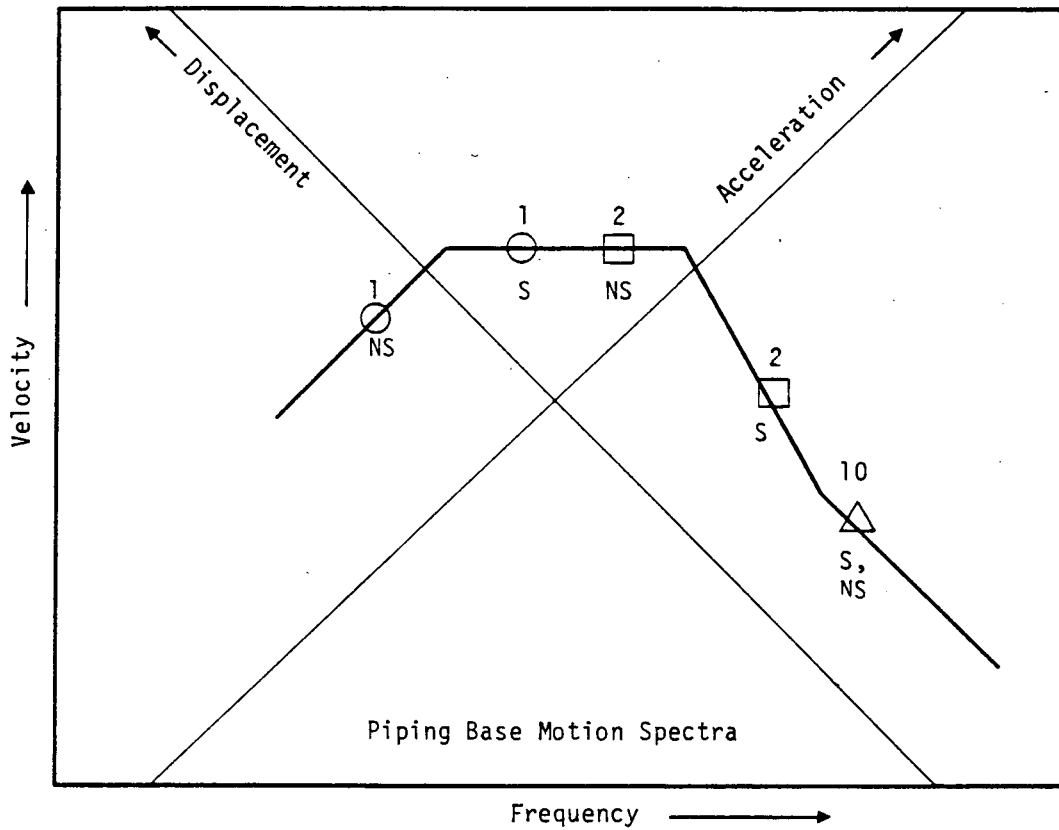
for the first and second modes, respectively. The natural frequencies for the pipe system without a midpoint support are 3.5 Hz and 12.2 Hz. Thus, a test with a complete break of the midpoint support would result in a decrease of the first and second natural frequencies by about 50% and 20%, respectively. Obviously, the lower modes changed radically. The higher modes would have been affected considerably less than the lower ones.

When there is complete snubber lockup during a test, the system modal properties change. This change is not very large because the snubbers, when excited by sufficiently large loads, are locked up for a considerable amount of time. This can be seen by the fact that the first two natural frequencies for a midpoint support were considerably higher than they were for no support. If the response levels for the tests used to obtain the frequencies for a midsupport were sufficiently low, the support would have not added any stiffness to the system and the snubber would not have locked up. Thus, the natural frequencies would increase for complete snubber lockup only to the degree that the snubber locked up more. A discussion of snubber lockup is given in Reference 4.

For a given earthquake base motion, when a support experiences a complete break, the response of the piping system can change radically. This is due to (1) a change in the modal properties, (2) a change in the damping, and (3) a change in which modes are excited the most. When the natural frequencies of a system change (increase or decrease), their corresponding modes will be excited differently. This obvious comment is expressed graphically by the example given in Figure 3-10.

Five tests were performed where the midpoint support failed (see Table 3-11). Obviously, the supports failed because they did not have the necessary load-carrying capacity. These supports were undersized for this pipeline and for the level of earthquakes used as base motion input. The other tests where a support failure was planned (see Table 3-2) did not result in a support failure because the supports were closer to being properly sized for the pipe system/earthquake-level. Several of the support failure tests (failure occurred) are discussed below.

The first support failure test to be discussed is test T3R13 with a PSA-1/4 mechanical shock arrestor. Figure 3-11 gives plots of snubber load and pipe



Indicator of Natural Frequency

<u>Mode</u>	<u>Symbol</u>
1	○
2	□
10	△

(Note: S and NS refer to midpoint support and no midpoint support, respectively.)

Mode	Natural Frequency Change	Change in Peak Response		
		Displacement	Velocity	Acceleration
1	decrease	increase	decrease	decrease
2	decrease	increase	increase	none
10	none	none	none	none

Figure 3-10. Example of Change in Peak Response Due to Complete Break of Midpoint Support

Table 3-11

EARTHQUAKE TESTS INDUCING PIPE SUPPORT FAILURE

<u>Midpoint Support</u>	<u>Test</u>	<u>Peak Pipe Support Load (lbf)</u>	<u>Percent of C/D Level</u>	<u>Comments on Support Failure</u>
Anchor/ Darling-40	T2R7	1,120	210	Failure of snubber internals (at rack gear) leaving them separated but impacting during earthquake.
PSA-1/4	T4R7B	1,900	380	Snubber partially locked up permanently, with travel limited to $\pm 1/2$ in.
PSA-1/4	T3R13	1,900	380	Failure of 1/8 in. diameter shaft support pin, resulting in complete separation of snubber into two halves.
Weak Strut 1	T4R3	1,670	106*	Support was fatigued to failure (rupture).
Weak Strut 2	T4R5	4,700	157*	Support was fatigued to failure (rupture).

* There was no C/D load rating for the struts; this is the percent of the minimum yield load for the strut.

midpoint displacement. Before the PSA-1/4 snubber was essentially unable to transmit a load to the pipe (see note (4) in Figure 3-11[a]), it was locked up a great deal of the time. This conclusion was reached because the snubber load was greater than the A/B load for the snubber for much of the time before the time corresponding to note (4). Thus, the first two natural frequencies of the system, before complete snubber break, were greater than those given in Table 3-8 for the case of no support. They were probably less than those for the PSA-1 snubber, because the PSA-1/4 snubber is less stiff than the PSA-1 snubber. However, once the PSA-1/4 snubber lost its ability to exert a force on the pipe (did not contribute to the stiffness of the system), the first two natural frequencies were equal to those for the case of no midpoint support (3.5 Hz and 12.2 Hz for the first two frequencies). This can be seen in Figure 3-11(b).

The above comments on the system natural frequencies before and after support failure, lead to some tentative conclusions about the support failure. The PSA-1/4 snubber experienced a considerable amount of loading greatly in excess of its C/D load rating. It is likely that it experienced some heavy wear because of this. The major portion of the damage probably occurred during the time up to and when the snubber load reached -1900 lbf (see Note 1 of Figure 3-11[a]). However, this did not result in complete snubber failure. As the snubber continued to displace, its internal mechanism still continued to function to some extent. This resulted in some load being exerted on the pipe. However, note (3) indicates that the first piping mode had a natural frequency of about 3.4 Hz; thus, a fair amount of separation (partial break) of snubber internals must have occurred, even though there was still some contact between them. The last major contact of the snubber internals occurred at Note 4. By this time there was basically a complete break at the snubber (the first natural frequency had been about 3.4 Hz for a couple of cycles of response). After Note 4, load was transmitted to the pipe at only a few points in time. This was due to the two halves of the snubber impacting each other or adjacent structures.

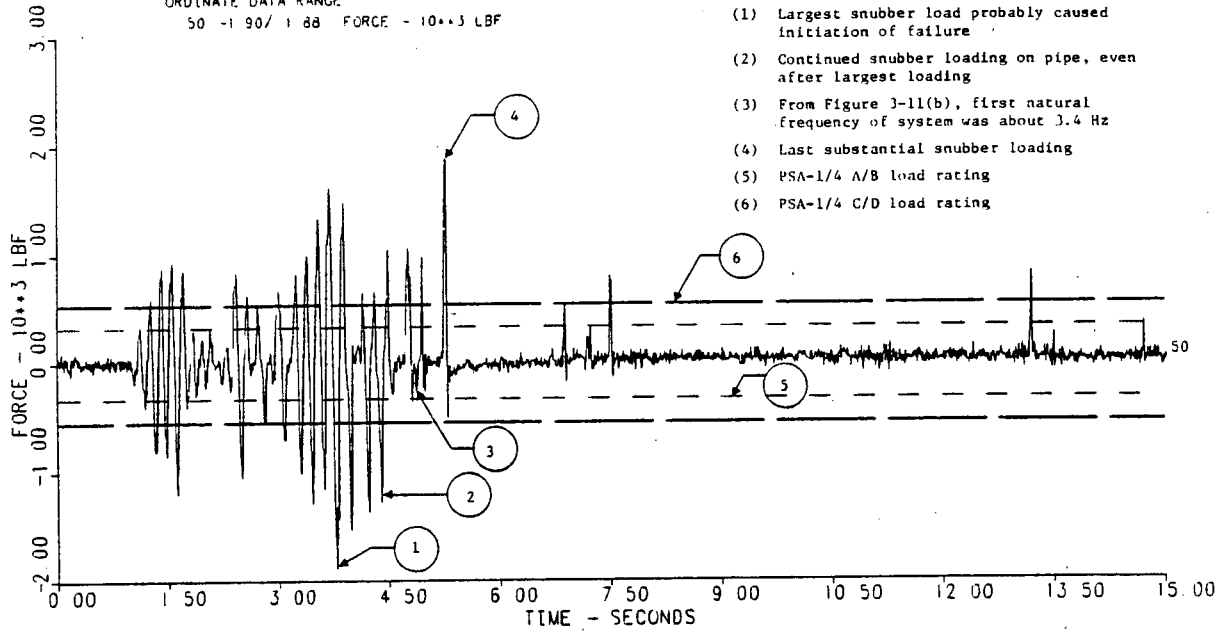
The second support failure test to be discussed is Test T4R5 with weak Strut 2. Figure 3-12 gives plots of strut load and pipe midpoint displacement. The failure (rupture) of the support is very apparent (it occurred at about 9.2 s). There were 19 cycles of oscillation with the peak support load greater than or equal to the minimum yield load. When the support ruptured, the displacement of the pipe at its midpoint increased dramatically.

HIGH LEVEL E Q WITH SNUBBER PSA-1/4

TEST 3 RUN 13
 ORDINATE DATA RANGE
 50 -1.90 / 1.88 FORCE - 10**3 LBF

Notes

- (1) Largest snubber load probably caused initiation of failure
- (2) Continued snubber loading on pipe, even after largest loading
- (3) From Figure 3-11(b), first natural frequency of system was about 3.4 Hz
- (4) Last substantial snubber loading
- (5) PSA-1/4 A/B load rating
- (6) PSA-1/4 C/D load rating

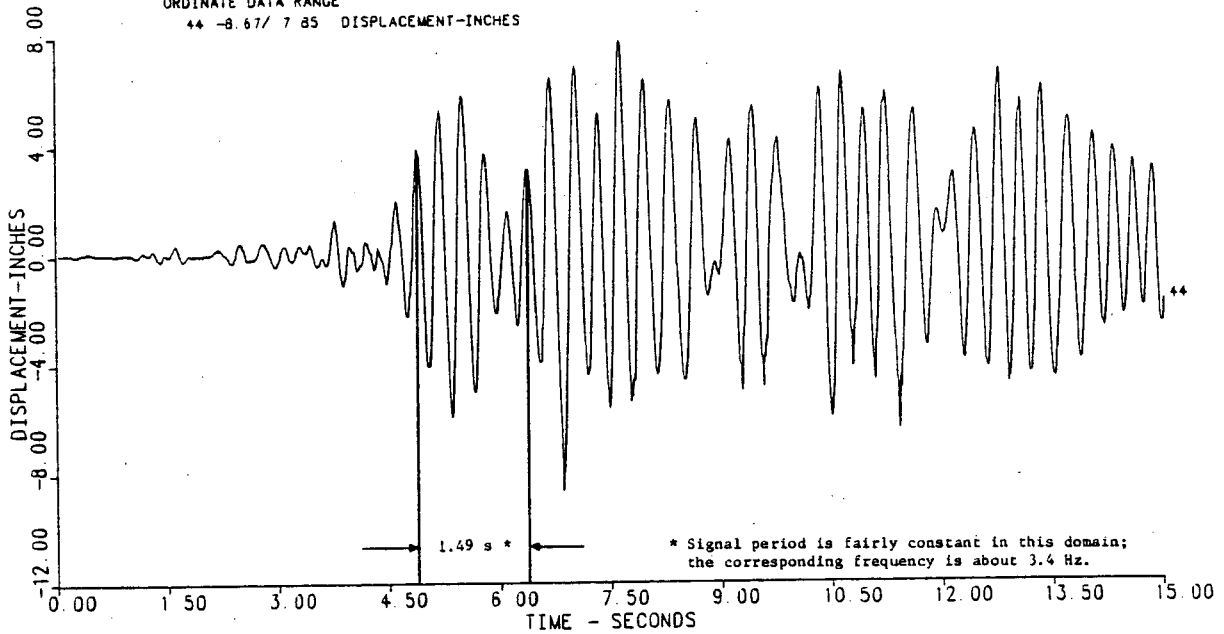


CHANNEL 50 007183 PT 1 + NORTH FORCE KIPS

(a) Snubber Force on Pipe

HIGH LEVEL E Q WITH SNUBBER PSA-1/4

TEST 3 RUN 13
 ORDINATE DATA RANGE
 44 -8.67 / 7.85 DISPLACEMENT-INCHES



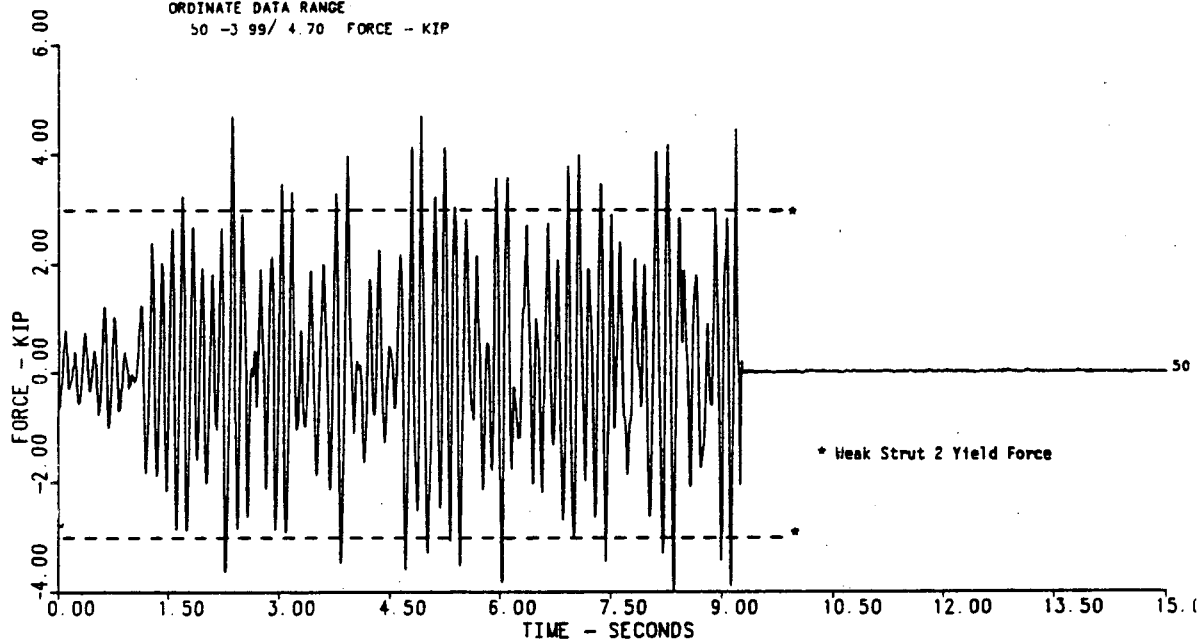
CHANNEL 44 A03350 PT 1 + Z DISPLACEMENT INCHES

(b) Pipe Midpoint Absolute Displacement

Figure 3-11. Snubber Failure Test with PSA-1/4 Snubber

MODERATE LEVEL E. Q. W/STRUT #2 TO FAILURE T4R5 12/28/81

TEST 4 RUN: 5
 ORDINATE DATA RANGE
 50 -3 99/ 4.70 FORCE - KIP

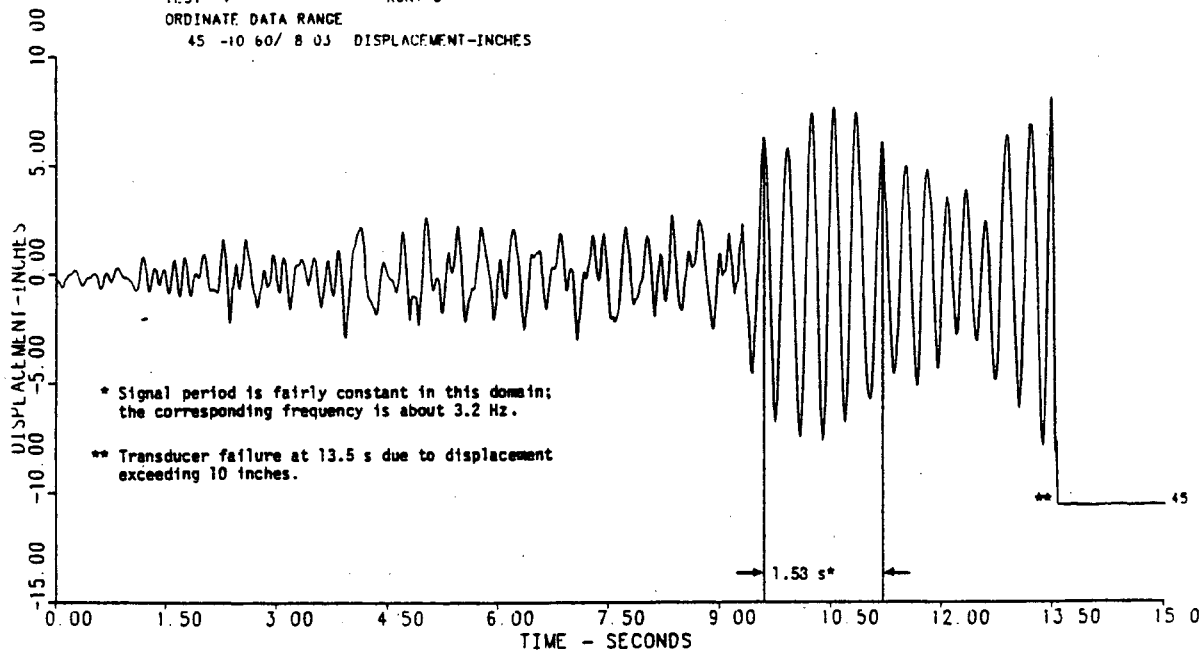


CHANNEL 50 007183 PT. 1.4 NORTH FORCE KIPS

(a) Snubber Force on Pipe

MODERATE LEVEL E. Q. W/STRUT #2 TO FAILURE T4R5 12/28/81

TEST 4 RUN: 5
 ORDINATE DATA RANGE
 45 -10 60/ 8 0.5 DISPLACEMENT-INCHES



CHANNEL 45 A0JJ49 PT. 1.6 Z DISPLACEMENT INCHES

(b) Absolute Displacement of Pipe Near Mid-Point

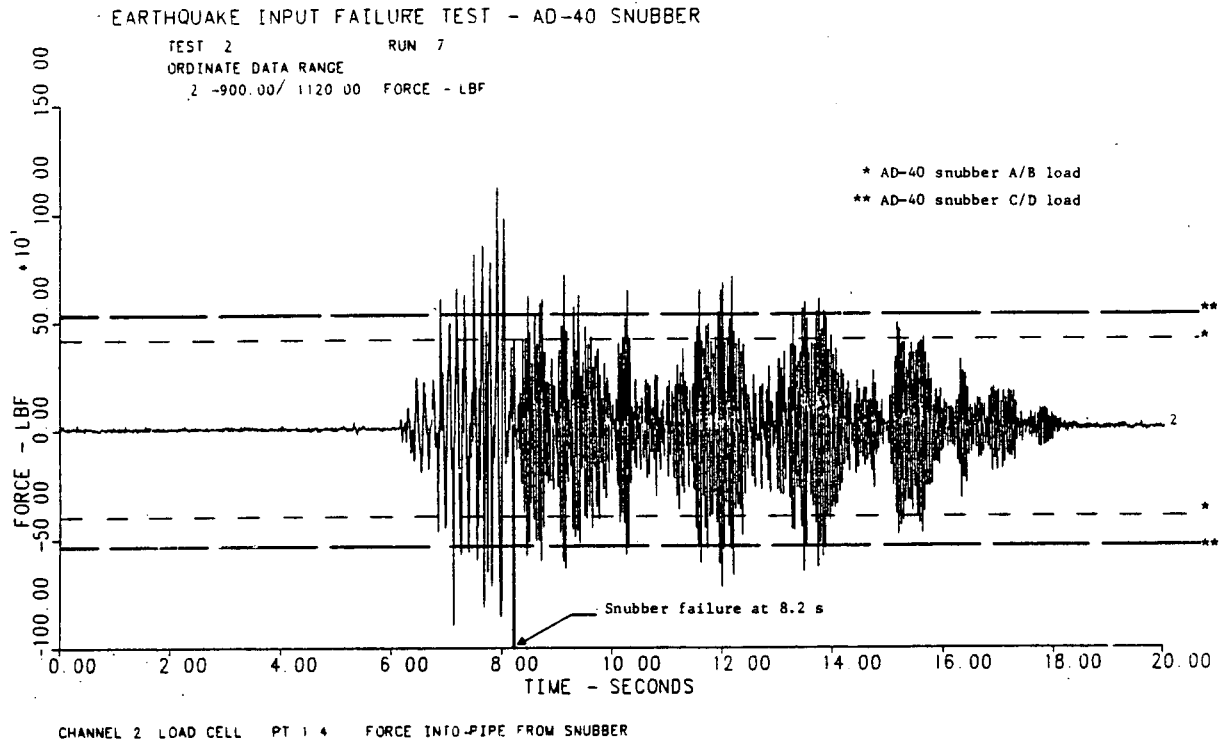
Figure 3-12. Snubber Failure Test With Weak Strut 2

The first natural frequency of the pipeline (after support failure), as determined from the displacement time trace in Figure 3-12, was about 3.2 Hz. This is approximately equal to the value of 3.5 Hz obtained from the sine dwell tests (see Table 3-8). Using the values from the sine dwell tests, the first two natural frequencies dropped from 7.4 Hz and 16.0 Hz to 3.5 Hz and 12.2 Hz, respectively, upon support failure.

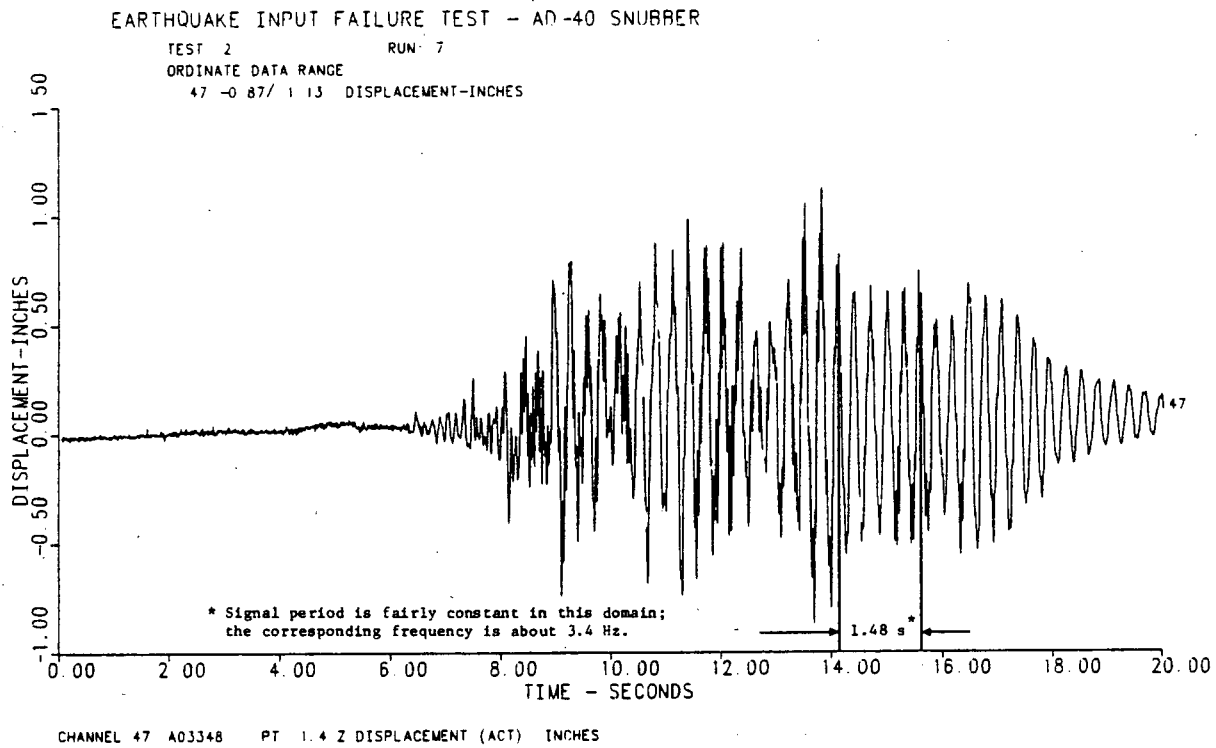
The final support failure test, where there was a midpoint support failure, to be discussed is Test T2R7 with an Anchor/Darling-40 snubber. Figure 3-13 gives plots of snubber force and pipe midpoint displacement. This snubber failure is not as apparent as the previous two support failures. However, a definite change in the snubber force time history is noted at about 8.2 s. There is a change in both the frequency content and the overall amplitude. The earthquake base motion had about the same frequency content and amplitude for the entire event. This indicates that the snubber force, without snubber failure, should have had the same general frequency content and amplitude for the entire event. Thus, the time point of the noticeable change in these properties of the snubber force is the time at which failure occurred (8.2 s).

The fact that the snubber force did not go to, and remain at, zero at 8.2 s is easily explained. After the test, the Anchor/Darling-40 snubber was inspected. It was very easily separated into two pieces--an inner shaft from one end of the snubber slid out of an outer shaft from the other end of the snubber with no resistance. (The snubber was separated at the rack gear.) When the snubber, after failure, was excited dynamically, the inner shaft remained inside the outer shaft, and snubber internals impacted with each other. This resulted in the very high-frequency content of the force signal after 8.2 s.

Two other failure type tests were performed. They were earthquake tests of an ITT Grinnell and Bergen-Paterson snubber (see Figures 3-14 and 3-15). Snubber failures were not experienced for the tests. This was possibly due to the fact that the snubbers did not experience as severe loading as did the failed supports. The C/D load rating for these hydraulic snubbers was considerably greater than that for the failed mechanical snubbers.



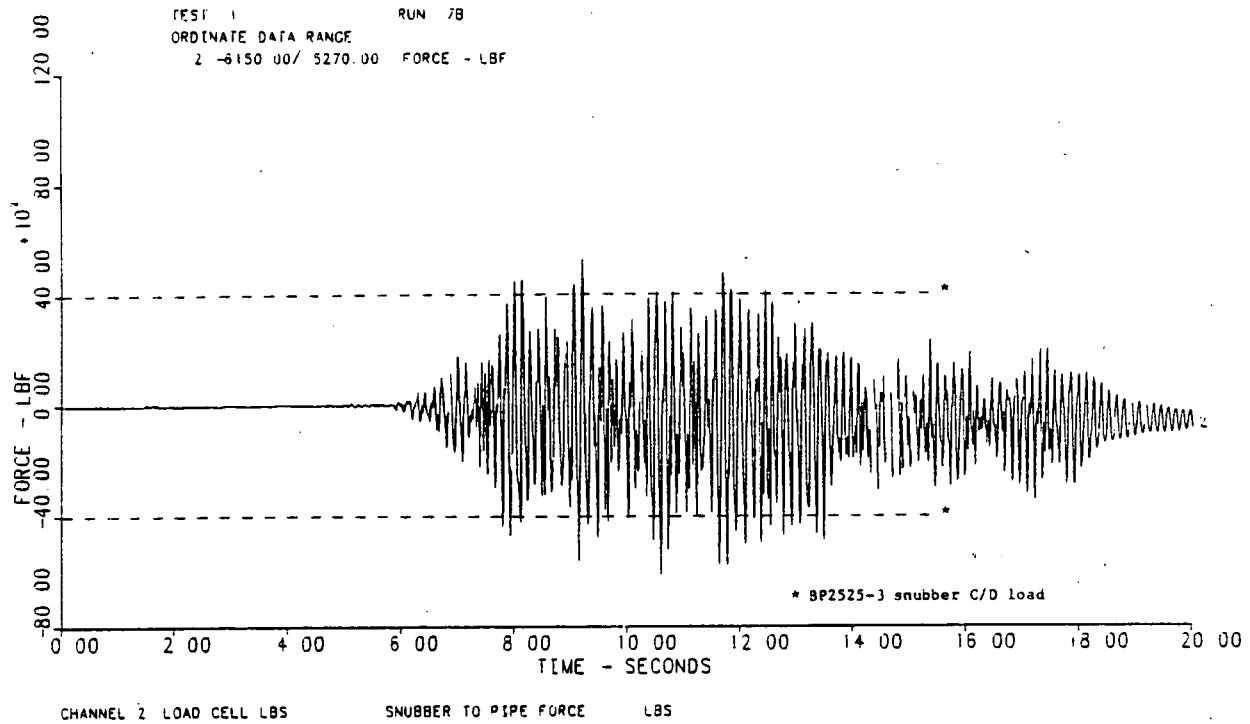
(a) Snubber Force on Pipe



(b) Pipe Midpoint Absolute Displacement

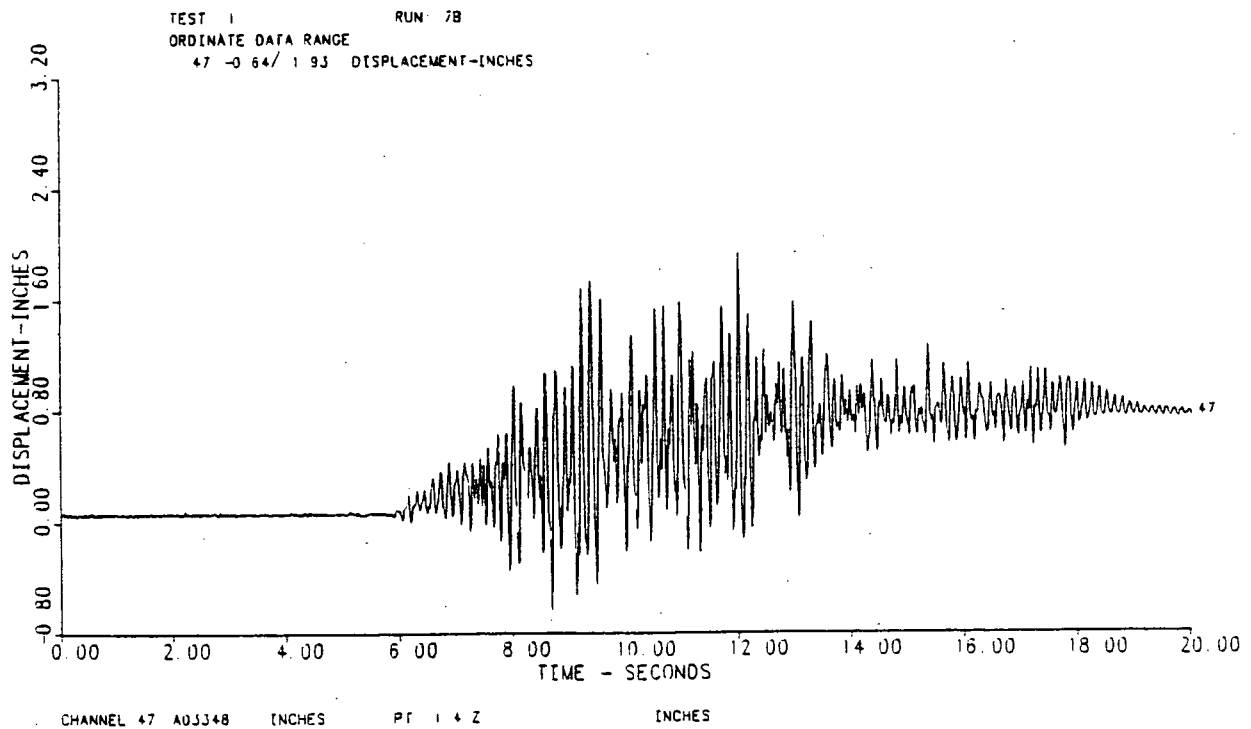
Figure 3-13. Snubber Failure Test with A/D-40 Snubber

FAILURE TEST REPEAT. EARTHQUAKE INPUT. BP-2525-3 SNUBBER



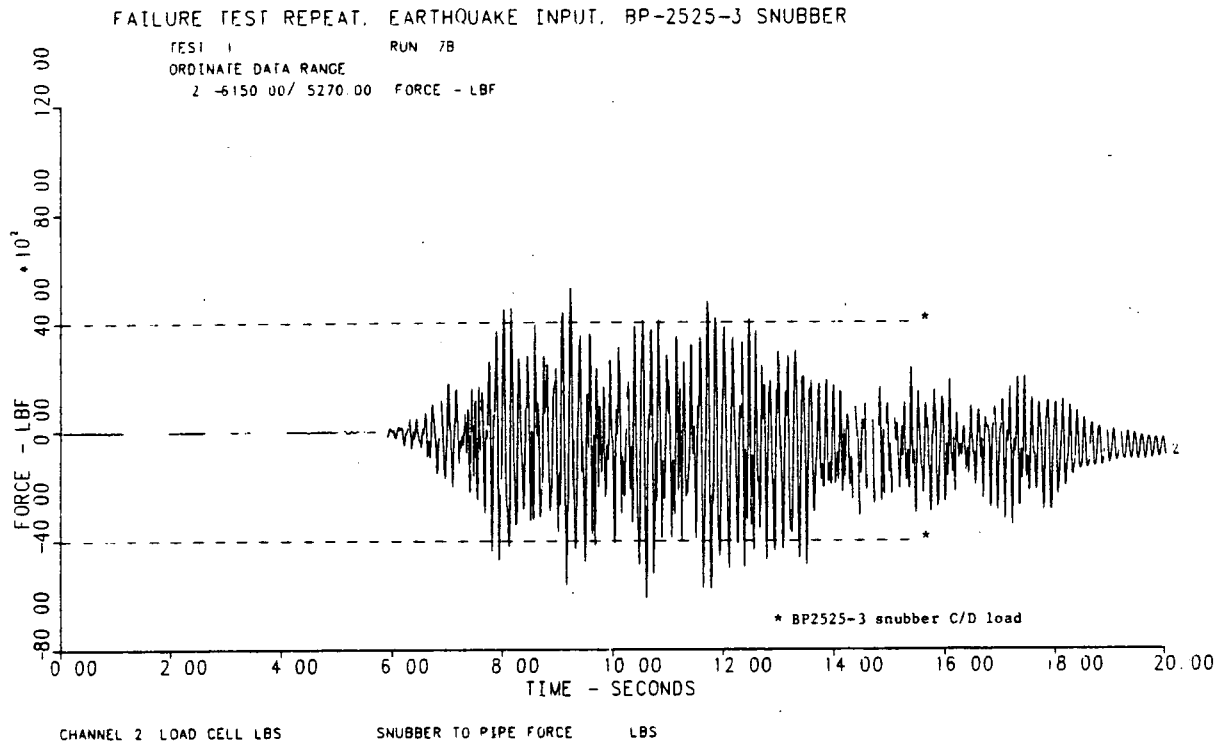
(a) Snubber Force on Pipe

FAILURE TEST REPEAT. EARTHQUAKE INPUT. BP-2525-3 SNUBBER

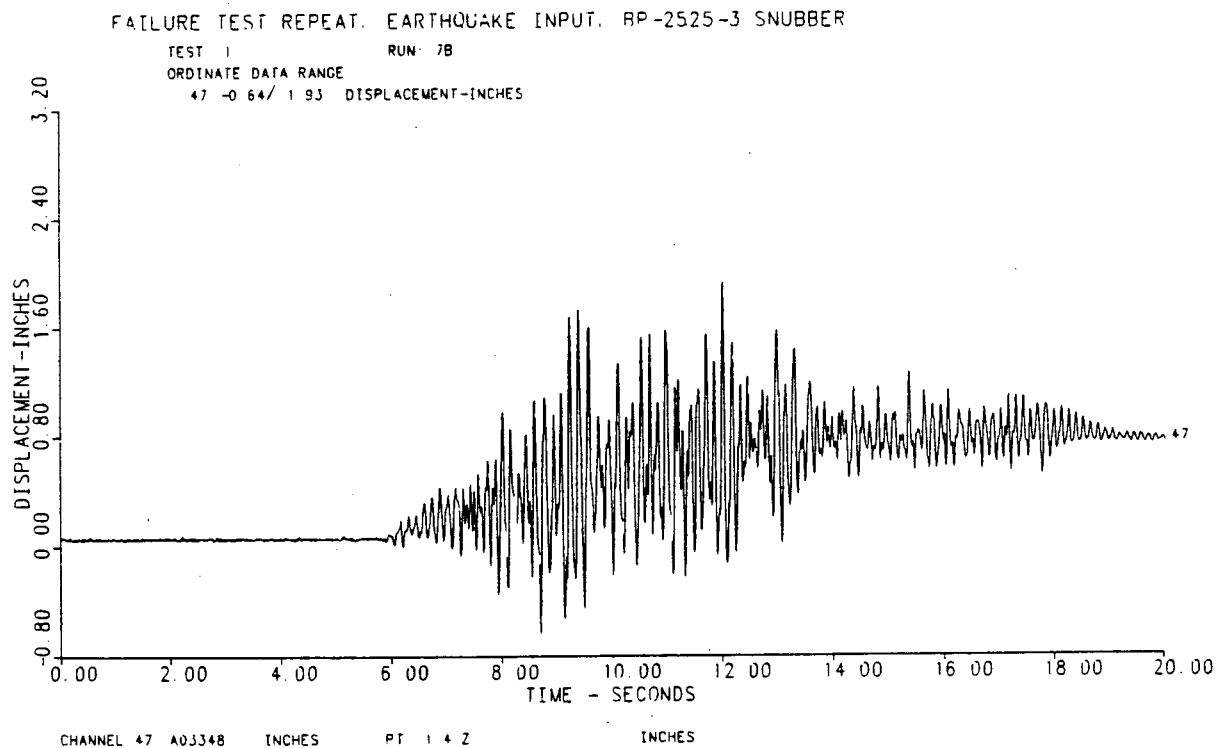


(b) Pipe Midpoint Absolute Displacement

Figure 3-14. Attempted Snubber Failure Test with ITT Grinnell Snubber



(a) Snubber Force on Pipe



(b) Pipe Midpoint Absolute Displacement

Figure 3-15. Attempted Snubber Failure Test with Bergen-Paterson Snubber

The two displacement traces (Figures 3-14[b] and 3-15[b]) show a permanent offset by the end of the earthquake events. There are several possible sources of the offsets; they are (1) plastic deformation of the pipe, (2) ratcheting of the midpoint snubber, and (3) the final positions of the bases are different from their initial positions. In looking at the strain time histories for the two tests, many of them indicate that there was permanent deformation of the pipe. Some of the permanent strain offsets were on the order of $250\mu\epsilon$. Also, the maximum ASME stress ratio (a value of one indicates a Level D stress condition) for the two tests was greater than 2.5. Even though this does not reflect how much plastic deformation has occurred, it does indicate that yielding has occurred. Therefore, some of the permanent offset in the displacement traces was probably due to plastic deformation of the pipe. Another possible source of the permanent displacement offset is the ratcheting of the snubbers. If, as the pipe response level increased, the snubbers tended to displace to the next displacement level and lock (against displacing less), eventually the snubbers would have a large permanent displacement. However, this is not too likely, as the snubbers would have to be in a failure mode for this to occur. In looking at the final position of the bases (see Figure 3-16), it is seen that the base at Point 4.0 did not return to its initial position. This could be due to plastic deformation, a locking snubber, or the operation of the hydraulic actuator system. From the available data, it is not surprising that there was some permanent offset in some of the displacements. The offsets could be due to any, or all, of the above-mentioned items.

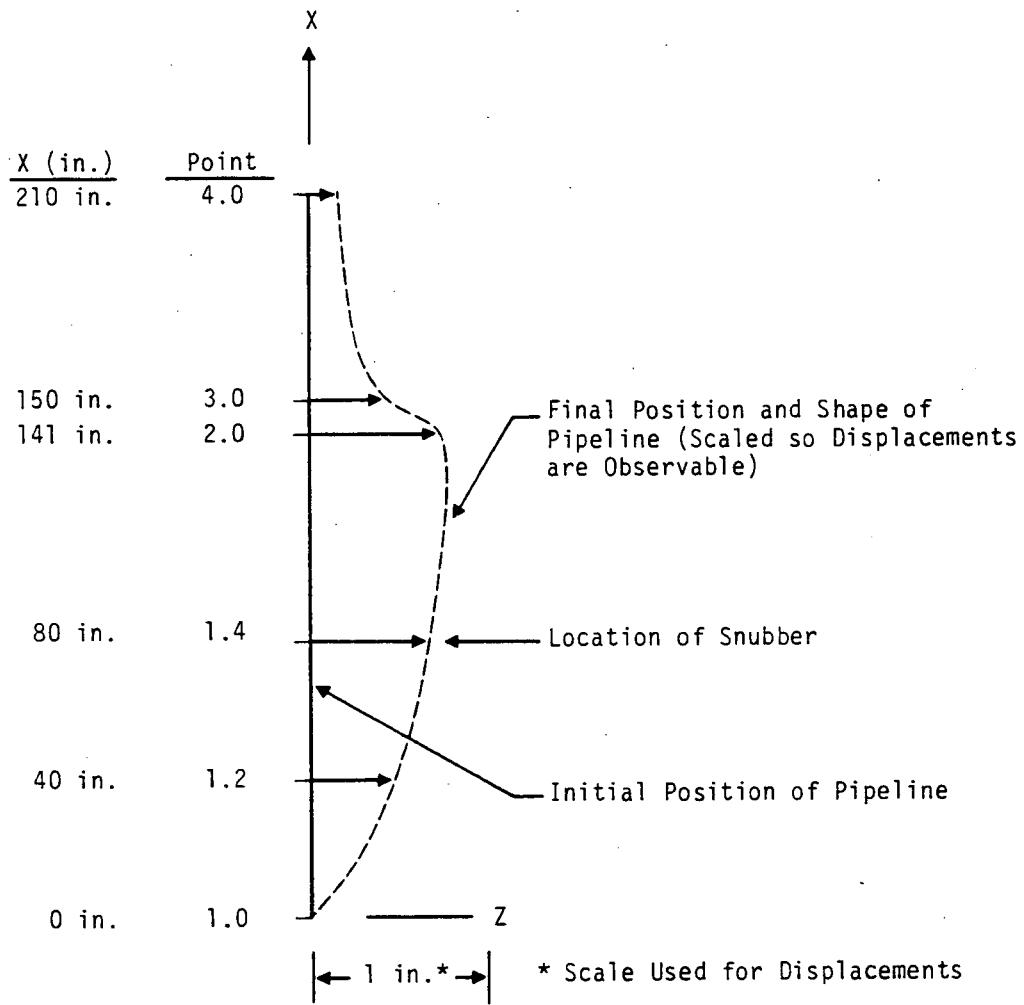


Figure 3-16. Final Position and Shape of Pipeline After High-Level Earthquake Test (T1R7B)--Bergen-Paterson Snubber Used

Section 4

FINDINGS

The limited testing conducted demonstrated the feasibility of executing, in a laboratory environment, multiple support excitation experiments inducing severe piping dynamic response. In addition, test data have been provided for a relatively simple piping system for benchmarking both linear and non-linear calculational tools. The data include the case of support failure in the course of dynamic loading.

The tested piping systems successfully withstood repeated earthquake-like loading at input levels from three to five times those necessary to exceed the ASME Class 2 Level D stress limit for primary loads. Even with midpoint support failure, piping pressure integrity was maintained. The tests demonstrated the difficulty of inducing pressurized piping failure (leakage or plastic collapse) with dynamic loads and provided evidence of the large safety margins that are believed to exist for nuclear power plant piping subjected to seismic loads.

In addition, the seismic testing of the piping indicated that the snubber hardware used had apparent failure loads that were two to four times the manufacturer's specified load limit. Piping system damping was observed to range from about two percent to four percent of critical, generally increasing somewhat with response amplitude and varying with support type. The observed damping was at least twice the one percent used in U.S. design practice for the Operating Basis Earthquake for four-inch piping, and up to twice the damping currently used for the Safe Shutdown Earthquake condition.

Section 5

REFERENCES

1. G.E. Howard, et al. "Piping Extreme Dynamic Response Studies." Nuclear Engineering and Design 77 (1984) 405-417, North Holland, Amsterdam.
2. "Testing and Analysis of Feedwater Piping at Indian Point, Unit 1, Volume 1: Damping and Frequency." Electric Power Research Institute Report EPRI/NP-3108, Volume I, July 1983.
3. P. Bezler, et al. "In-Situ and Laboratory Benchmarking of Computer Codes Used for Dynamic Response Predictions of Nuclear Reactor Piping." Department of Nuclear Energy, Brookhaven National Laboratory, Upton, Long Island, New York, NUREG/CR-3340, May 1983.
4. "Testing and Analysis of Feedwater Piping at Indian Point, Unit 1, Volume 2: Piping Response and Support Load." Electric Power Research Institute Report EPRI/NP-3108, Volume 2, forthcoming.

Appendix A
ULTRASONIC THICKNESS MEASUREMENTS
OF PIPING RUNS

Extensive pipe wall thickness measurements were made of the Phases I and II pipelines. The results obtained are presented herein.

Table A-1
PIPE WALL THICKNESS MEASUREMENTS--PHASE I PIPELINE

Location (Coordinate in Inches)	Circumferential Location				
	X	Y	-Y	Z	-Z
16	.236	.237	.223	.236	
36	.227	.228	.231	.230	
56	.228	.230	.229	.237	
72	.227	.232	.230	.234	
88	.228	.231	.233	.236	
104	.226	.232	.229	.236	
108	.241	.225	.245	.237	
119	.232	.228	.241	.242	
130	.241	.216	.240	.240	
Lower Bend	Z	-Z	45° Top	45° Bottom	
Center	.232	.236	.278	.195	
Y	X	-X	Z	-Z	
11	.215	.237	.236	.239	
23	.223	.237	.236	.241	
35	.227	.229	.226	.236	
49	.230	.236	.236	.230	
Upper Bend	Z	-Z	45° Top	45° Bottom	
Center	.229	.238	.197	.269	
X	Y	-Y	Z	-Z	
152	.231	.230	.225	.224	
166	.233	.224	.232	.228	
180	.233	.230	.230	.227	
194	.237	.223	.233	.223	

Table A-2

PIPE WALL THICKNESS MEASUREMENTS--PHASE II PIPELINE

Location (Coordinate in Inches)	Circumferential Location				
	X	Y	-Y	Z	-Z
16		.222	.221	.242	.244
31		.234	.225	.241	.246
46		.229	.228	.245	.237
61		.227	.233	.245	.241
76		.236	.233	.239	.245
84		.242	.234	.242	.245
95		.243	.243	.245	.254
107		.249	.249	.253	.255
111		.231	.223	.226	.235
123		.223	.234	.225	.232
135		.252	.218	.236	.236
Lower Bend		Z	-Z	45° Top	45° Bottom
Center		.222	.230	.258	.194
	Y	X	-X	Z	-Z
11		.242	.238	.243	.237
23		.237	.227	.238	.238
35		.238	.230	.230	.233
49		.242	.232	.230	.231
Upper Bend		Z	-Z	45° Top	45° Bottom
Center		.221	.232	.196	.282
	X	Y	-Y	Z	-Z
157		.230	.243	.236	.237
169		.236	.238	.234	.238
181		.240	.232	.240	.244
194		.243	.230	.234	.252

All measurements made with Nortec ultrasonic digital thickness gage. Model: NDT-123 S/N 123-311

Gage calibrated according to Nortec manual before testing and checked after testing.

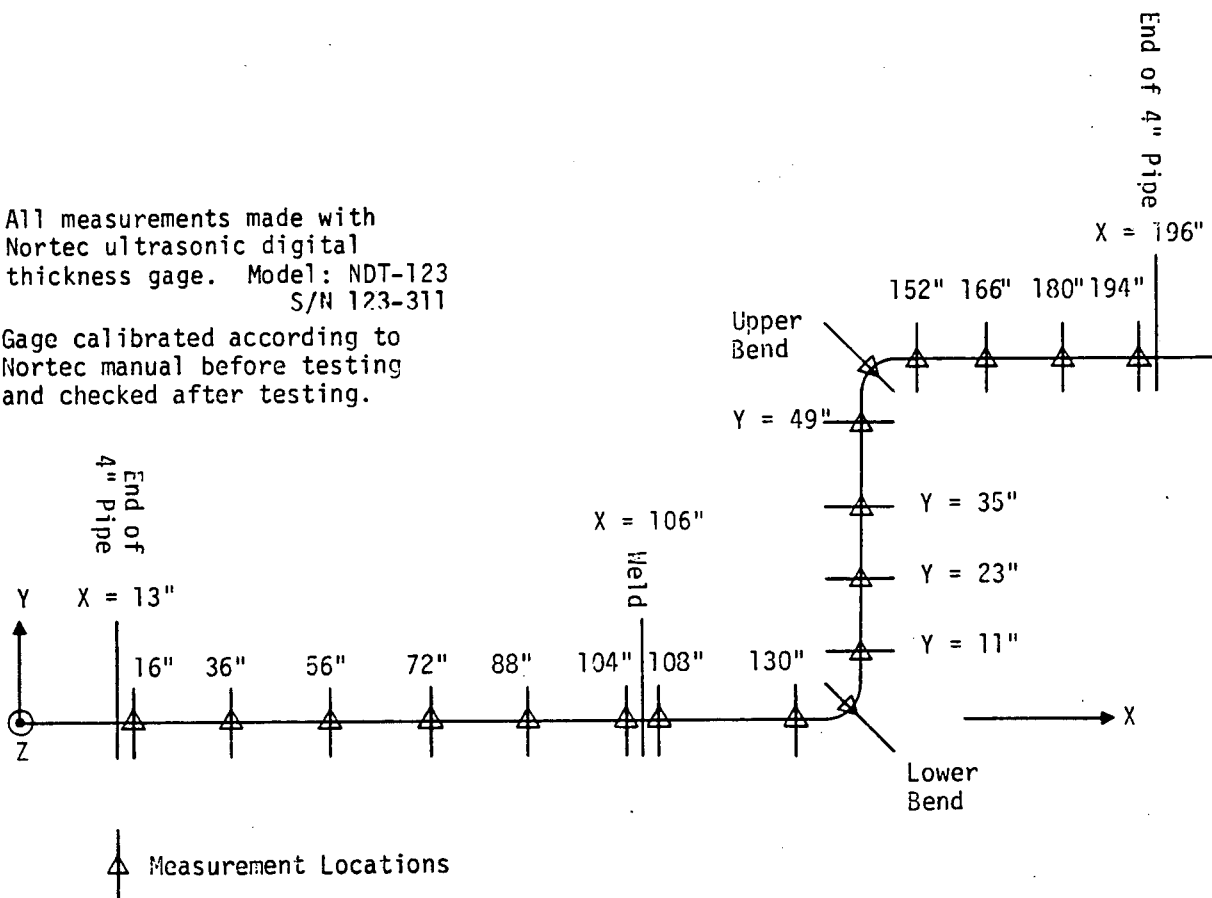


Figure A-1. Locations for Pipe Wall Thickness Measurements--Phase I Pipeline

All measurements made with Nortec ultrasonic digital thickness gage. Model: NDT-123 S/N 123-311

Gage calibrated according to Nortec manual before testing and checked after testing.

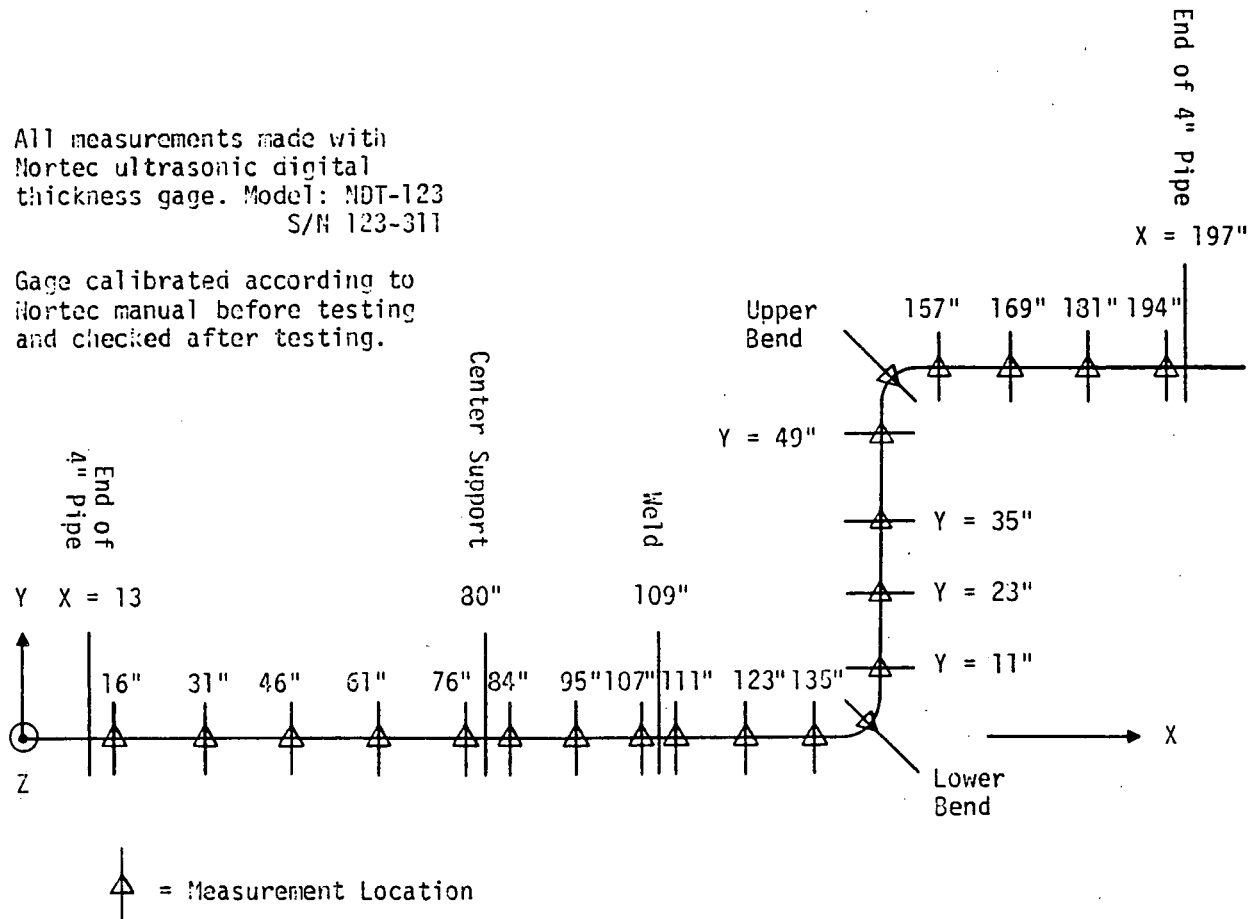


Figure A-2. Locations for Pipe Wall Thickness Measurements--Phase II Pipeline

Appendix B
INSTRUMENTATION LAYOUTS

The instrumentation layout for each phase of testing is described in this appendix. Figures B-1 and B-2, B-3 and B-4, and B-5 and B-6 give the instrumentation layout for Phases I, II, and III, respectively.

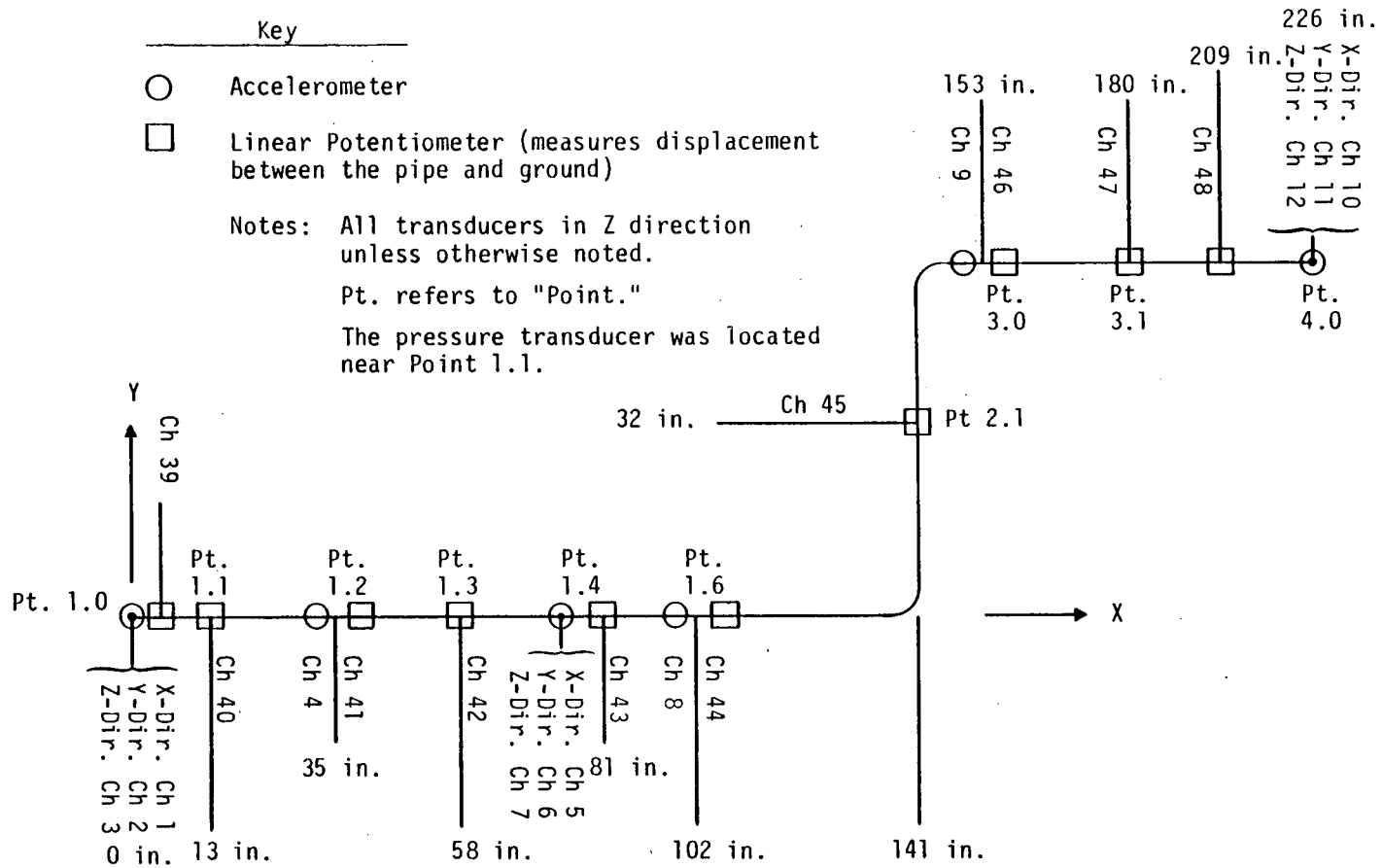


Figure B-1. Accelerometer, Displacement, and Pressure Transducer Locations--Phase I Tests

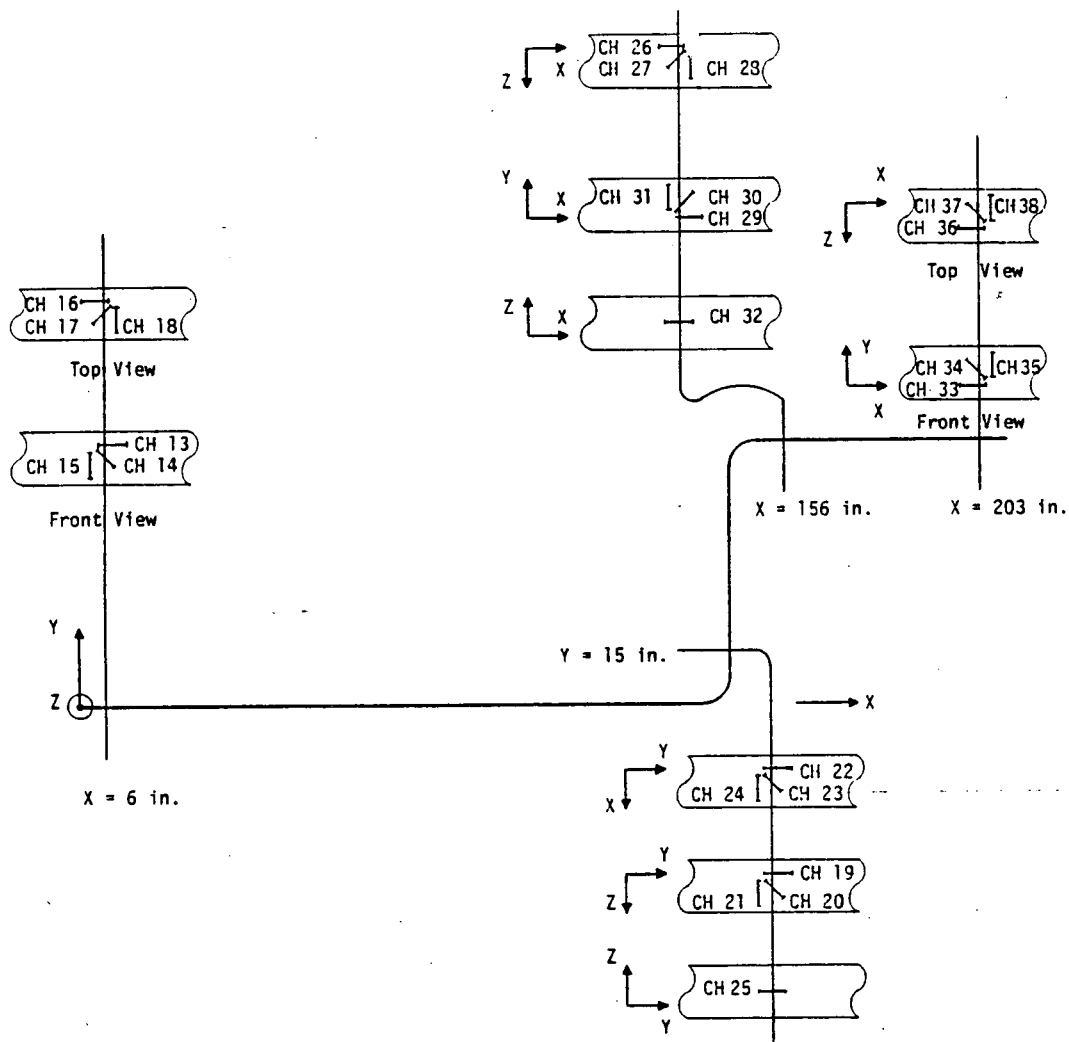


Figure B-2. Strain Gauge Locations -- Phase I Tests

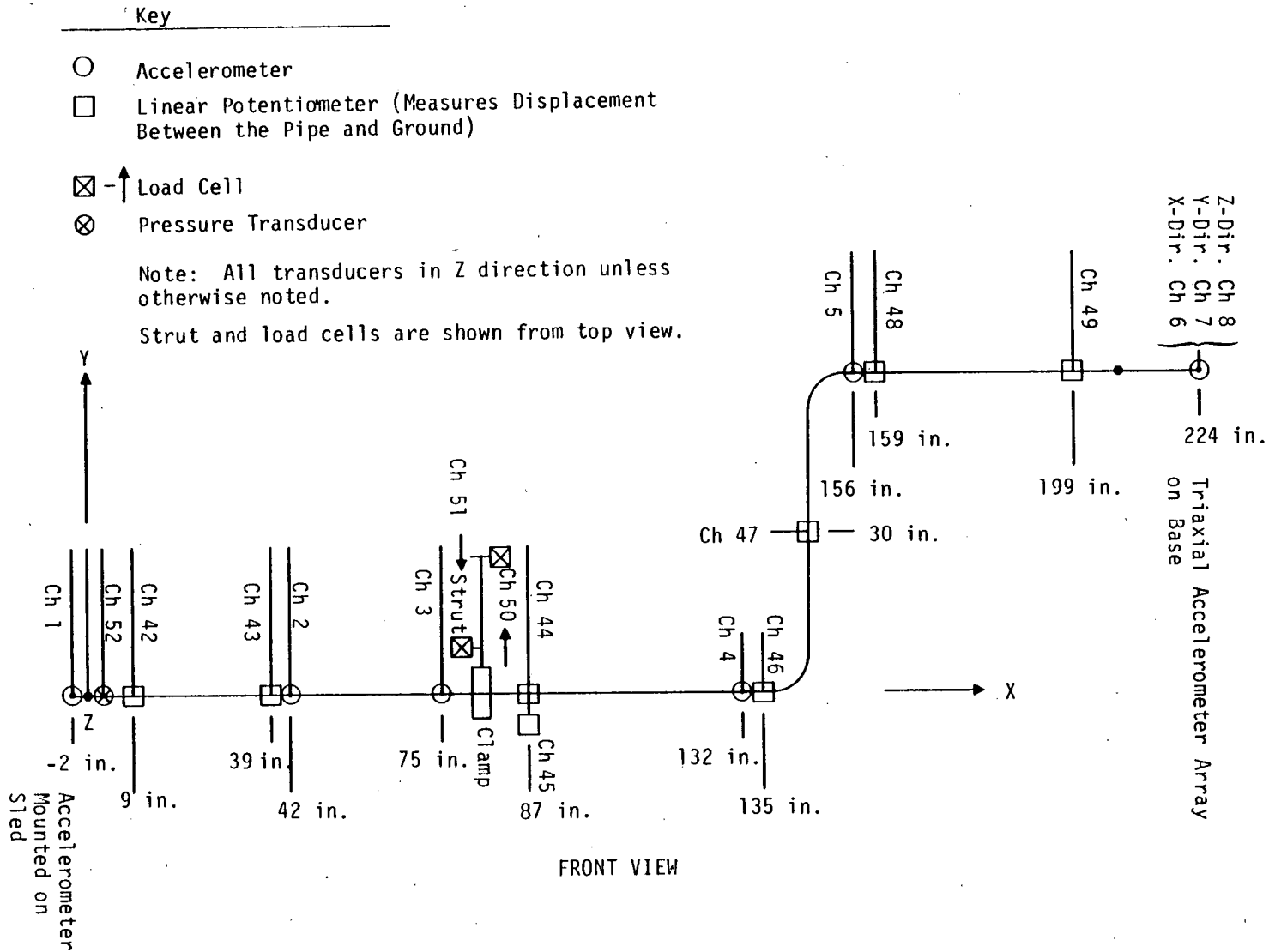


Figure B-3. Accelerometer, Displacement, Force, and Pressure Transducer Locations--Phase II Tests

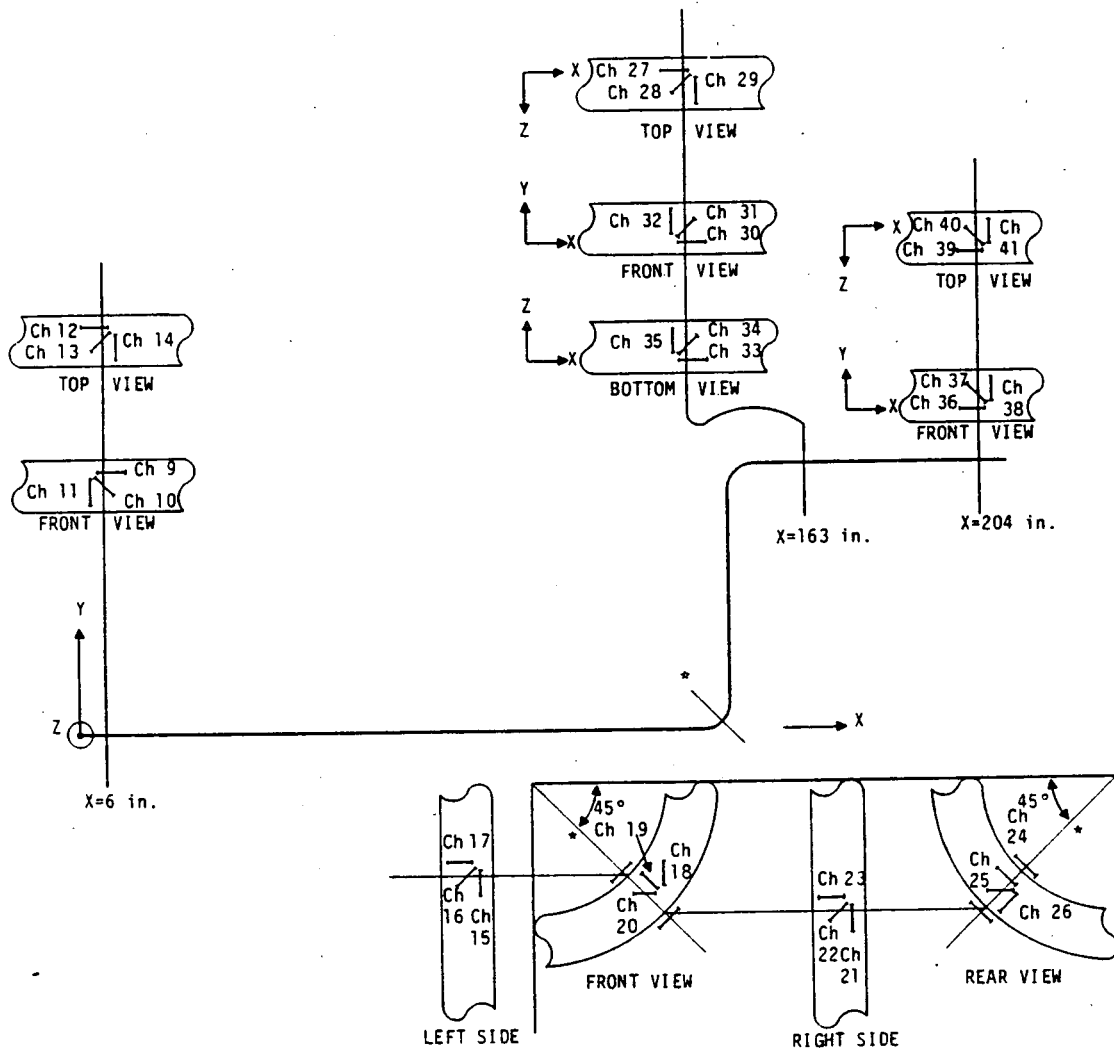
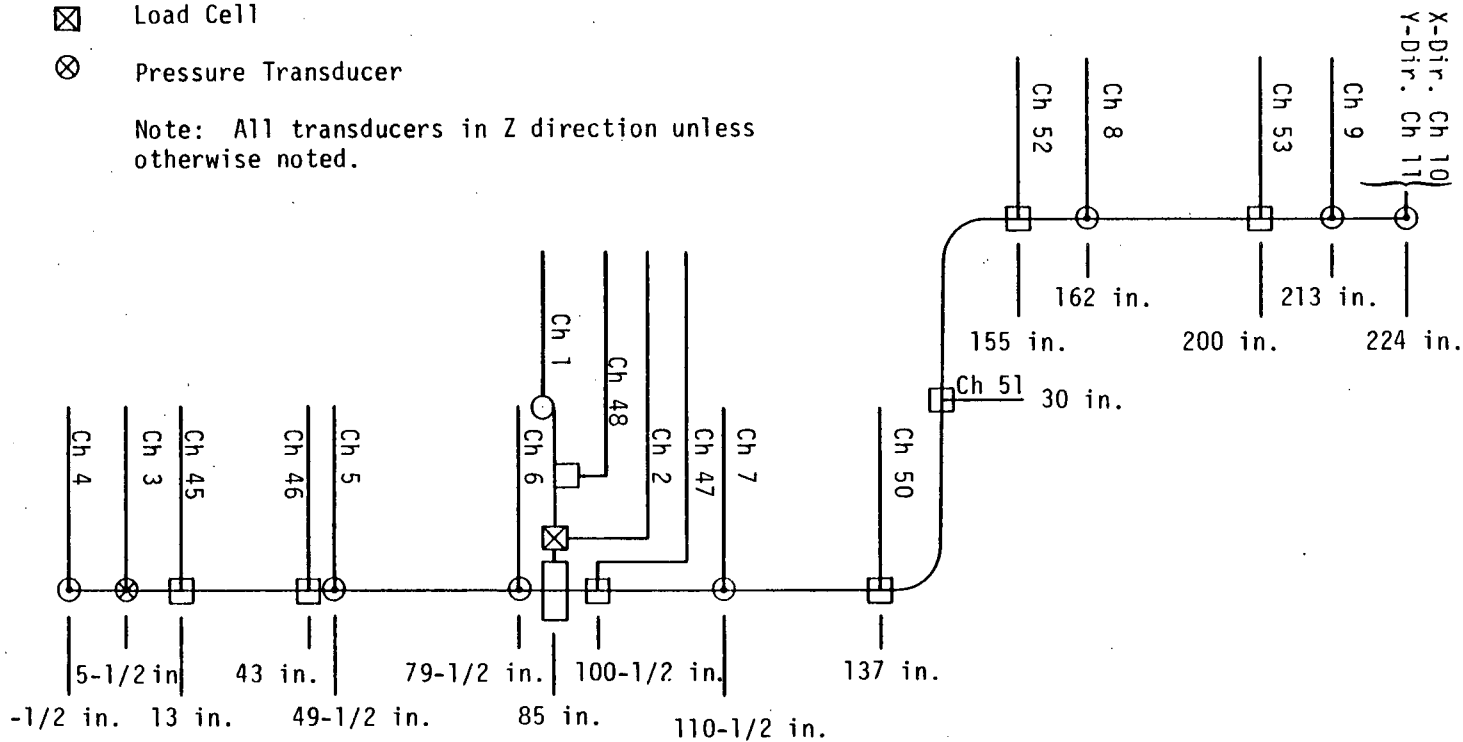


Figure B-4. Strain Gage Locations--Phase II Tests

Key

- Accelerometer
- Linear Potentiometer (Measures Displacement Between the Pipe and Ground)
- ⊗ Load Cell
- ⊗ Pressure Transducer

Note: All transducers in Z direction unless otherwise noted.



B-6

Figure B-5. Accelerometer, Displacement, Force, and Pressure Transducer Locations--Phase III Tests

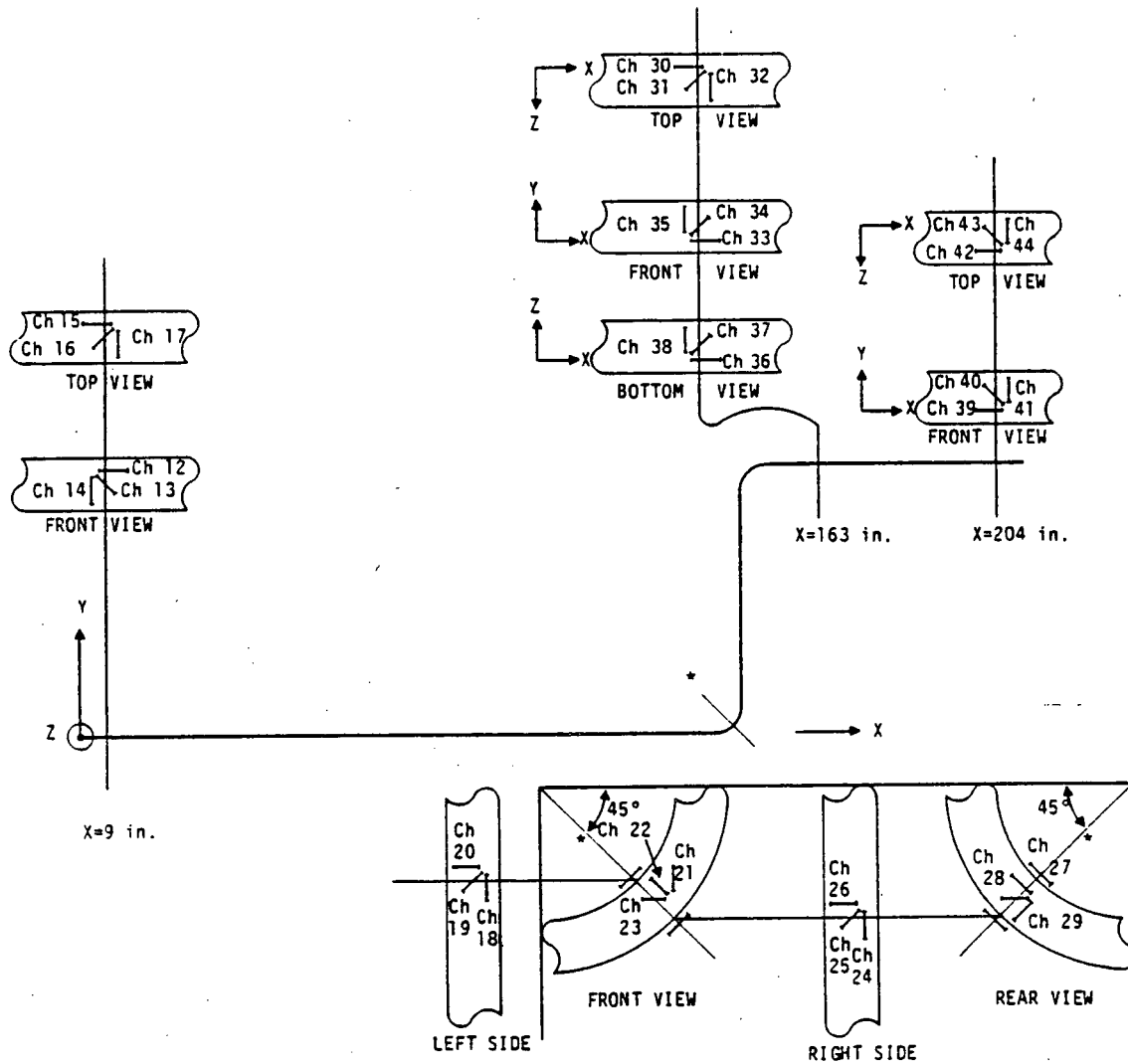


Figure B-6. Strain Gage Locations--Phase III Tests

Appendix C
PHOTOGRAPHS OF PIPING SETUP

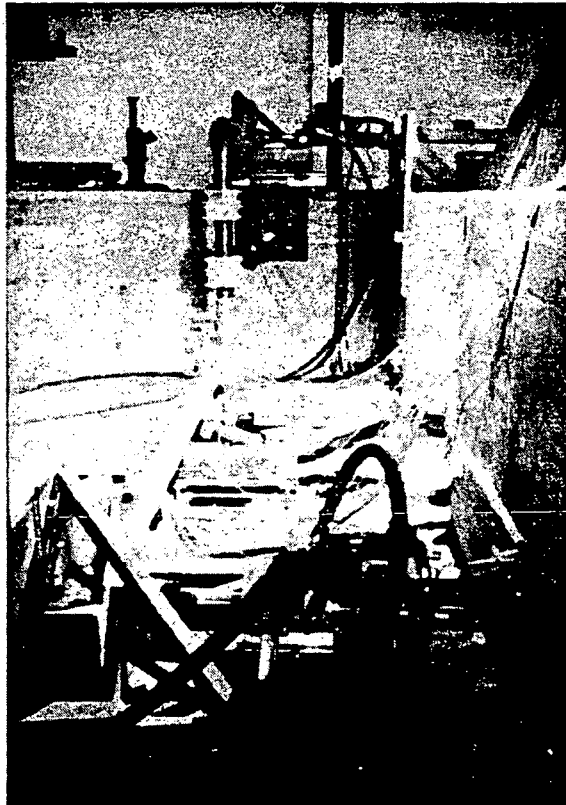
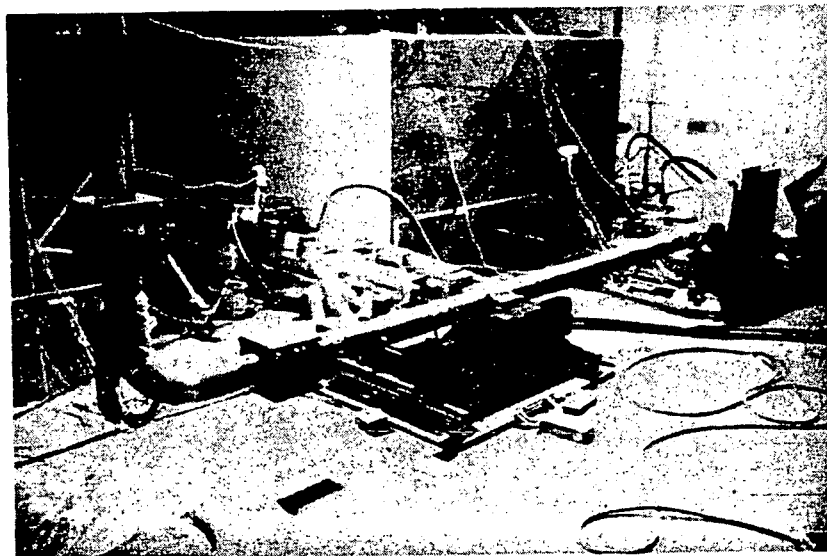
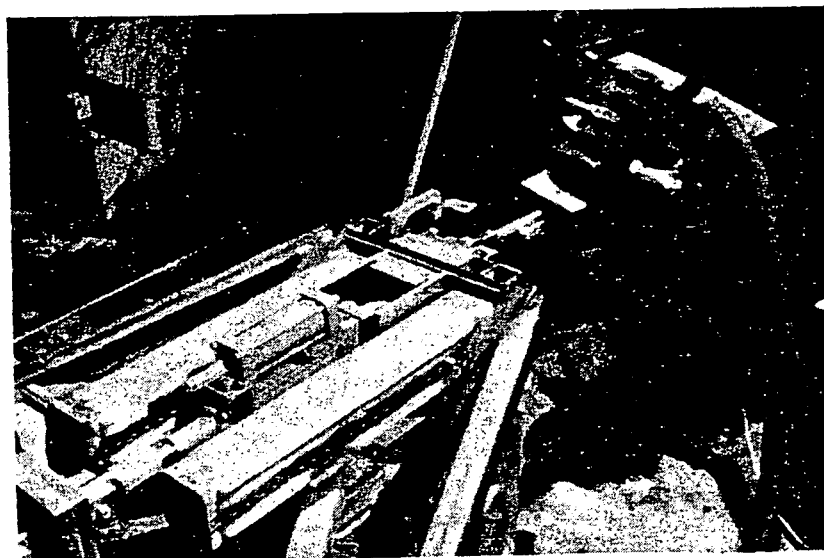


Figure C-1. End View of Z-Bend Piping System
(as Seen From Point 1.0)

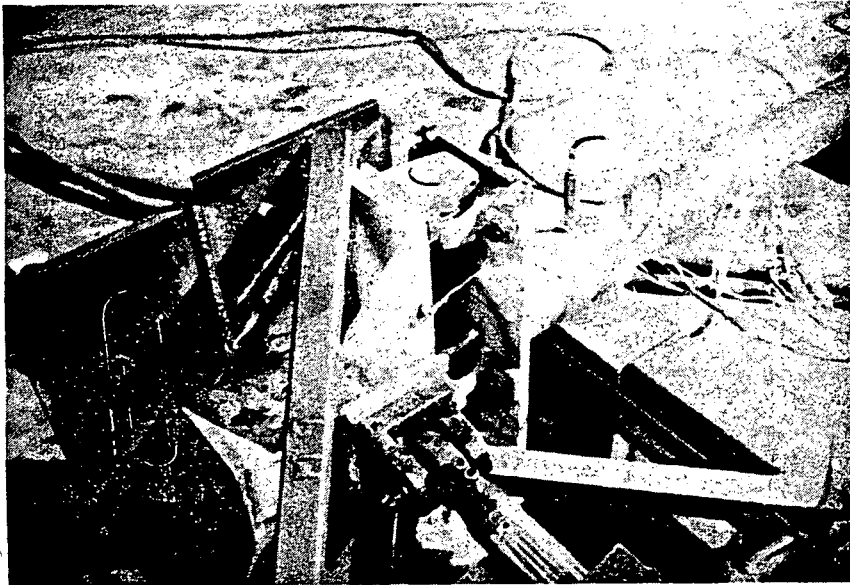


(a) Side View of Z-Bend Piping System

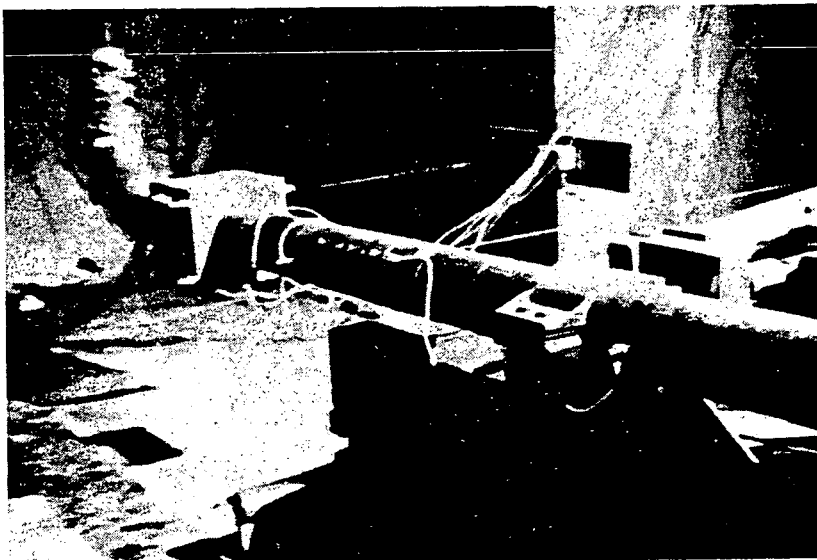


(b) Connection Between Hydraulic Actuator and Midpoint Base

Figure C-2. Overall View of Z-Bend Piping System

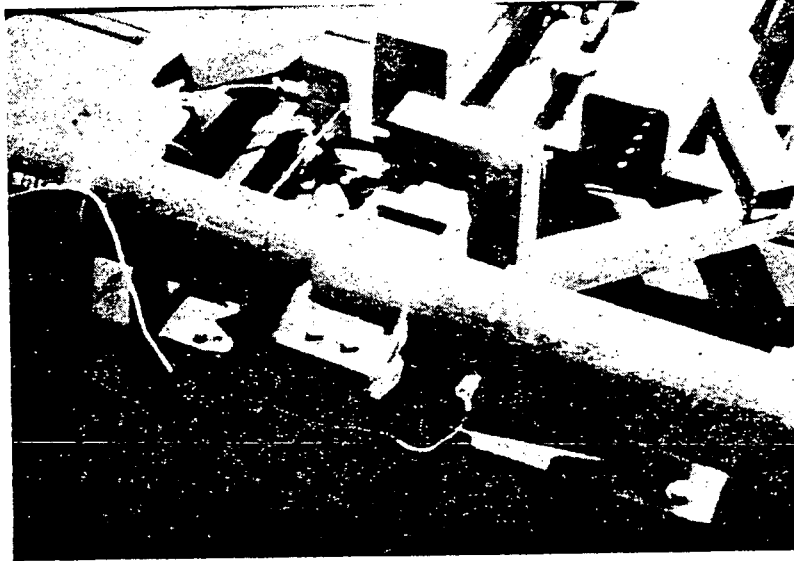


(a) End of Piping System at Point 1.0 (View Shows Pin Connection)

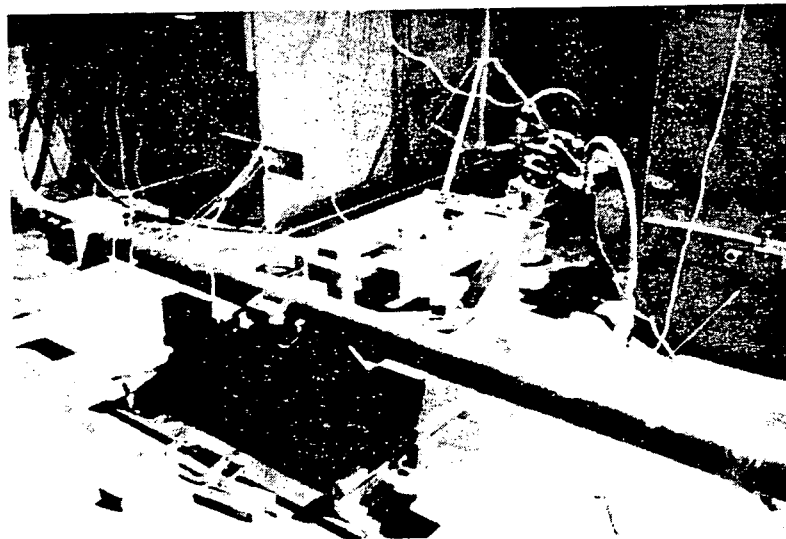


(b) Center Portion (Near Point 1.4) of Piping--Concentrated Mass on Right Side of Picture

Figure C-3. Z-Bend Boundary Conditions



(a) Snubber Connection to Pipe at Point 1.4--Phase III Tests



(b) Midpoint Base (at Point 1.4) and Snubber

Figure C-4. Midpoint Support